IEC-14

July 10-13, 2022

Lyon - FRANCE

14th International Eclogite Conference (IEC-14)

POST-CONFERENCE FIELD EXCURSION GUIDEBOOK

June 14-16, 2022, Aosta valley (Italy)

Structural and mineralogical fingerprints of eclogite-facies metamorphism in the W. Alps meta-ophiolites and associated continental margins

---

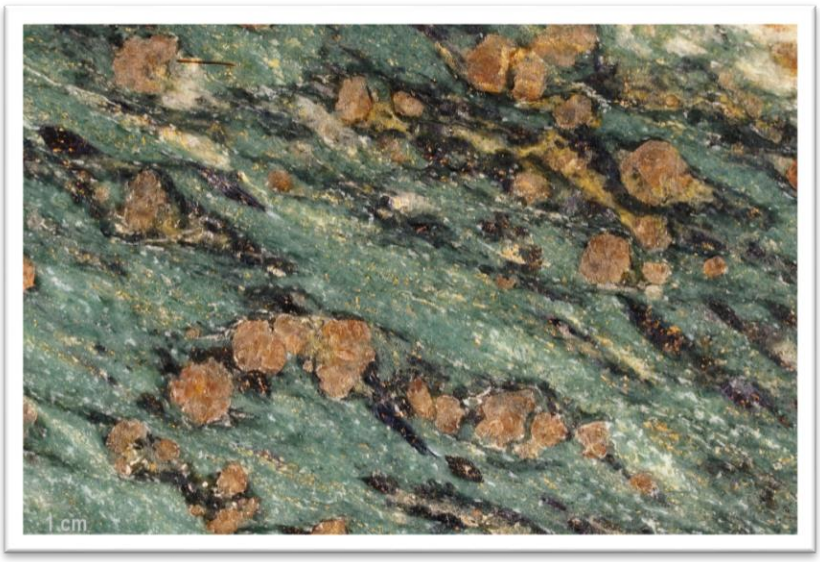

Valtournanche eclogite, Aosta valley, Italy

CONTENTS

Introduction and general geological context

The Western Alpine case study has many advantages: it gives fruitful insights from a well-constrained geological setting studied for over 200 years, it offers the opportunity to evaluate the extent of lateral variations along a continuous subduction zone, and the lack of post-subduction collisional-related heating ensures a good record of subduction processes.

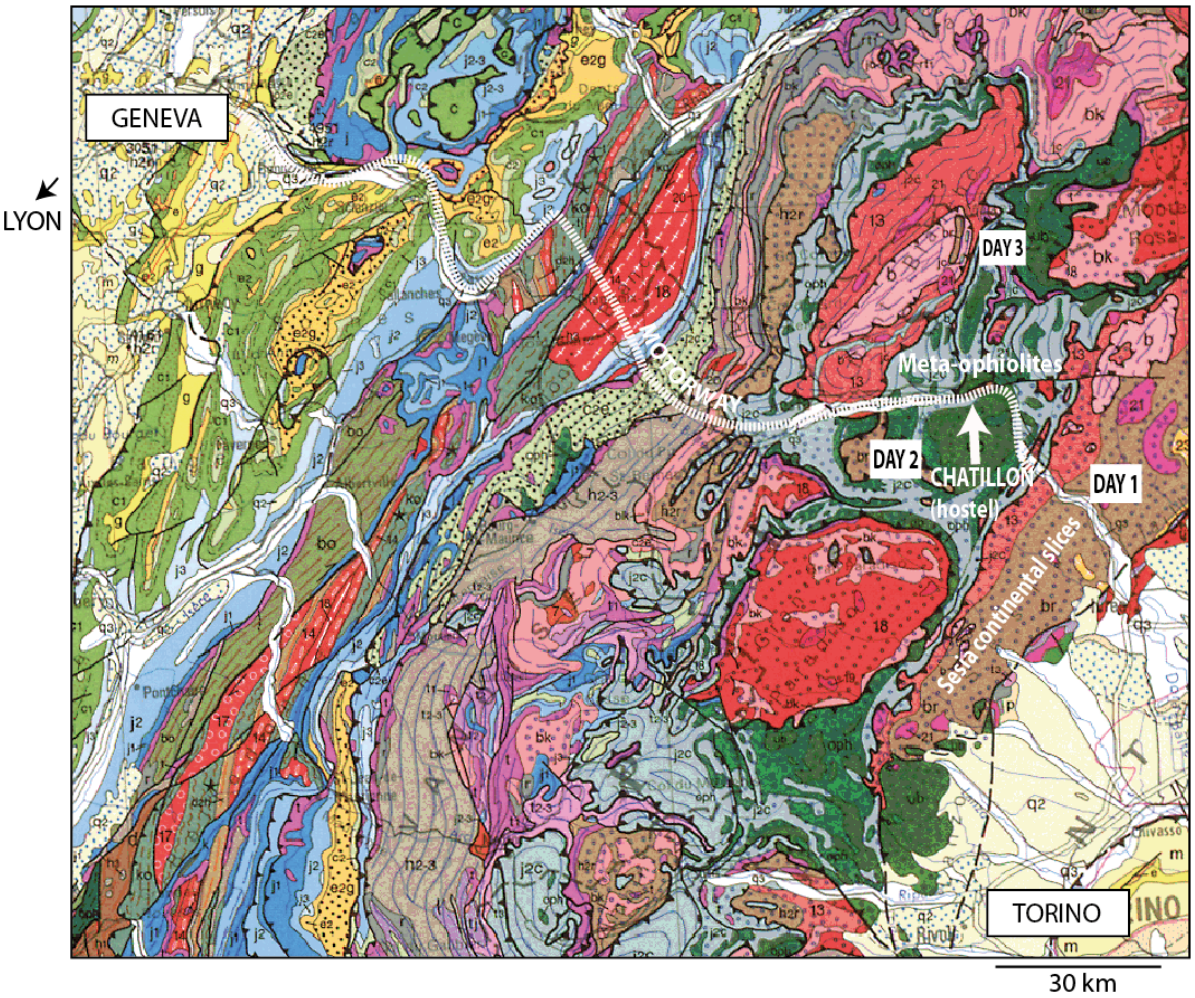

Fig. 1: Extract of the French Geological map (1/1000000, French Geological Survey - BRGM) showing the architecture of the main nappes across a GENEVA-TORINO transect. The trace of the motorway that will be used is depicted as a thick white-dashed line. The visited area is located in the region of Chatillon, in the Aosta valley. Eclogitized continental crust will be studied on the first day (Sesia zone, brown lithologies), which eclogite-facies meta-ophiolites (the Zermatt-Saas zone) will be visited on the second and third days (light blue (sediments) and deep green (mafics and ultramafics).

1. Overview of the geological context of the Western Alps

The Western Alps (**Fig.1**), one of the best studied mountain belts worldwide, results from successive subduction, accretion and collision between the European and Apulian/African plates from the Cretaceous to the present (Coward & Dietrich, 1989; Rosenbaum & Lister, 2005; Agard et al., 2022). The internal Western Alps, with their HP imprint, represent the W-verging stack of continental and oceanic nappes formed during subduction and (partial) exhumation of the Jurassic Tethyan seafloor and associated European thinned margin below the Apulian plate (e.g., Ernst & Dal Piaz, 1978; Agard et al., 2002, 2009; Rubatto & Hermann, 2003; Oberhänsli et al., 2004; Beltrando et al., 2010; Masini et al., 2013; **Fig.2**). Remnants of this ocean form the Liguro---Piemontese domain, now sandwiched between the Penninic front and eclogitized portions of the European continental margin (e.g., Dora Maira, Gran Paradiso). Eclogitized

portions of the Liguro-Piemontese oceanic lithosphere are found along 200 km, from the Zermatt---Saas area in the north to the Monviso area in the south, and further to the SE in Voltri, and constitute some of the largest and deepest ophiolitic slices detached from a subduction zone (Reinecke, 1998; Bucher et al., 2005; Angiboust et al., 2009). Peak HP-LT metamorphic conditions grade eastward in the Internal zones, from high-pressure greenschist to blueschist facies in the Schistes Lustrés complex and in the Briançonnais (Goffé &Velde, 1984; Agard et al., 2001; Oberhänsli et al., 2004) to eclogitic facies conditions in the oceanic Zermatt-Saas / Monviso / Voltri units, and in the continental Dora Maira / Gran Paradiso / and Sesia massifs (Chopin, 1984; Philippot & Kienast, 1989; Pognante, 1991; Lardeaux & Spalla, 1991; Spalla et al., 1996; Van der Klauw et al., 1997; Reinecke, 1998). Closure of the approximately ~1000 km wide, NS-trending Liguro--Piemontese slow-spreading ocean occurred from ~100 Ma onwards (for complete reviews of the Alpine geodynamic context: Lemoine et al., 1986; Coward & Dietrich, 1989; Polino et al., 1990; Lagabrielle & Lemoine, 1997; Stampfli et al., 1998; Dal Piaz, 2001; Agard et al., 2002; Oberhänsli et al., 2004; Rosenbaum & Lister, 2005; Ford et al., 2006), through an E-dipping subduction zone below Apulia/Africa at rates ~ 20 mm/yr (Le Pichon et al., 1988; Dragovic et al., 2020). During the Eocene (45-40 Ma), the thin, leading edge of the continental European margin reached the subduction zone and a short-lived (~10 My; Duchêne et al., 1997a; Rubatto & Hermann, 2001) period of continental subduction (30-40 Ma; Bonnet et al., 2022) took place before the onset of collision between Eurasia and Apulia/Africa (at ~35-30 Ma; Sinclair& Allen, 1992). During subsequent collision (~35-30 Ma onwards) the continental crust of the Western Alps underwent only moderate medium-pressure medium-temperature metamorphism (unlike in the Central Alps: Todd & Engi, 1997).

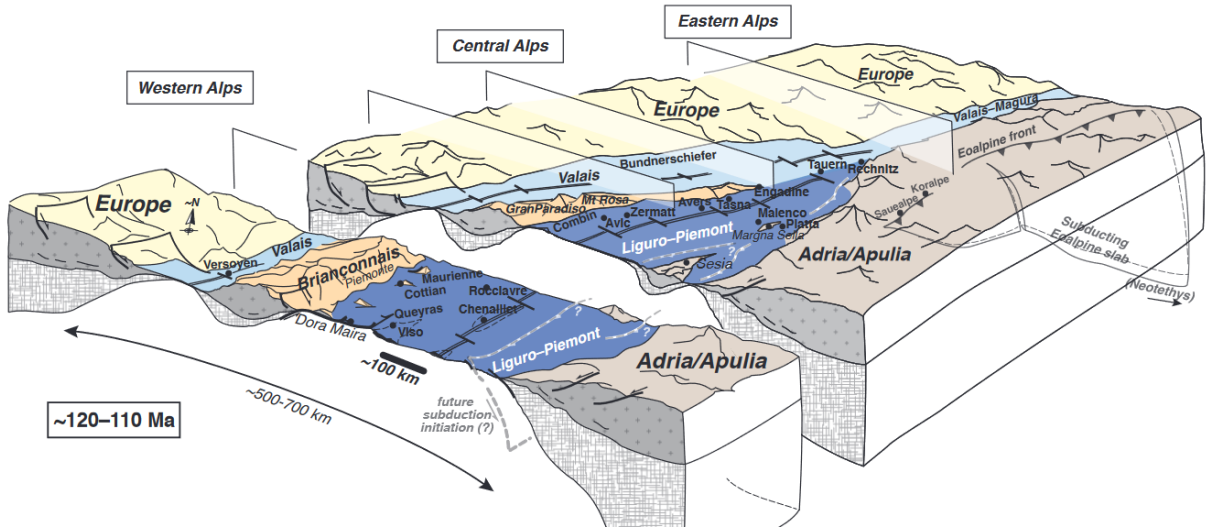

Fig. 2: Western Tethys paleogeography (Agard & Handy, 2021) at the peak of basin expansion in the lower Cretaceous. The studied transect during this field excursion corresponds to the left one from "Central Alps".

In the northern side of the Aosta valley (W. Central Alps transect on **Fig.2**), the Alpine collisional wedge (Penninic-Austroalpine nappe stack) is characterized, from bottom to top, by (**Fig. 3**):

- the eclogite-facies Monte Rosa unit (European continental margin);
- the eclogite-facies Zermatt-Saas meta-ophiolite (Tethys ocean; in purple color on **Fig.4** and see PT paths on **Fig.5**);
- a few eclogite-facies Austroalpine slices (outliers) and/or a Permian-Mesozoic decollement cover unit of debated continental origin (the Pancherot-Cime Bianche unit);
- the blueschist-facies Combin (or Tsaté) meta-ophiolite (Tethys ocean);
- finally, the capping upper Austroalpine units (Adria/Apulia continental margin) consisting of the eclogite-facies Sesia-Lanzo inlier and blueschist-facies Dent Blanche-Mont Mary-Pillonet klippen (outliers) (Ballèvre et al., 1986; Polino et al., 1990; Dal Piaz, 1999; Dal Piaz et al., 2001; Beltrando et al., 2014; Angiboust et al., 2014; Manzotti et al., 2014).

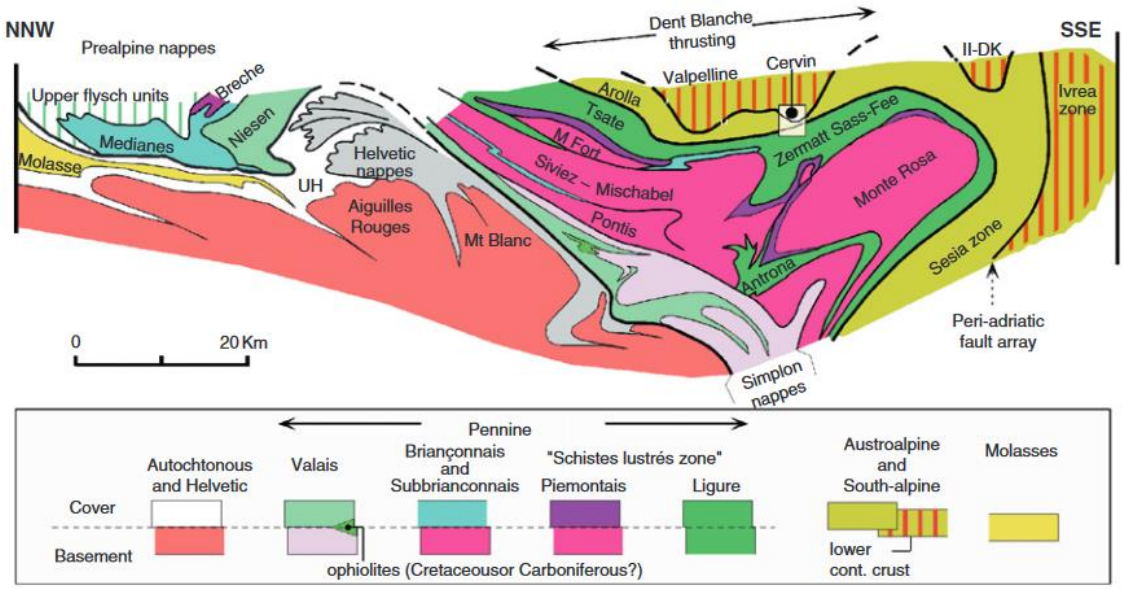

Fig. 3: Cross-section of the Alps passing through the Cervino-Matterhorn (white square). De Graciansky et al., 2011, after Escher & Beaumont, 1997.

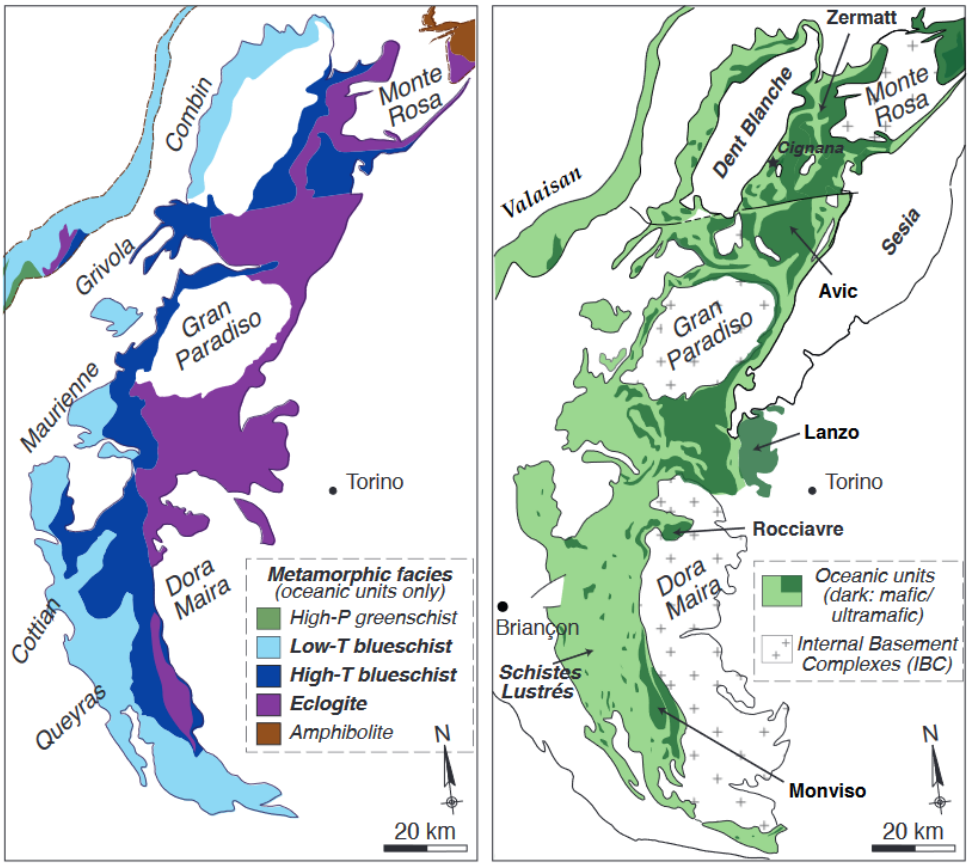

Fig. 4: (left) Distribution of metamorphic facies across the Western Alps for the material derived from the oceanic Tethyan realm. See how the peak burial metamorphic grade increases from W to E. (right) Distribution of sedimentary- and mafic-ultramafic-dominated units, also for the Tethyan realm (after Agard & Handy, 2021). Note that the proportion of mafic and ultramafic-derived material increases when reaching higher metamorphic grades.

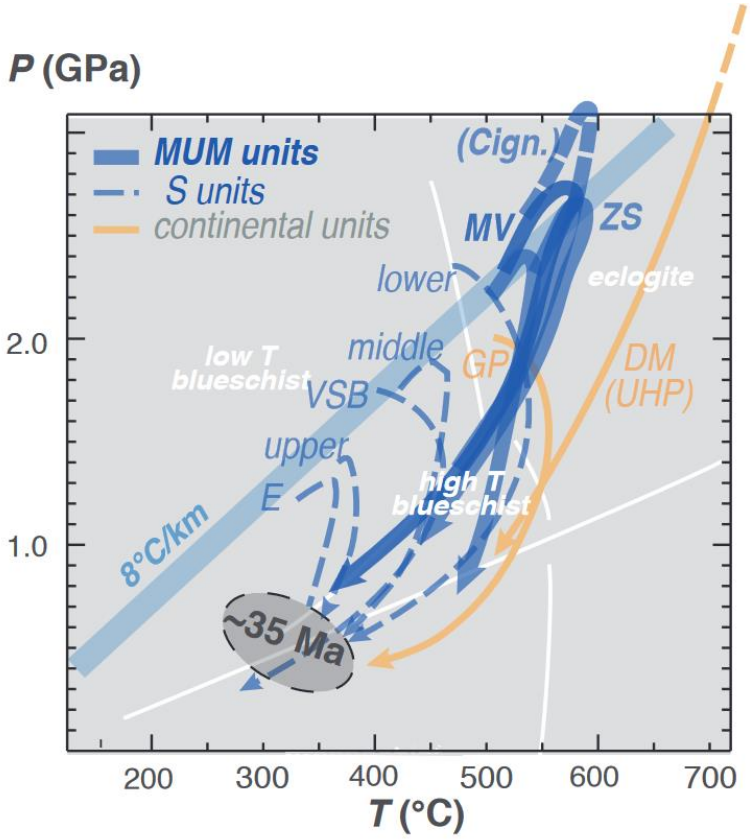

***Fig. 5**: Pressure-Temperature paths characteristic of western Alps tectonic trajectories for HP meta-ophiolites (after Agard & Handy, 2021). ZS: Zermatt-Saas meta-ophiolites, and MV: Monviso (both in blue) are typical of Mafic and Ultramafic-dominated (MUM) lithologies localized in figure 4. S units: (meta-)sedimentary units. Cign: Lago di Cignana subunit. VSB: Valaisan Petit-Saint-Bernard unit. E: Engadine. DM: Dora Maira UHP unit. This sketch shows that the downgoing oceanic lithosphere typically passes through the lawsonite blueschist facies until reaching the lawsonite-eclogite facies. It is subsequently exhumed through the epidote-blueschist facies before reaching shallow structural level within the greenschist facies, that typically overprints many of the HP lithologies visible in the field in the Alps.*

2. Evolution of the oceanic lithosphere from seafloor hydrothermalism to eclogitization

The meta-ophiolites of the composite Piedmont nappe extend along the entire arc of the Western Alps up to the Central Alps (Bigi et al., 1990). They form numerous metamorphic units, which are scattered at different structural levels of the Alpine nappe pile, from the uppermost Platta-Arosa unit (Central Alps) to the lowest and outermost Versoyen unit (in the Western Alps). Argand (1916) attributed these meta-ophiolites to the Penninic domain. Since the development of the plate tectonics, they are considered as derived from the oceanic lithosphere of the Liguro-Piedmont branch of the Tethys that opened in the Middle-Late Jurassic between Europe and Adria (Africa) passive continental margins (see historical review in Dal Piaz et al., 2001). The oceanic lithosphere forming the Tethyan realm in this region was inferred to belong to a slow-spreading type, similarly to the present-day Atlantic Ocean, with denudated serpentinized mantle directly exposed on the seafloor (Lagabrielle & Cannat, 1990). This oceanic lithosphere was sliced and dismembered during the plate margin convergence that led to the subduction of the oceanic and continental crusts under the Adriatic margin and to their partial exhumation. The occurrence of either a single Piedmont ocean or two separated oceanic branches (South-Penninic / Piedmont and North-Penninic / Valais basins) has been envisaged since the first work of Sturani (1973) to the last contribution of Rubatto et al. (1998), who tried to date both oceans.

On the basis of the metamorphic evolution of these meta-ophiolites, Dal Piaz (1965, 1974), Bearth (1967) and Kienast (1973) distinguished two main units, namely the Combin (blueschist-facies, named Tsaté on the Swiss side) and Zermatt-Saas (eclogite-facies) units. This discrimination has been accepted by many authors

(e.g., Elter, 1971), who also used lithostratigraphic and structural criteria to distinguish between these two units. Here, we only emphasize the features of the lower Zermatt-Saas meta-ophiolite.

The rocks of Zermatt-Saas unit are serpentinite with locally preserved mantle peridotite relics, abundant ophicalcitic breccias, minor metagabbro with magmatic mineral or textural relics (e.g., Allalin, Mellichen, Crepin), metabasalts with N-MORB affinity (Dal Piaz et al., 1978; Dal Piaz 1981; Beccaluva et al., 1984; Pfeiffer et al., 1989; Fontana et al., 2015a) and metasediments derived from the internal part of the Tethys (e.g., Bearth, 1967; Ernst &Dal Piaz, 1978; Deville et al., 1992).

The meta-ophiolites originally closer to oceanic hydrothermal out-flow zones show occurrences of Fe-Cu sulphide and Mn ore deposits (e.g., Dal Piaz & Omenetto, 1978; Martin et al., 2008). The formers are located within metabasalts, the latter in siliceous sediments (metacherts). The most important Cu-Fe sulphide deposits of the Zermatt-Saas unit are within high-pressure metabasalts with strong oceanic alteration (garnet glaucophanite, chloriteschists and talcschists). They are located in the southern Aosta valley, noticeably at Saint-Marcel (see below) and Champ-de-Praz. The Mn deposits occur mainly as metamorphosed boudinaged quartzites rich in braunite, piemontite and spessartine (Castello, 1981). At Praborna (Saint-Marcel), which is by far the most important and famous occurrence, the ore deposit includes very peculiar Mn-bearing silicates (e.g., Martin-Vernizzi, 1982; Martin & Kienast, 1987; Krutow-Mozgawa, 1988). It is thought to derive from an oceanic hydrothermal system, or accumulation of Mn-rich oceanic nodules and “umbers”, as evidenced by high Sb-, Sr- and Ba-contents (Perseil, 1988; Perseil & Smith, 1995; Tumiati et al., 2010). Further details about sulphide and Mn-related mineralizations will be given below in the section presenting the second-day excursion.

The effect of oceanic hydrothermalism and alteration on the mafic rocks is also evidenced by abnormal contents in various elements (Na, OH, Mg, Ca) (Beccaluva et al., 1984; Barnicoat & Bowtell, 1995; Widmer et al., 2000; Martin & Cortiana, 2001; Angiboust & Agard, 2010) and the scattering of $d^{18}O$ values (Cartwright & Barnicoat, 1999).

The subduction and exhumation history of the Zermatt-Saas unit is signed by prograde relics as pseudomorphs after lawsonite, eclogite-facies assemblages and by greenschist-facies assemblages indicating retrogression. The Zermatt-Saas rocks yield P-T estimates for the peak metamorphism with values mostly comprised between 2.0-2.5 GPa and 520-570°C (Martin & Tartarotti, 1989; Bucher et al., 2005; Angiboust et al., 2009). In the Lago di Cignana locality, the finding of coesite-bearing metasediments (Reinecke, 1991) indicates slightly higher P-T conditions, most likely in the range 3.0-3.2 GPa and up to 600°C (Groppo et al., 2009d; Frezzotti et al., 2011). These deeper conditions may reveal the presence of a thin tectonic sliver that has been subducted deeper than the rest of the Zermatt-Saas zone (Forster et al., 2004a), even though the contact zone is difficult to evidence. Overall, it is important to note that the Zermatt-Saas zone (and its lateral equivalent the Monviso complex further south) represent among the largest coherent massifs of eclogitized oceanic lithosphere known on Earth (Angiboust et al., 2009, 2012a).

The formation of the Zermatt-Saas oceanic crust is attributed to the Jurassic (164-153 Ma: Rubatto et al., 1998). Geochronology yielded a range of ages between 52 and 43 Ma (Eocene) for its high-pressure metamorphism, depending on the technique used (Botwell et al., 1994; Barnicoat et al., 1993; Rubatto et al., 1998; Mayer et al., 1999; Dal Piaz et al., 2001; Dragovic et al., 2020). The different results may correspond to different steps of the P-T path between the peak conditions and the retrogression below 500°C.

The structure of the Zermatt-Saas meta-ophiolite in the Saint-Marcel valley and Monte Avic massif is generally characterized by a N-S-trending lineation parallel to the axes of isoclinal folds, and related to a D2 deformation phase that occurred under eclogite facies (Tartarotti, 1988; Martin et al., 2004). Relics of an earlier prograde deformation (D1) have been recognized only in the core of garnet crystals. The D2 foliation is further folded by a D3 deformation phase with axes still oriented N-S. An E-W-trending D4 regional tectonic phase developed under greenschist facies (e.g., Elter, 1960). South dipping fault planes belonging to the Aosta-Ranzola normal fault system (Bistacchi & Massironi, 2000), locally reactivated as N-vergent thrusts, represent the last deformation episode D5 (Martin & Tartarotti, 1989).

3. Metamorphism and deformation of the continental margins

The Austroalpine domain is represented, in the Aosta Valley, by two first-rank units, namely (i) the Sesia-Lanzo internal zone, a 90-km long and 25-km large belt bounded to the east by the Canavese fault, and (ii) numerous external slices of continental crust, traditionally grouped as Dent Blanche nappe (Argand, 1916; Stutz & Masson, 1938; Compagnoni et al., 1977). The paleo-geographic origin of the continental slivers involved in the alpine nappe-stake has been debated for decades (e.g. Mattauer, 1986; Dal Piaz et al., 2001). While it is likely that some tectonic erosion of the upper continental plate has occurred throughout the entire alpine subduction history (Polino et al., 1990), available geological evidence corroborates the model where many of these continental allochthons were inherited from crustal thinning during the continental rifting and were actually drifting together with the ophiolites in the middle of the oceanic basin (Beltrando et al., 2010 and references therein).

The Sesia-Lanzo zone mainly consists of

(i) the internal Micaschist Eclogitic complex (Stella, 1894; Franchi, 1900, 1902),

(ii) the external greenschist-facies Gneiss minuti complex (Gastaldi, 1871) and

(iii) some klippen of the Adria lower crust (e.g., II zona Dioritico-Kinzigitica).

The Dent Blanche nappe (s.l.) is subdivided into two main groups of units, which are characterized by a contrasting subduction metamorphism and a different structural position:

(i) the blueschist-facies Dent Blanche (s.s.), Mont Mary and Pillonet thrust units (Diehl et al., 1952; Ayrton et al., 1982; Dal Piaz & and Martin, 1988; Canepa et al., 1990; Dal Piaz et al., 2001), which, like the Sesia-Lanzo zone, override the entire ophiolitic Piedmont Zone and therefore may be reported as upper Austroalpine outliers (Dal Piaz, 1999);

(ii) the eclogite-facies lower Austroalpine outliers

The pre-Alpine Adriatic crust was mainly composed of felsic and mafic granulites (e.g., Nicot, 1977; Lardeaux and Spalla, 1991), kinzigitic gneiss (e.g., Diehl et al., 1952; Canepa et al., 1990), a few slices of serpentinized mantle peridotite (e.g., Cesare et al., 1989), marble, abundant Late Palaeozoic granitoids (e.g., Gneiss Arolla) and gabbros (e.g., base of the Cervino/Matterhorn: Dal Piaz et al., 1977). A Mesozoic sedimentary cover, composed of quartzite, marble, dolostone, sedimentary breccia, conglomerate etc. is locally preserved in the Dent Blanche-Mont Mary system (Roisan zone, Mont Dolin; Manzotti et al., 2014) and has been metamorphosed together with the basement (Ayrton et al., 1982; Canepa et al., 1990). Similarly, a metamorphosed sedimentary cover has been described in the Sesia-Lanzo zone (Venturini, 1995).

During the Alpine orogeny, the high-grade metamorphic and igneous basement was metamorphosed under eclogite-facies (Sesia-Lanzo and lower Austroalpine outliers, such as the Chatillon slice, Dal Piaz & Martin, 1988) or blueschist-facies (upper Austroalpine outliers: Dent Blanche, Mont Mary, Pillonet) conditions, giving rise, respectively, to Eclogitic Micaschists and chloritoid-bearing micaschists (Lardeaux et al., 1983; Giuntoli & Engi, 2016), phengite-jadeite orthogneiss and Na-amphibole mafic boudins (Pillonet: Dal Piaz, 1976). As for the leucocratic granitoids that intruded the Adria basement during the Permian, they were transformed into Gneiss minuti (Sesia-Lanzo) and Gneiss Arolla (Dent Blanche s.l.).

The metagranitoids and metapelites of the Sesia-Lanzo zone are of particular interest, because they have preserved rather well the eclogite-facies paragenesis. The Eclogitic Micaschists, first defined and studied by Stella (1894) and Franchi (1900, 1902), are coarse-grained micaschists, with quartz, phengite, paragonite, large garnet crystals, omphacite, glaucophane, chloritoid and rutile. Some granites gave rise to the famous eclogite-facies rocks, with jadeite, quartz, phengite, garnet (e.g., Monte Mucrone: Compagnoni & Maffeo, 1973; Compagnoni et al., 1977; Oberhänsli et al., 1982, 1985; Rubbo et al., 1999).

In the Dent Blanche nappe, the blueschist-facies P-T conditions were estimated at 400-500°C and in the range 1-1.5 GPa (Angiboust et al., 2014b; Manzotti et al., 2014), whereas higher P-T-values have been obtained for the Sesia-Lanzo eclogite-facies rocks (e.g., 550±50°C and 1.4-2.1 GPa: Oberhänsli et al., 1985; Inger et al., 1996; Tropper et al., 1999; Zucali et al., 2002).

Extensive geochronological investigations in the last twenty years has led to a re-appraisal of previously published relatively old ages for the Sesia-Lanzo nappe and of the upper Austroalpine. The wealth of recent geochronological data, using garnet, phengite and allanite dating techniques converge towards ages at the transition between the very end of the Cretaceous and the Paleocene (69.2±2.7 Ma, Duchêne et al., 1997; 65±5 Ma, Rubatto et al., 1998; 77-55 Ma, Giuntoli et al., 2018). A similar age was obtained for the Pillonet klippe (75-73 Ma: Cortiana et al., 1998). These ages have been interpreted as the crystallization age of the eclogite-facies paragenesis at a depth of 50-100 km. Younger Ar-Ar white mica deformation ages (~65 Ma) have been related with exhumation of the Eclogitic micaschists in the blueschist facies (Halama et al., 2014), likely during the tectonic juxtaposition with the underlying Arolla-Gneiss Minuti slivers (Angiboust et al., 2014b; **Figs. 6 and 7**).

There are a number of Austroalpine derived outliers (derived from the stretching of the continental margin during rifting) that were reported by previous studies (Dal Piaz et al., 2001; Beltrando et al., 2010c; Weber & Bucher, 2015; Fassmer et al., 2016) and that appear either embedded or capping the summit of the Zermatt-Saas unit. Most peak burial ages cluster between 58 and 45 Ma (Bucher et al., 2020 and references therein). Monte Emilius massif (that will be visible in the landscape above the Zermatt-Saas unit on day 2) occupies this structural position too and could correspond to another one of these outliers, subducted down to eclogite-facies conditions together with some segments of the Zermatt-Saas unit (Dal Piaz et al., 2001; Angiboust et al., 2017).

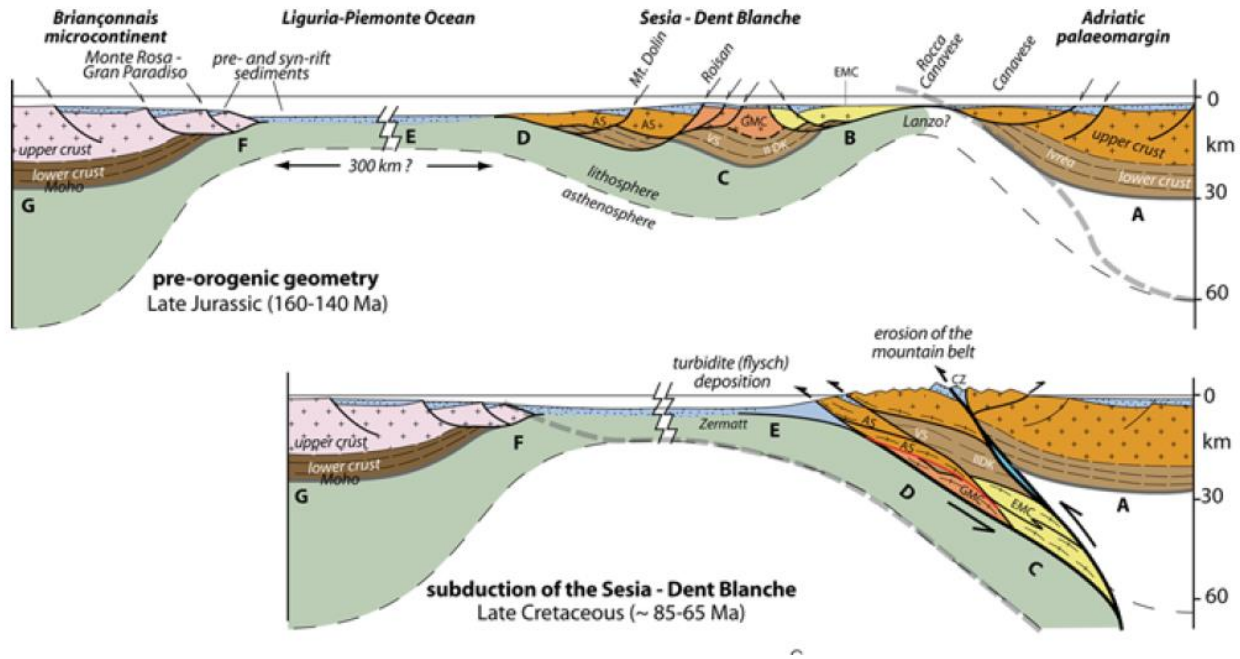

***Fig. 6**: Simplified kinematic model in six sketches for the evolution of the Sesia-Dent Blanche from the rifting stage (top) until the collisional stage (bottom). Modified from Manzotti et al. (2014). AS: Arolla Series, VS: Valpelline Series, IIDK: Seconda Zona Dioritico-Kinzigitica, EMS: Eclogitic Micaschist Complex, GMC: Gneiss Minuti Complex, RCTS: Rocca Canavese Thrust Sheets, CZ: Canavese Zone. The internal structure of the Liguro-Piemontese units is not shown. In the Sesia-Dent Blanche nappes, thicker lines mark the location of the main shear zones (in red: the intra-Dent blanche Roisan shear zone).*

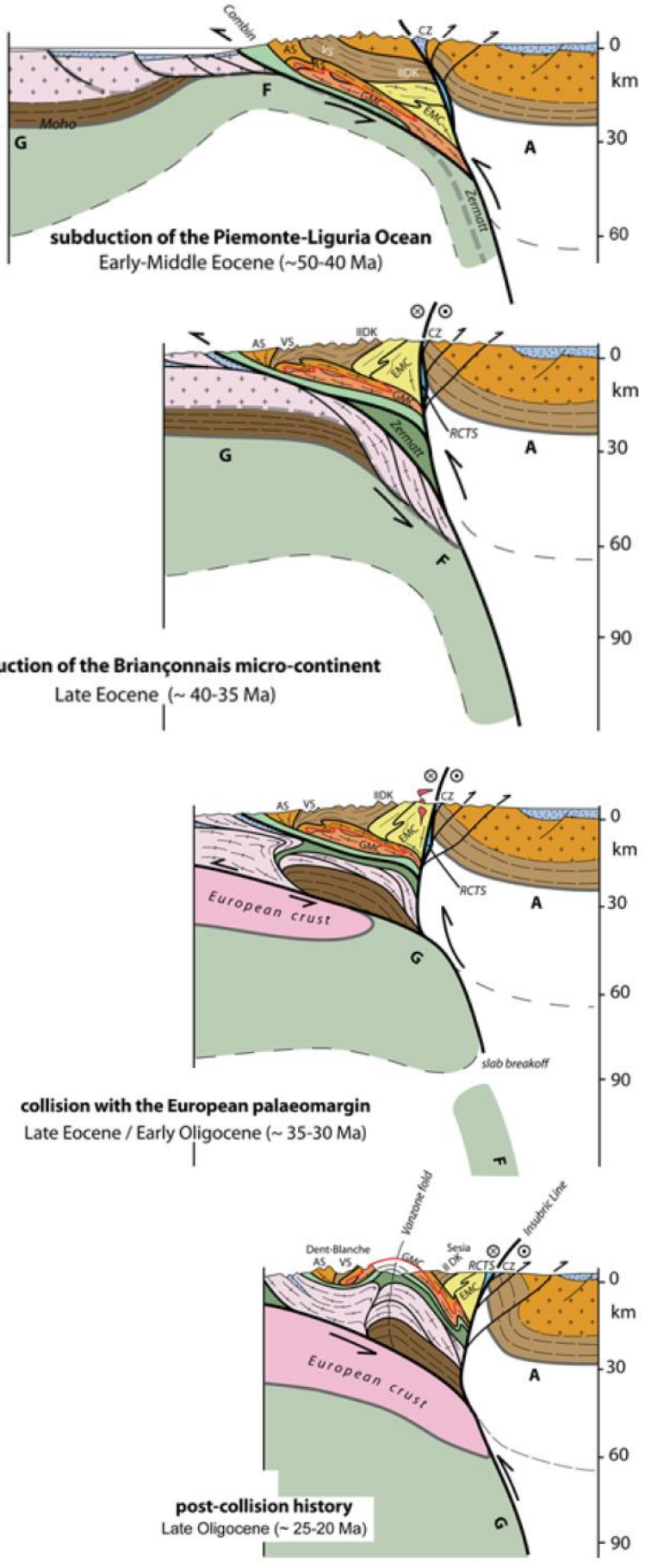
Combin
AS
VS
CZ
IIDK
EMC
F
Moho
G
A
Zermatt
0
km
30
60
subduction of the Piemonte-Liguria Ocean
Early-Middle Eocene (~50-40 Ma)
RCTS
90
subduction of the Briançonnais micro-continent
Late Eocene (~ 40-35 Ma)
GMC
European crust
slab breakoff
collision with the European palaeomargin
Late Eocene / Early Oligocene (~ 35-30 Ma)
Vanzone fold
Insubric Line
Dent-Blanche
Sesia
post-collision history
Late Oligocene (~ 25-20 Ma)

In the Aosta valley area, the vast amount of available petrological and geochronological data helped Angiboust et al. (2014b) to propose a tectonic model where each of the shear zones bounding the different oceanic and continental tectonic slices in the Sesia-Dent Blanche edifice could be viewed as former transient plate interface boundaries which have been gradually abandoned upon basal accretion and downstepping of the active deformation front (**Figs. 6 and 7**). In this framework, the Eclogitic Micaschist complex (already eclogitized at 60 Ma) has been juxtaposed on its way up under blueschist facies conditions meanwhile the adjacent Sesia gneiss minuti (and their lateral equivalent the Arolla gneiss from the Dent Blanche) where accreted at their peak burial conditions in the blueschist facies at around 450-500°C and 1.2 GPa. Even though a HP imprint has been earlier noted in the entire Sesia complex (Compagnoni et al., 1977b), a recent study questions the existence of a blueschist-facies imprint in the westernmost part of the Sesia complex (Gneiss Minuti), inferring a late juxtaposition together with the eclogitic micaschist sequence only at greenschist-facies conditions (Giuntoli et al., 2018).

Most of the early tectonic contacts have been extensively reworked upon exhumation, leading in some extreme cases to a complete erasing of the high pressure memory (Wheeler & Butler, 1993).

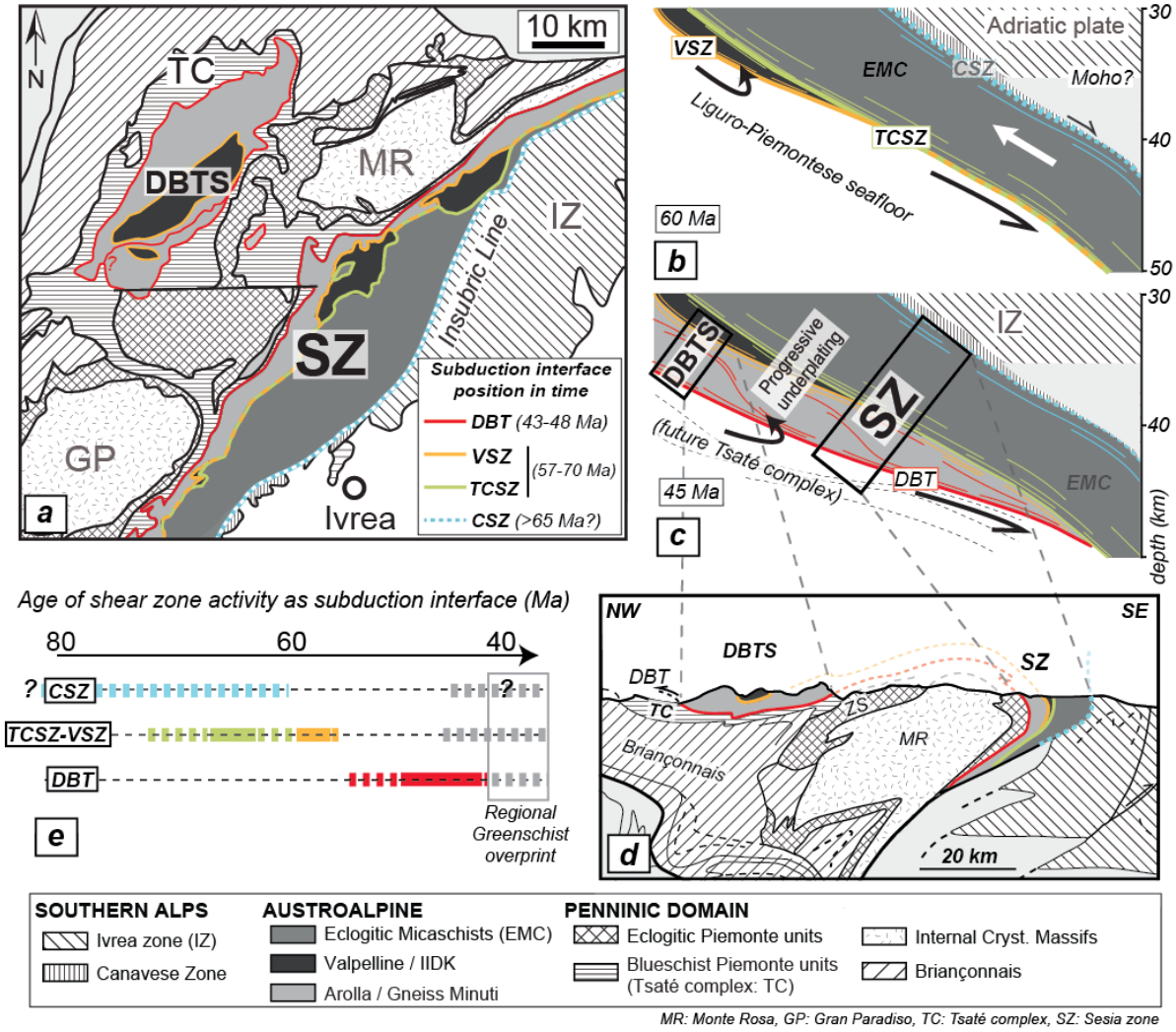

***Fig. 7**: Conceptual sketch depicting a structural evolution model for explaining nappe distribution and juxtaposition in the NW Alps internal metamorphic zones (Angiboust et al., 2014). **a**. Geological map of the studied region showing the trace of the Dent Blanche Thrust (DBT, red) and other blueschist-facies shear zones from the Sesia Zone, interpreted as ancient, transient subduction interfaces (modified from Beltrando et al., 2010). **b**. Cross-section showing the location of the Canavese (CSZ), Tallorno-Chiusella (TSZ) and Valpelline shear zones (VSZ) at 60 Ma. Note that the CSZ would have been active as a detachment fault at that time because of ongoing exhumation of the Eclogitic Micaschist Complex (EMC) slice. **c**. Cross-section of the Alpine plate-interface geometry at ca. 45 Ma showing the most plausible location of Dent Blanche*

Tectonic System (DBTS) and Sesia Zone (SZ) sections. Progressive underplating of continental slices led to significant thickening of the subduction channel and migration of the active subduction interface towards the lowermost structural level. ***d****. Simplified cross-section of the studied area localizing the present-day position of these ancient subduction interfaces (modified from Dal Piaz et al., 2003).* ***e****. Geochronological constraints on shear-zone activity in the DBTS-SZ area (references in Angiboust et al., 2014).*

In the Sesia-Lanzo zone, Gosso (1977) and Gosso et al. (1979) identified four Alpine deformation phases (D1-D4), on the basis of field interference structures and microstructures (see also Zucali et al., 2002). The D1 phase was coeval to the eclogite-facies event and produced an almost complete transposition, whereas D2-D4 are post-nappe deformation phases, which occurred at different steps of the retrogression or during the late mesoalpine greenschist-facies overprint.

4. The closure of the Tethyan basin and the structuration of the W. Alps internal zones

Geological reconstructions consider that the meta-ophiolites now exhumed in the internal zones of the Alps were geographically close to the European continental margin given their tight spatial correlation with exhumed eclogitized remnants of the continental margin (Beltrando et al., 2010 and references therein). In other words, the vast majority of the Tethyan basin seafloor got subducted in the mantle and has never been exhumed (e.g. Agard et al., 2009). When the last portions of the Tethyan oceanic realm were subducted below the Apulian margin, the thinned segments of the rifted European margin started entering the trench and follow the ocean-continent transition (OCT) zone into the subduction zone (Beltrando et al., 2010; Bonnet et al., 2022 and references therein). Several decades of field and petrological investigations have confirmed that the European margin got subducted down to various depths, from blueschist facies conditions (e.g. Briançonnais, Vanoise) down to eclogite facies for the internal crystalline massifs (Gran Paradiso, Monte Rosa, and Dora Maira; Chopin, 1984; Gasco et al., 2013 and references therein). Geochronological studies have demonstrated that some of the deepest subducted slivers (namely the UHP Dora Maira Brossasco-Isasca unit; **Fig.8**) have been exhumed along the subduction interface/channel as fast as several cm per year as indicated by zircon U-Pb dating (Rubatto & Hermann, 2001; Compagnoni et al., 2012). It remains a matter of discussion whether the burial and exhumation of meta-ophiolitic bodies has been disconnected from the (fast) uplift of UHP continental margin units. While Lapen et al. (2007) consider that the internal crystalline massifs may have contributed to the exhumation of the large volumes of eclogitized oceanic crust, recent geochronological data question this model (Angiboust & Glodny, 2020; Bonnet et al., 2022). Indeed, exhumation-related overprint of eclogitic meta-ophiolitic massifs in the epidote blueschist facies (1.5 GPa) has been dated at 38-36 Ma (multi-mineral Rb-Sr method; Angiboust & Glodny, 2020), which corresponds to an age at which Dora Maira UHP unit was not yet reached peak burial conditions (35 Ma; 3.5 GPa). Overall, further studies are needed to better decipher the dynamics of coupling and juxtaposition of oceanic and continental tectonic slices during the transition between oceanic and continental subduction, as suggested by the complex interlayering visible in the Dora Maira complex (Henry et al., 1993; **Fig.8**) or in the Gran Paradiso-Monte Rosa area (**Fig.3**).

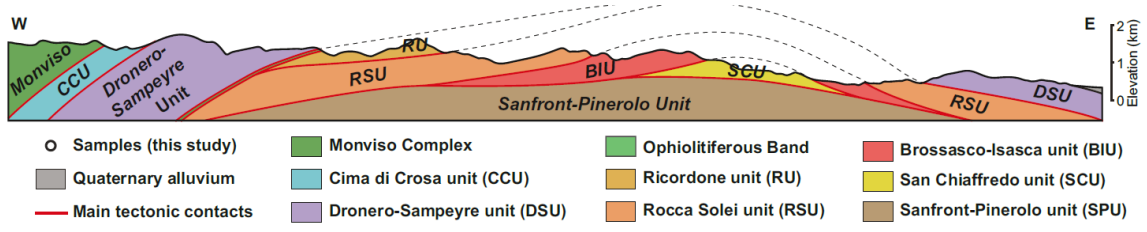

Fig. 8*: Cross section across the Dora Maira massif showing the complexity of tectonic thrust sheets imbricated in this massif (from Bonnet et al., 2022).*

During ongoing convergence in the Oligocene and collision with the thick European margin, a proper collisional orogen developed in the western and northwestern Alps including (i) the formation of an antiformal stack of high pressure rocks in the internal zones, (ii) a stack of nappes progressively younging from east to west (iii) the west-ward transport over large distances of continental and sedimentary nappes (Briançonnais, Pre-alps, and the Dauphinois nappes) and (iv) the development of foreland molassic troughs (Rosenbaum & Lister, 2005; **Fig.9**).

Some conventional elements typically visible in collisional belts are not or weakly represented in the Alps, such as the magmatic arc that is missing. Yet, the presence of an Oligocene magmatism has been documented by the Biella intrusive vs effusive complex (Callegari et al., 2004, with refs.) and minor volumes of Oligocene andesitic dykes crop out in the Sesia zone region (Dal Piaz et al., 1979; Venturelli et al., 1984). Some andesitic clasts are found in the Eocene basins an Ruffini et al. (1997) described volcanic clast-rich turbidite in the Oligocene Taveyanne sandstones (Savoie, France). This point will be discussed during the first day excursion.

The Alpine collision may not be fully over yet as indicated by the active seismicity monitored, in particular on the regions surrounding the Penninic front (the main contact that separates the internal zones from the external zones), where normal-faulting focal mechanisms are common associated with vertical motion of internal domains (e.g. Sue et al., 1999). From the Jura fold-and-thrust belt to the French Riviera area, west directed thrust faults accommodate the recent thickening of the Outer zone. Strike-slip faults in the Belledonne External crystalline massif accommodated the southeastward extrusion of the southern part of the Western Alps.

As a conclusion, the western Alps belt provide a unique opportunity to document the evolution of a convergent system from an oceanic subduction stage (well preserved along the Grenoble-Torino transect) to continental subduction stage (well visible in the Aosta valley region) until full continental collision which is more developed further east in Switzerland and Austria. The Alps are thus constituted by a series of imbricated wedges passing from an oceanic accretionary wedge that developed in the late Cretaceous until an orogenic wedge that formed from the Eocene until today (**Fig.9**). The lack of pervasive collisional overprint in the Western Alps makes this area a perfect natural laboratory for understanding deep-seating petrological and tectonic processes related with the HP-LT subduction event, from paleo-seismicity to fluid flow and subduction interface rheology.

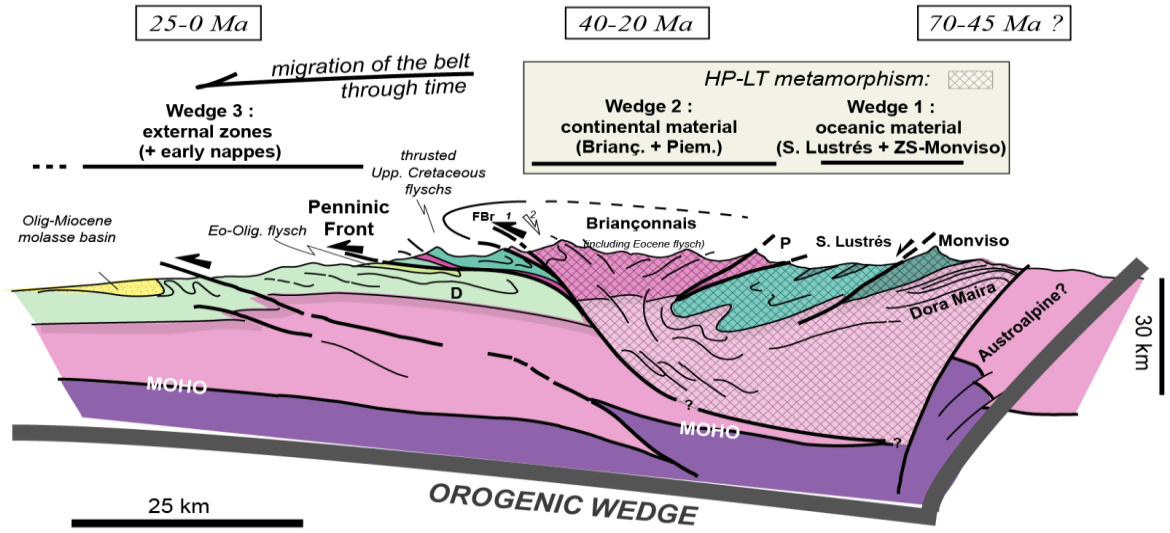

Fig. 9: Simplified cross section (passing through the Grenoble-Monviso transect) revealing the diachronism of the structures and detrital deposits, showing the imbrication of units at various scales, and the evolution from the inner oceanic accretionary wedge to a wedge involving continental material, until the formation of a crustal-scale orogenic wedge. P: Piemontese metasediments; ZS: Zermatt-Saas; D: Dauphinois; FBr: Briançonnais Front; 1: initial thrust movement across the FBr; 2: extensional reworking of the FBr from 20-15 Ma onwards. Modified after Agard & Lemoine, 2005.

FIELD TRIP 1:

Exhumed remnants of eclogitized continental margins

(*Lower Aosta valley* – Sesia zone)

Please note that sampling is not allowed at any of the stops.

1. INTRODUCTION

This half-day field trip is located at Montestrutto, a small village set near the entrance of the Aosta Valley and at the nearby Ivozio locality, in the very core of the Eclogitic Micaschists Complex, a sub-unit of the Sesia Zone that was also the subject of the 10th IEC Syn-conference Excursion (Compagnoni et al., 2014). During this field trip, after reviewing the most common HP paraschists, eclogites and orthogneisses of the Eclogitic Micaschists Complex, we will mainly focus on the Ivozio Metagabbro Complex. This Complex is one of the main pre-Alpine mafic complexes of the Sesia Zone, and was first described by the late Ugo Pognante (Pognante, 1979; Pognante et al., 1980). It consists of different types of eclogites with minor chlorite-bearing amphibolites and metaultramafites, interpreted as the products of Alpine metamorphic re-equilibration and polyphase deformation after Devonian-Carboniferous arc magmatism (Delleani et al., 2018; Vho et al., 2020).
The excursion will take place at very-low altitude along easy paths.

The Sesia Zone
The Sesia Zone (also known as the Sesia-Lanzo Zone) is the most easterly unit of the axial belt of the Western Alps. It is bounded by the Insubric Line (locally called External Canavese Line) to the east, the Piemonte Zone to the west, and the Lanzo Ultramafic Massif to the south (**Fig. 10**). The Sesia Zone is a composite unit that consists predominantly of Palaeozoic continental basement similar to the Ivrea Zone, which is an equivalent block in the Southern Alps. The Ivrea zone is characterized by Permian amphibolite- to granulite-facies metamorphism and lacks Alpine overprint. Within the Sesia Zone, a Mesozoic sedimentary cover is locally found (Venturini et al., 1994); it underwent Alpine metamorphism together with the basement rocks (Compagnoni et al., 2014 with refs.). A post-metamorphic volcano-sedimentary cover of Oligocene age crops out close to the Insubric Line (Ahrendt, 1969; Kapferer et al., 2012; Zanoni et al., 2022; with refs).
Various subdivisions of the Sesia Zone have been suggested (e.g. Venturini et al., 1994; Babist et al., 2006; Regis et al., 2014), but the classical four sub-units, as defined by Compagnoni et al. (1977) and subsequent update by Pognante (1989) on the grounds of metamorphic grade and prevalent rock types, are used below: Eclogitic Micaschists Complex (EMC), Gneiss Minuti Complex (GMC), Second Diorite-Kinzigit Complex (IIDK), and Rocca Canavese Thrust Sheets Unit (RCTU).
Focusing on the Eclogitic Micaschists Complex (EMC), it consists of a polycyclic basement comprising paragneisses, minor metamafic rocks, orthogneisses and impure marbles (Compagnoni, 1977; Compagnoni et al., 2014, with refs.). This basement is intruded by abundant Palaeozoic granitoids and minor gabbros (e.g. Bussy et al., 1998; Rubatto, 1998; Rubatto et al., 1999), which are present also to the south (Rebay & Spalla, 2001; Rebay & Messiga, 2007). Granitoids are dominant in the northeastern part of the Sesia Zone; they are traditionally labelled "Sesia Gneiss" (Dal Piaz et al., 1972). A probably Mesozoic sedimentary cover, with monometamorphic paragneiss, carbonate schist and locally manganiferous impure quartzite, is found in the central part of the EMC, along the Aosta Valley (Venturini et al., 1994). The EMC reached maximum pressures less than 2 GPa at temperatures lower than 600 °C (e.g. Tropper et al., 1999; Tropper & Essene, 2002; Zucali et al., 2002). To the NW, in proximity of the Gneiss Minuti Complex, pervasive, greenschist-facies assemblages overprint the eclogite-facies parageneses of the EMC (e.g. Dal Piaz et al., 1972, Compagnoni et al., 1977; Konrad-Schmolke & Halama, 2014; Giuntoli & Engi, 2016).
Polyphase deformation related to the Alpine tectonic evolution has been documented in detail, both in the external and internal parts of the Western Alps (e.g. Passchier et al., 1981; Zucali, 2002; Babist et al., 2006; Giuntoli et al., 2018). The Sesia Zone was exhumed as a coherent HP-terrain, but it comprises at least three continental nappes. The evidence gathered strongly suggests that the pre-orogenic structure at lithospheric scale fundamentally affects where, when and how HP-rocks are formed. Recent studies have discovered

unexpected complexities in the kinematic evolution of the Sesia Zone (Rubatto et al., 2011; Regis, 2012; Regis et al., 2014), with some tectonic slices having experienced substantial pressure cycles at eclogite-facies conditions ("yo-yo tectonics", see also Compagnoni et al., 2014 for a discussion).

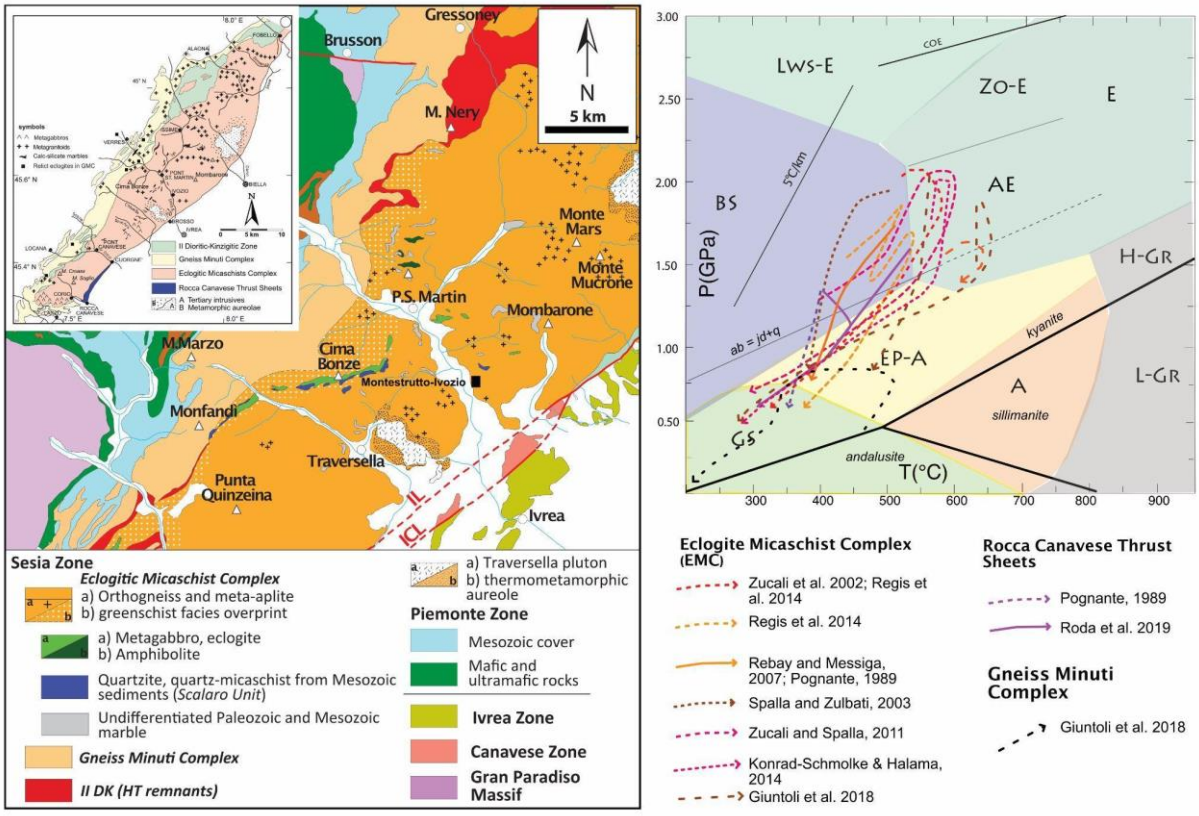

***Fig. 10**: Geotectonic map of the central Sesia Zone and adjoining units along the lower Aosta Valley. The square locates the Montestrutto-Ivozio area (modified after Regis et al., 2014); inset: Sesia Zone overview, with the main subdivisions. P-T-paths of the Sesia Zone, for Eclogitic Micaschist Complex, Rocca Canavese Thrust Sheets Unit and Gneiss Minuti Complex.*

Stop 1.1 - EMC at the Montestrutto cliff (*45.53858° N, 7.84067° E)*

<u>Paraschists, eclogite boudins, layers of leucocratic orthogneiss and HP metamorphic veins</u>

This stop is located along the cliff of Montestrutto, a hamlet of the nearby Settimo Vittone village (**Fig.11**). The three-hundred-meters cliff, initially popular in the 1980s for bouldering, today includes some 120 bolted routes that develop on walls with a height ranging from a few meters up at 80 meters (https://www.montestrutto.it/la-falesia/).

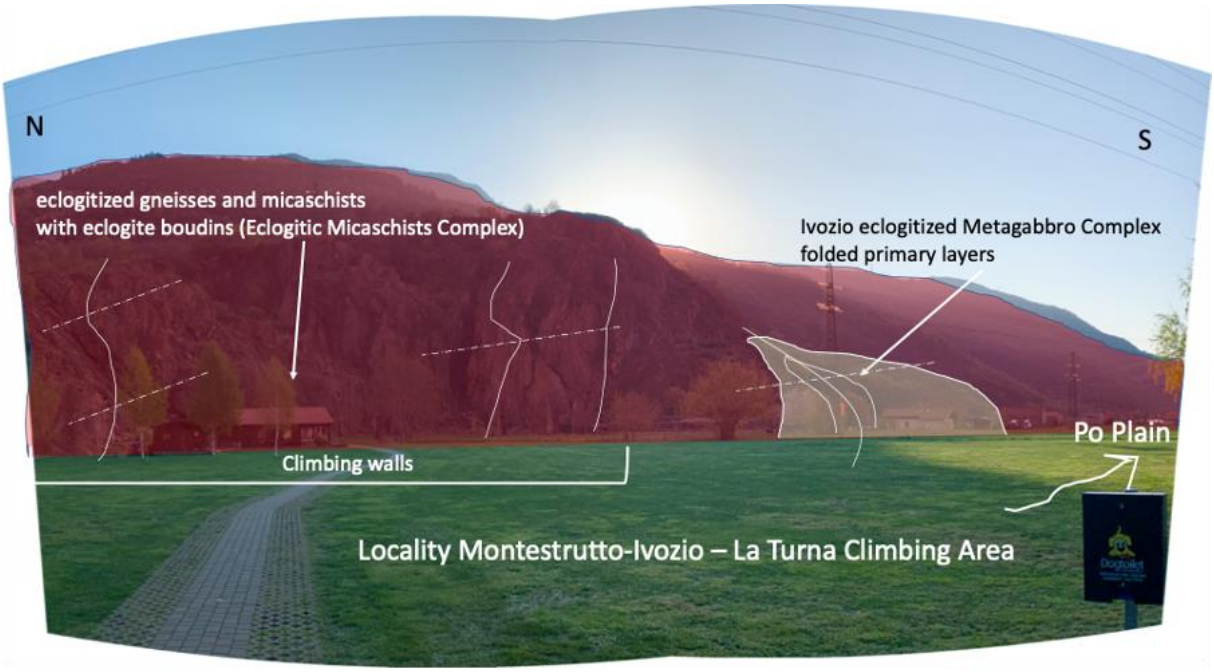

Fig.11: *Geologic overview of the EMC at the Montestrutto cliff and relations with the Ivozio Metagabbro Complex.*

The most frequent lithology is a banded, medium- to coarse-grained, phengite paraschist with garnet, pale-green omphacite ± finer-grained, dark-blue glaucophane and accessory rutile, apatite and zircon. The main foliation is defined by both phengite and omphacite, and the banded fabric reflects a wide range of relative modal proportions and grain sizes. Isoclinal folding and transposition are responsible for the nearly-parallel association of dm-thick layers of leucocratic orthogneiss with the darker paraschists. These latters often include cm- to dm-thick boudins of garnet omphacitite and glaucophane eclogite, with coarse-grained, idioblastic omphacite and finer-grained garnet and glaucophane (**Fig.12**). Refolded, dm-thick, quartz veins with minor phengite, coarse-grained rutile and local carbonate rhombohedra are also common.

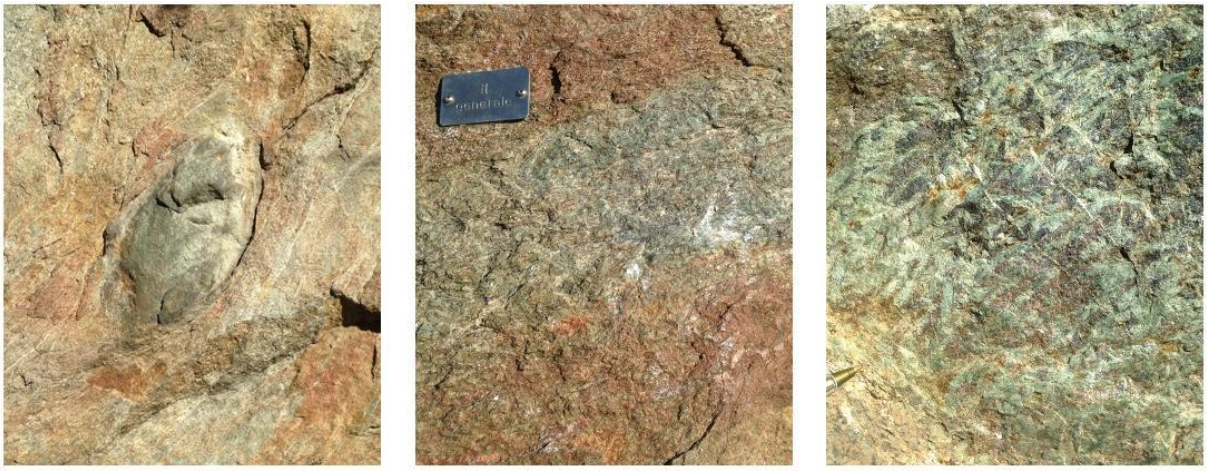

Fig. 12*: Outcrop images of the eclogite boudins wrapped within eclogitized paraschists at Montestrutto.*

On the very top of the cliff, a m-thick, leucocratic orthogneiss layer (not to be visited during the excursion) displays megablasts of very-pale-green-grayish jadeite (~ Jd_{95}, ca. 5 cm across) that are coarser-grained at the very contact with the country paraschists. Contrary to the widespread orthogneiss bodies derived from Permian granitoids such as the well-known Monte Mucrone metagranitoids (e.g. Compagnoni & Maffeo, 1973; Oberhänsli et al., 1985; Zucali, 2011), this layer, together with a thicker and refolded one on the same side of the valley (medium-grained, homeoblastic, and quarried as "Verde Argento"), are leucomonzogranitic in composition and Silurian in age (Liermann et al., 2002). The leucocratic, "Verde Argento" orthogneiss consists of quartz, jadeite, K-feldspar, phengite ± minor garnet and glaucophane, with

accessory Al-rich titanite, metamictic allanite, zircon, apatite, and scanty fluorite, Fe-sulphide and carbonate. Locally, jadeite is surrounded by a thin retrogression corona mainly consisting of albite (Compagnoni et al., 2014).

Stop 1. 2 - The Ivozio Metagabbro Complex (*45.53531° N, 7.84537° E)*

Amphibole-bearing eclogite

This stop is located at the base of the Ivozio village vineyard terraces.
The Ivozio Metagabbro Complex consists of amphibole-bearing eclogite, lawsonite/zoisite-bearing eclogite, amphibole-epidote-bearing eclogite, quartz-bearing eclogite, chlorite-bearing amphibolite, and ultramafites (**Figs.13-15**). Five Alpine deformation phases occur (D1 to D5) and consist of folds, foliations and shear zones. They developed during the Upper Cretaceous to Eocene subduction-exhumation path. The metamorphic mineral assemblages related to the deformation stages indicate a polyphase deformation, started with a prograde evolution under blueschist to eclogite-facies conditions, followed by a blueschist retrograde re-equilibration (D4), and discrete late shearing (D5) under greenschist-facies conditions. In addition, four veining stages developed under eclogite- to blueschist-facies conditions.

Amphibole-bearing eclogite, with medium- to fine-grained blue-green amphibole, and garnet eclogite with minor omphacite, phengitic white mica and zoisite constitute the main lithologies. A spaced S1 foliation marked by garnet trails and amphibole-rich layers occurs. Localized brittle veins occur, related to the growth of cm-sized omphacite. Locally, the S1 foliation is deflected along cm-thick shear zones, where blue-green amphibole occurs. S1 foliation is folded, with meter wavelength, during the D3 deformation phase. Zoisite- and blue-amphibole-bearing veins postdate S1 foliation and D3 folding.

In this eclogite type amphibole-, garnet- and omphacite-rich layers frequently alternate. This layering, transposed parallel to D1 axial planes, is mapped as S1. The boundary between juxtaposed layers can be transitional or discrete and locally is marked by mm-thick epidote-rich layers. The gradual transition between amphibole- and garnet-rich layers can result from the metamorphic transformation of a poorly deformed original igneous layering. At the meso-scale these alternating layers do not show mineral Shape Preferred Orientation (SPO).

Amphibole-rich layers are composed of medium- to fine-grained blue/blue-green amphibole (50-70%), garnet (15-30%) and omphacite (10-30%). Amphibole has blue rims around blue-green coloured cores and is fine-grained. Garnet is pinkish, and fine-grained with rare poikiloblasts of cm-size. Green omphacite occurs in medium-grained crystals, up to cm-long, and as fine-grained, 1 to 3mm long needles.
Garnet rich layers contain medium- to fine-grained garnet (60-80%), blue-green amphibole (40-20%) and omphacite (5%). Garnet is pinkish, medium-grained, and locally in poikiloblasts. Amphibole is blue-green and fine-grained; rare acicular omphacite is fine-grained.

Omphacite-rich layers generally lie between amphibole- and garnet-rich layers. These layers are composed of medium- to coarse-grained omphacite (40-60%), amphibole (20-30%), white mica (15-25%) and garnet (5%). Omphacite is coarse-grained, up to cm-size, with emerald green colour. Amphibole is fine-grained, with blue-green colour, and occupies the interstices between omphacite and white mica. White mica is medium- to coarse-grained, up to cm-size, and is pale-grey with silky sheen. Rare pinkish, fine-grained, garnet crystals occur. Omphacite and white mica crystals are randomly oriented in these layers.

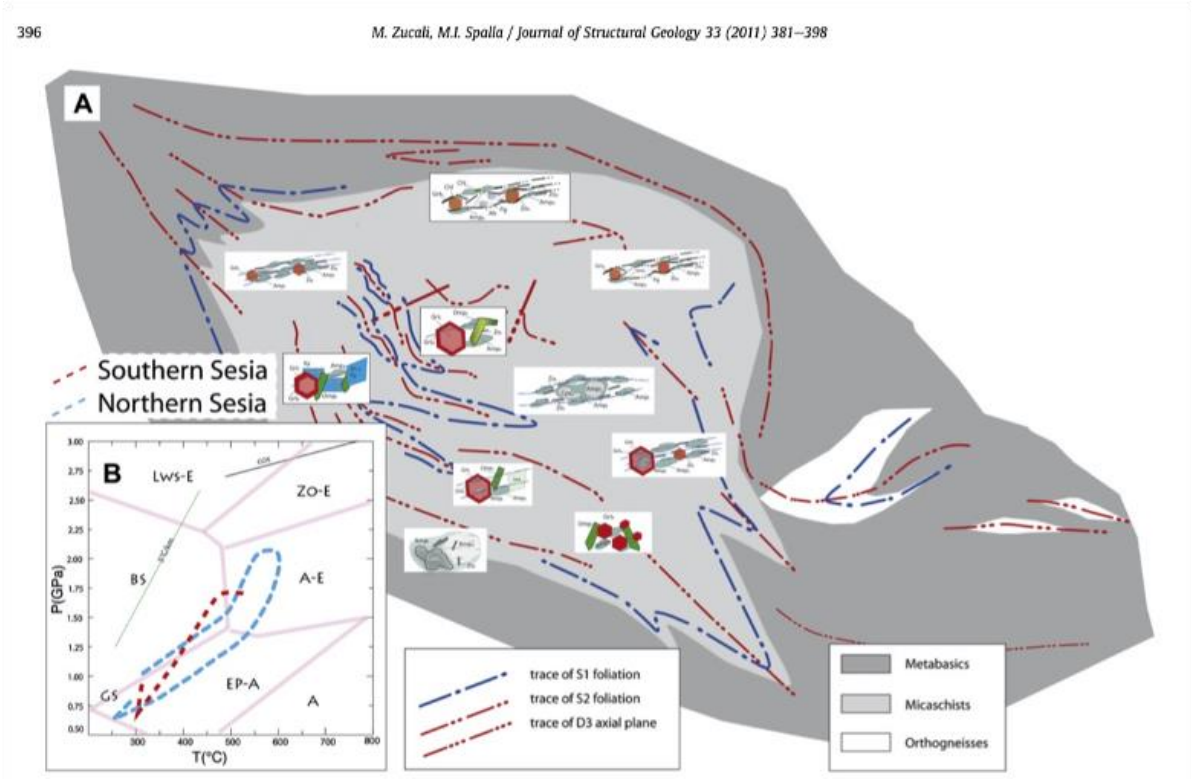

***Fig.13**: Simplified structural and metamorphic map of the Ivozio Metagabbro Complex (A) and P-T-t-d paths of the Northern and Southern Sesia-Lanzo Zone (B).*

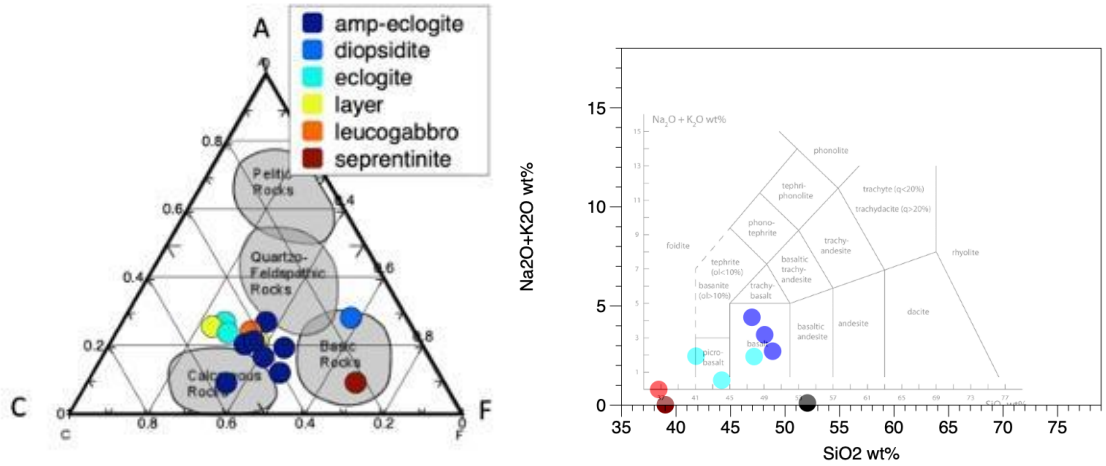

***Fig.14**: ACF and TAS plot of bulk-rock chemistry analyses for main Ivozio Metagabbro lithologies.*

Fig.15*: Outcrop images of amphibole-bearing eclogites showing mm- to cm-thick omphacite (upper left and right images). Garnet-rich trails parallel to S1 are locally cut by garnet-veins (lower left) or zoisite-veins (lower right).*

Stop 1.3 - The Ivozio Metagabbro Complex (*45.53643° N, 7.84617° E)*

<u>Lawsonite-bearing Eclogite</u>
This stop is located within the vineyard terraces.
Lawsonite crops out within layered bodies of zoisite-bearing eclogites alternate with amphibole-bearing eclogites. Lawsonite occurs as lozenge-shaped mm-thick individuals, layered at cm-scale (**Fig.16,17**). Lawsonite-rich layers alternate with white zoisite-rich mm-thick layers. Layers and mineral foliation is named S1 as it results from the prograde deformation path. The S1 foliation is here folded at cm- to dm-scale during D2. D2 developed under eclogite facies conditions and locally developed an axial planar foliation marked by SPO of omphacite.

In general, zoisite-bearing eclogites contain at least 30% (vol.) of white zoisite. They are medium- to coarse-grained rocks constituted by zoisite (30-60% vol.), blue amphibole (15-35% vol.), white mica (15-25% vol.), garnet (10-20% vol.), omphacite (10-20% vol.) and quartz (5-15% vol.). Zoisite is medium- to coarse-grained,

up to cm-size and tabular-shaped. Blue amphibole is fine- to medium- grained. White mica is medium-grained, pale-grey phengite and silver white paragonite. Garnet is reddish and medium- to coarse-grained, with up to cm-grain size. Coarse-grained emerald green crystals omphacite are up to 5 cm in length. Quartz is fine-grained and occurs within mm- to cm-thick lenses. Locally these rocks contain up to 10 cm porphyroblasts of garnet and up to 35% of white mica. Chlorite, epidote, rutile, titanite and albite are accessory minerals. These eclogites generally preserve textural relics of lawsonite, as prismatic coarse-grained domains, up to 3 cm in length, pseudomorphosed by whitish aggregates of zoisite + paragonite. Locally these domains are bluish and made by kyanite, testifying the replacement of lawsonite, as described by Zucali et al. (2004) and Zucali & Spalla (2011). Coarse-grained zoisite, white mica and blue-amphibole show Shape Preferred Orientation parallel to S1; lawsonite pseudomorphs are preferentially aligned within S1. In places S2 marked by fine-grained omphacite, white mica and zoisite wrap around pseudomorphosed lawsonite porphyroblasts and around omphacite and garnet large-sized porphyroblasts (3-10 cm).

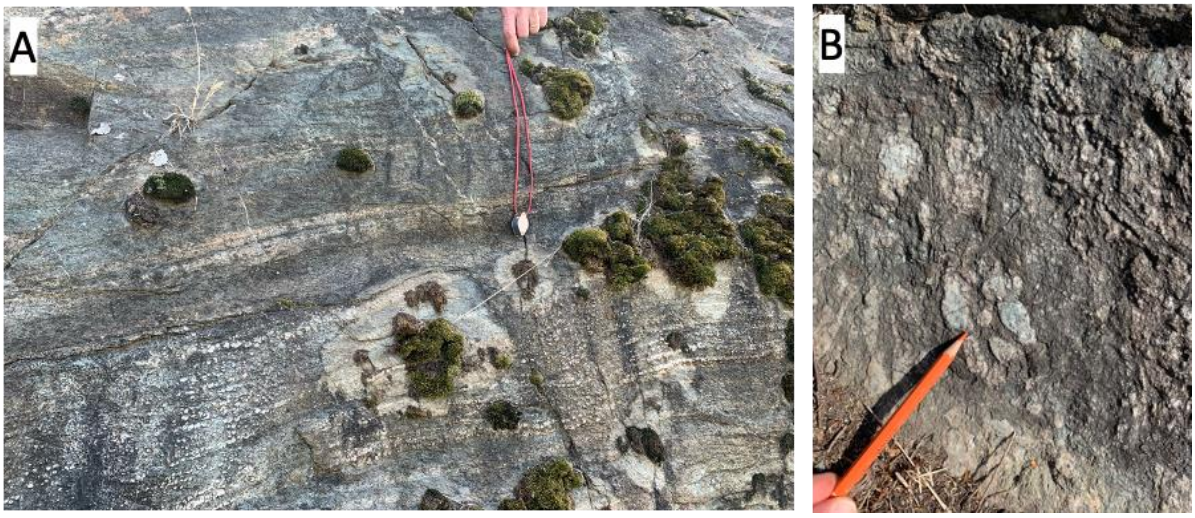

***Fig.16**: Outcrop images of the lawsonite/zoisite eclogites. (A) S1 foliation defined by lawsonite-rich layers locally replaced by zoisite-rich aggregates. (B) cm-sized lozenge-shaped lawsonite replaced by kyanite showing a light blue color.*

Stop 1.4 - The Ivozio Metagabbro Complex (*45.53545° N, 7.84660° E)*

<u>Lawsonite-bearing Eclogite</u>

This stop is located within the Ivozio vineyard terraces.

At this last stop, lawsonite displays the typical bluish replacement to lawsonite, testifying the prograde reaction *lawsonite => kyanite + zoisite + H2O* in association with omphacite, as described by Zucali et al. (2004) and Zucali & Spalla (2011) (**Fig.18**). Lawsonite mm- to cm-sized individuals generally display whitish replacement commonly due to zoisite ± paragonite, here few grains preserve their shape and clearly display the pale blue color due to the kyanite substitution.

The S1 foliation developed during prograde blueschists to eclogite facies conditions, while the kyanite-bearing pseudomorphs likely occurred at peak eclogite conditions, before retrogression. Retrogression is generally marked by paragonite-rich replacement of lawsonite. Where replacement is volumetrically significant, the SPO of paragonite also defines the pervasive foliation.

Close to this stop, quartz-rich eclogites occur. *Quartz-bearing eclogites* have ≥ 30% (vol.) quartz. They contain zoisite (30-50% vol.), quartz (30-50% vol.), omphacite (20-40% vol.) and white mica (5-15% vol.), and are coarse-grained. Zoisite occurs in coarse-grained (up to 3cm) prismatic white crystals, quartz is medium- to fine-grained and occurs within cm-thick lenses, omphacite is emerald green and coarse-grained (locally up to 5cm in length), and white mica is pale-grey. Blue amphibole, garnet, chlorite, epidote, rutile, titanite and albite are accessory phases. Quartz-bearing eclogites mainly show a 5-cm-spaced discontinuous S1 foliation marked by SPO of coarse-grained zoisite and white mica, and by lenticular quartz domains. Minor volumes record cm-spaced discontinuous S2 foliation marked by medium- to fine-grained zoisite and white mica wrapping around large omphacite porphyroblasts (3-5 cm) and quartz elongated lenses.

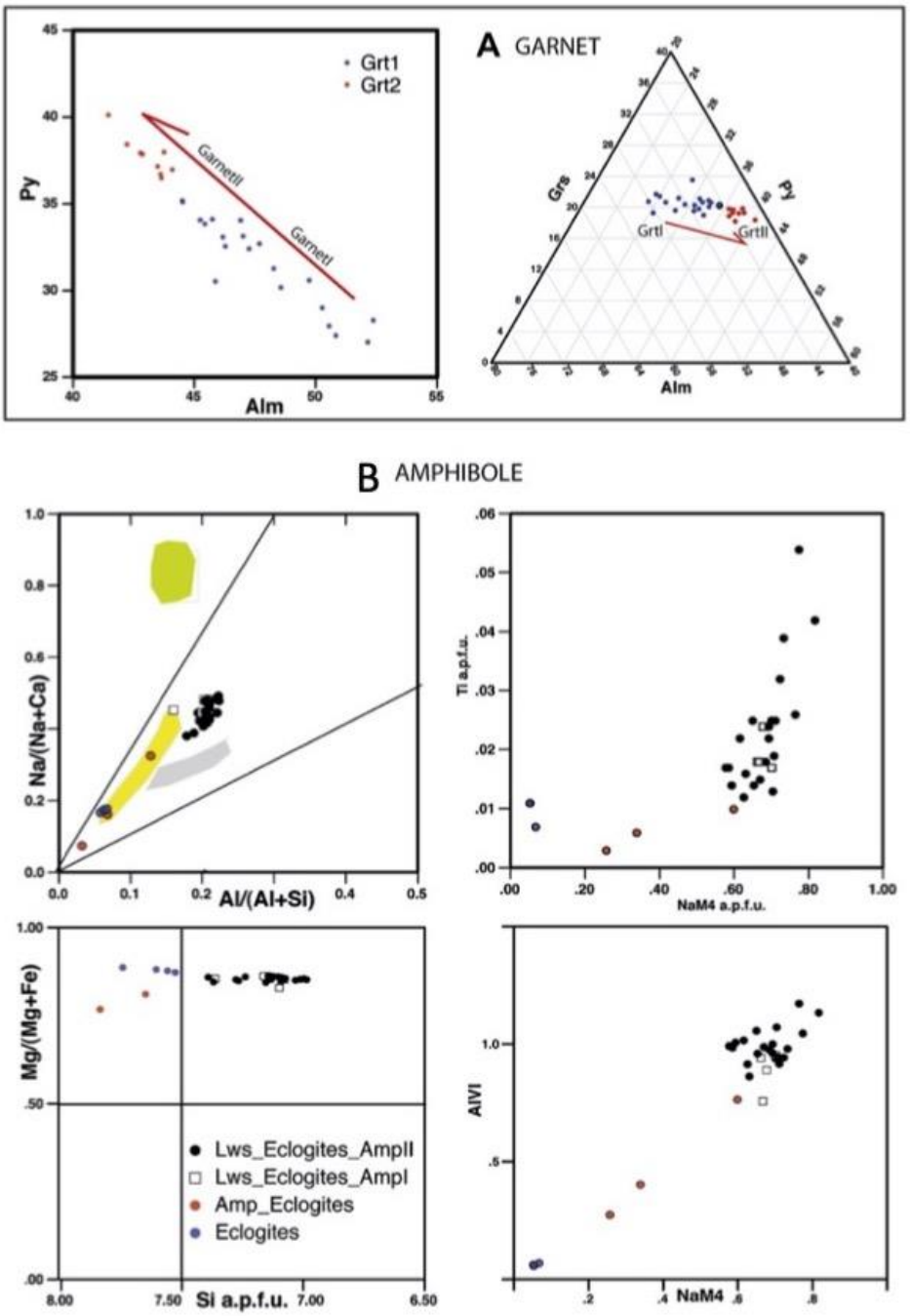

***Fig. 17**: Mineral chemistry diagrams showing chemical variations with respect to microsites occurrence. A) Garnet compositional variation (Alm, Py, Grs). B) Minerochemical variations of amphibole within lawsonite-bearing eclogites, Amp-eclogites and eclogites.*

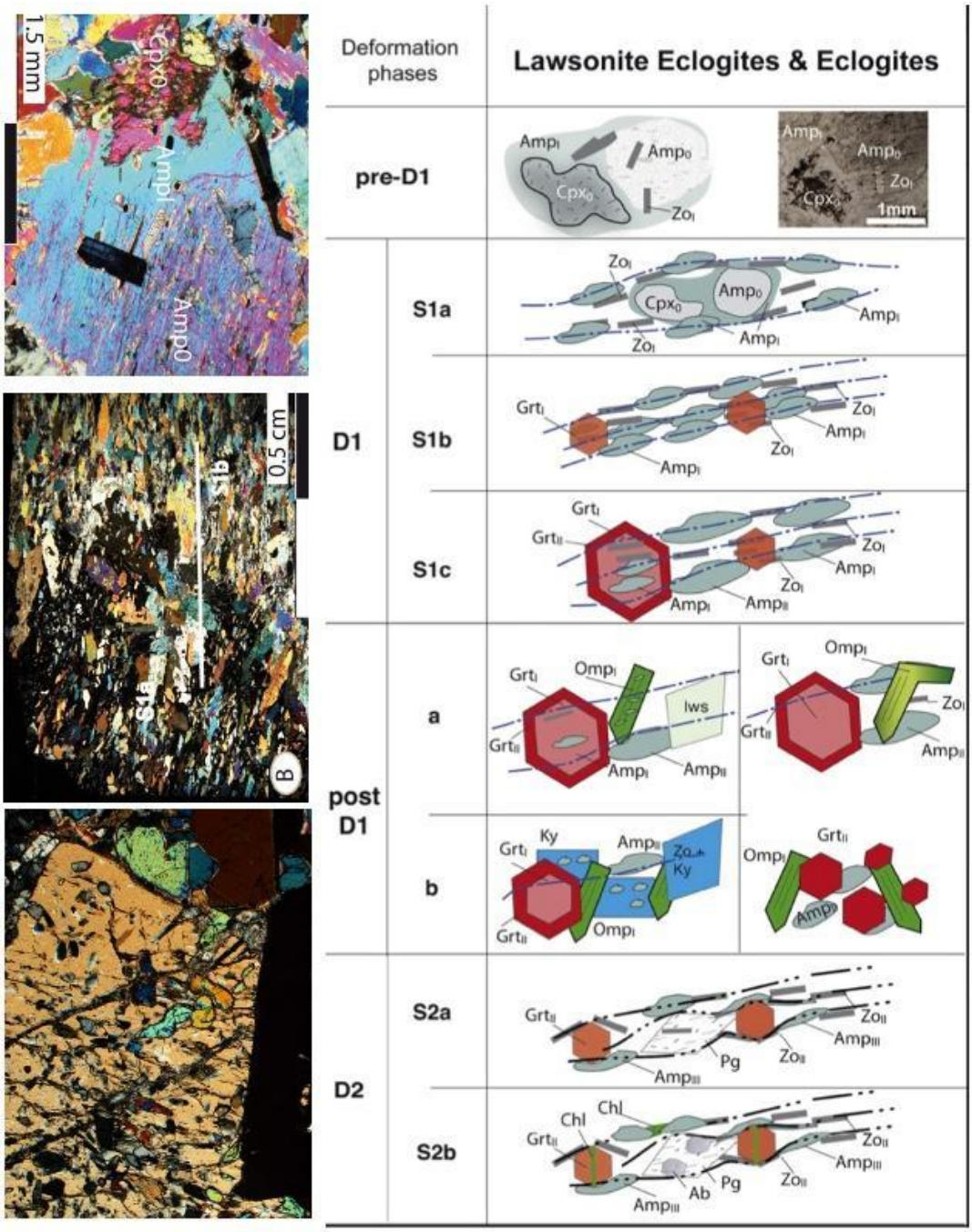

***Fig.18**: Microstructural and petrographic evolution of the lawsonite-bearing eclogites.*

FIELD TRIP 2:

A journey inside a hydrothermal field subducted in the eclogite facies

(*Saint Marcel Valley, Zermatt-Saas zone*)

The aim of this short excursion is (i) to (ii) observe some of the typical eclogite-facies lithologies from hydrothermally altered oceanic rocks and the Cu-Fe- and Mn- ores in the St. Marcel valley, a dextral tributary valley of the Aosta Valley.

NB: this excursion will involve a whole day in the field, walking along paths at altitudes between 1600 and 1900 m.a.s.l. Please bring appropriate equipment, i.e. proper shoes, warm clothes, water bottles and sunscreen.

Please note that this is a protected area and it is forbidden to collect samples.

1. *Localization of the excursion, tectonic framework and itinerary*

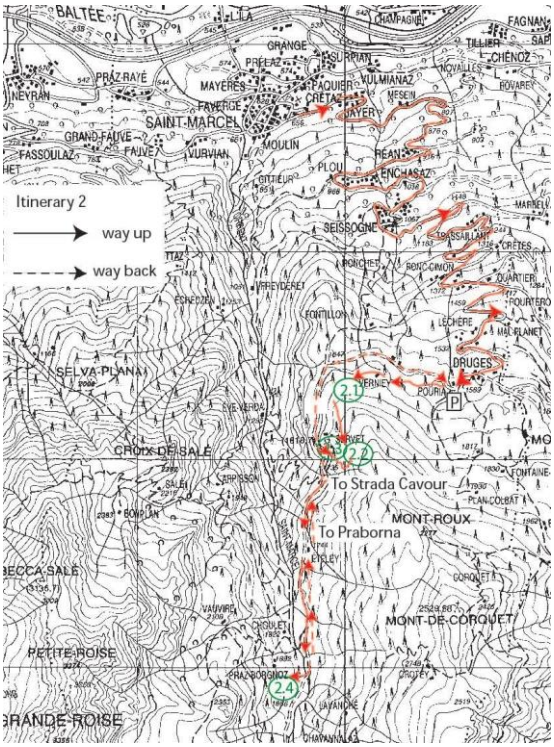

This excursion proposes the visit to Servette and Praborna mines (**Fig.19**), both deriving from ocean floor hydrothermal activity, and presently preserving HP imprints acquired during Alpine orogeny. Servette mine is a Cu_Fe sulphide deposit (mainly pyrite and chalcopyrite) hosted in garnet-bearing quartzite, within lawsonite- chloritoid- garnet- bearing glaucophanites, chloritoid- garnet- bearing talc schists, and garnet chlorite schists.

Similar rocks are found near the Mn-bearing ores of Praborna, which is by far the most important and famous occurrence worldwide of Mn-rich HP minerals. It is the type locality for several rare Mn minerals: violan, a semiprecious violet-blue Mn-bearing clinopyroxene, piemontite, the manganic epidote, alurgite, the Mn-bearing variety of muscovite, that are found in the ores together with braunite, Mn-garnets, rhodonite, rhodochrosite, to mention a few.

Fig.19: *Itinerary of day 2 excursion.*

The structure of the Zermatt-Saas meta-ophiolite in the Saint-Marcel valley and Monte Avic massif is generally characterized by a N-S-trending lineation parallel to the axes of isoclinal folds related to a D1 deformation phase that occurred under eclogite facies (visible within garnet), reworked by a D2 shearing deformation phase and a D3 under retrogressed conditions, having axes parallel to D1 one characterized by open folds (**Fig.20**). The subduction and exhumation histories are here testified by prograde relics, such as pseudomorphs after lawsonite, eclogite-facies assemblages and by greenschist-facies assemblages indicating retrogression. Peak PT conditions for the Servette (and Praborna) rocks have been suggested to be 540 ± 30°C and pressures in the range 2.1 - 2.5 GPa (Angiboust et al., 2009; Rebay & Powell, 2012). Recent in situ Sm-Nd garnet dating has shown that the garnet cores grew at 46.9 +/- 1.6 Ma (at PT conditions

of c.500°C and 1.85 GPa) while the rims inferred to have grown at peak conditions yield an age of 43.5 +/- 1.3 Ma. From this P-T-t data, an extremely cold and steep paleo-thermal gradient of c.3°/km can be estimated between 60 and 80 km in the late Eocene (Dragovic et al., 2020).

2. *Servette*

The Saint-Marcel eclogite-facies meta-ophiolite, making part of the Zermatt-Saas unit, are overthrust by the Austoalpine Monte Emilius klippe continental slice. The uppermost section of this metaophiolite, well exposed at Servette, consists of interlayered chlorite schists, talc schists, glaucophanite, quartzite, rodingite and slices of eclogite-facies metagabbro and serpentinite (**Fig.20**).

Servette is the site of a Fe-Cu sulfide deposit that has been interpreted as the product of extensive hydrothermal alteration of the seafloor. The rocks underwent eclogite-facies metamorphism, but eclogites sensu stricto (omphacite-garnet rocks) are rare at Servette. Interlayered glaucophanites, chlorite schists, and talc schists are the dominant lithologies (Castello, 1981; Cartwright & Barnicoat, 1999; Martin et al., 2008; Rebay & Powell, 2012).

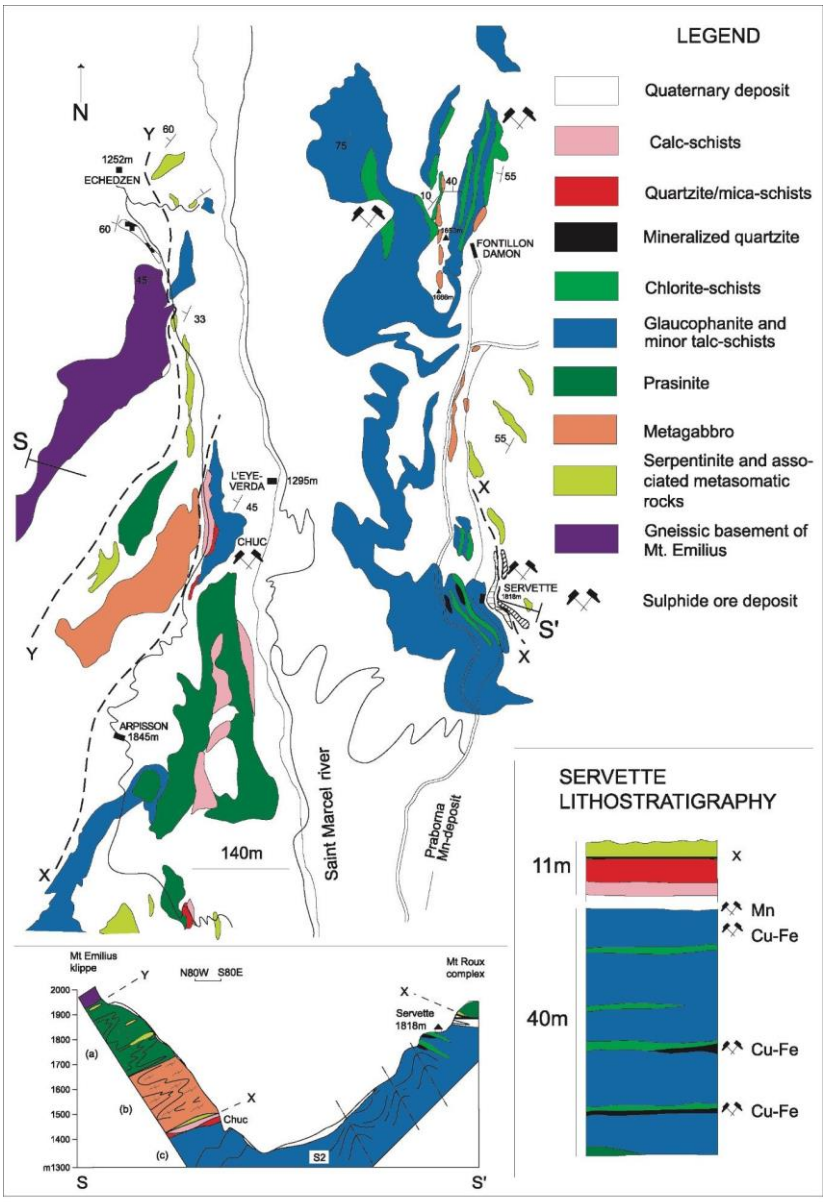

These different rock types have been attributed to different styles of hydrothermal alteration. The talc schists were considered as evidence of up-flow zones in black smoker-type environments, whereas the glaucophanites and chlorite schists formed in zones of downward, up-temperature, pervasive, fluid flow (Cartwright & Barnicoat, 1999; Martin et al., 2008). Cu-Fe sulphide ore at Servette includes pyrite, chalcopyrite with accessory sphalerite, bornite, pyrrhotite, neodigenite, marcasite, mackinawite, and rare native copper (e.g., Tartarotti et al., 1986; Krutow-Mozgawa, 1988; Martin et al., 2008; Rebay & Powell, 2012; Dragovic et al., 2020).

Fig. 20: *Map of Servette ridge (from Martin et al., 2008).*

The deposit occurs between 1717 and 1890 m of altitude. It is concentrated in two major ENE-dipping layers of 3-4 m in thickness, and some minor levels (less than 1 m) located at the boundary between chlorite

schists and glaucophanite, but it is also disseminated in the surrounding rocks. The Servette mine was exploited during the ancient times, probably in the Middle Ages, as testified by the slag dating (1120±40 BP; Tumiati et al., 2005) and the existence of old excavations (Lorenzini, 1998). Recently, a Roman melting site dating first century after Christ has been discovered near the dated slag deposit (Castello e Cesti, 2017).

Martin et al. (2008) proposed a polymetamorphic evolution for Servette, starting with ocean-floor metamorphism followed by Alpine prograde blueschist facies toward peak eclogite-facies metamorphism at 550-660°C and 2.1 ±0.3 GPa. P-T-peak conditions at P=2.3 GPa and T=540 – 560°C were proposed by Dragovic et al. (2020) using garnet isopleths. Two cm-sized garnet crystals from Servette were dated using Sm/Nd. Garnet cores were dated to 46.9 ±1.6 Ma, signifying an approximate age for the initiation of garnet growth. Garnet rims were dated to 43.5 ±1.3 Ma, signifying the timing of peak metamorphism. These ages agree with the ^{40}Ar-^{39}Ar age of 42 Ma obtained from alurgite of the Servette quartzite (Dal Piaz et al., 2001).

The extent of greenschist-facies retrogression is variable at Servette (Martin et al., 2008).

Stop 2.1 – Old foundry of Treves (*45.7074° N; 7.4572° E*; alt. 1672 m, **Fig.21**)

Similar blast furnaces have been known since the 15th century in the Alps. They were designated to produce iron, which therefore should have been a by-product of the nearby copper Servette mine. The Treves blast furnace was loaded by the top, through a path coming from the Servette mine (see the pillars that supported the catwalk). Layers of mineralized stones and carbon, used as combustible, were interlayered in the furnace. The process produced gas, iron-rich silicate slags and iron. Slags heaps are visible along the main road during the whole excursions. (Tumiati et al 2005; Castello & Cesti, 2017).

Fig. 21: *Old Treves foundry.*

Follow the pathway that climbs southwards in the woods towards the ancient mine of Servette. Along the path, some outcrops of magnetite-bearing serpentinite can be observed. At a fork, take the left branch of the way that leads to the uppermost level of the Servette mine, which was dug in sulphide-bearing meta-ophiolite. Cross the debris, where you can see several blocks of sulphide bearing garnet-quartzite, massive sulphide mineralization, and all lithologies typical of Servette, with dispersed sulphide or without them. Refer to the detailed descriptions of these rocks here below.

Stop 2.2 - Uppermost level of the Servette mine (*45.70185° N, 7.45545° E*, alt. 1820 m)

A few steps eastwards to the entrance of the uppermost gallery (*45.70098° N; 7.45565° E'*, alt. 1829 m), opened in glaucophanite and Mn-rich quartzite, cm-to-dm-thick layers that grade into carbonate-rich micaschists. This Mn-bearing rock is rich in alurgite (pink Mn-muscovite), yellow Mn-garnet, red piemontite or/and Mn-epidotes. The main schistosity dips 20-30° towards ENE. North of the entrance (*45.701022° N; 7.45563° E*), a rodingite (grossular-rich garnet + diopside + epidote**: Fig.22**) formed by metasomatism at the expense of a metagabbro, at the contact with an overlying serpentinite slice. Over this one, crops out the metaophiolite sequence belonging to the overlying Mont Roux rock complex, which is made of retrogressed metagabbro, prasinite and minor serpentinite.

Fig. 22: *garnet-diopside rodingite.*

Stop 2.3 – **Eclogitized oceanic hydrothermal ore of the Servette mine**

Descending from the top to the bottom, following the path to the left, there is the opportunity to see all lithologies of Servette. Outcrops are oxidized, but the compositional banding is observable. The best way to see the rocks is to look at the walls of the mine houses, which date from the last period of exploitation of the mine (1854-1950) and have been recently restored. Please refrain from sampling!

Below the mine house, several remnants of the exploitation are still visible: powder magazine, gallery entrances, tailings (Lorenzini, 1998; Zinetti, 2002), and you can enjoy wonderful rocks in the walls and outcrops along the path.

Servette rocks are rather heterogeneous, and the main lithologies may be summarized as follows:

(a) Sulphide-bearing quartzite (**Fig.23a**) forms thin layers. Pyrite, chalcopyrite, magnetite, garnet, cummingtonite and blue amphibole (crossite) are the major minerals besides quartz (Martin &Tartarotti, 1989; Tartarotti & Caucia, 1993). Sulphides may include silicates, but garnet in turn includes sulphides and amphibole.

(b) The ore assemblages, hosted by glaucophanite, chlorite schists (**Fig. 23b**), talc schists and quartzite, consist of sulphides and oxides: pyrite (FeS_2), chalcopyrite ($CuFeS_2$) with minor sphalerite (ZnS_2), bornite (Cu_5FeS_4), other secondary sulphides such us digenite (Cu_9S_5), pyrrotine, marcassite, mackinawite ($(Fe,Ni)_9S_8$) (Natale, 1969; Gruppo ofioliti, 1977; Castello, 1979; Castello et al., 1980), native copper (Jervis, 1873), rutile, ilmenite, hematite and magnetite. Chalcopyrite generally defines “flames” in pyrite, or it borders earlier pyrite suggesting exsolution. Occasionally, earlier pyrite has been observed inside ilmenite. Chalcopyrite and sphalerite may crystallise later as interstitial phases and fill fractures of garnet. Bornite has been observed only as small crystals inside pyrite. Ilmenite is observed both in the main foliation and in cores and rims of zoned garnet crystals. It includes rutile and exsolved ilmeno-hematite, which were generated after the eclogite peak. In the matrix, ilmenite may show hematite rims.

(c) Chlorite schists (**Fig.23c**) have chlorite, garnet, quartz, ±talc, ±chloritoid, ±crossite, ±paragonite and accessory sulphides, rutile, epidote, ilmenite, all aligned along the main foliation. These rocks display S1 planes (schistosity) and C-planes (shear planes), outlined by large flakes of primary chlorite, and which intersect each other at about 35°. The C-planes coincide with the main foliation of the associated glaucophanite. Garnet occurs as zoned euhedral porphyroclasts up to 1 cm in diameter, with inclusion trails (ilmenite, apatite and epidote) occurring in the core, whereas rare inclusions of rutile, crossite and chloritoid are observed in the rim. Chloritoid forms cm-sized porphyroclasts elongated along the schistosity and stretched grains along the C planes. It is often replaced by secondary chlorite. Rare blue amphibole (crossite) crystals show rims of blue-green secondary hornblende (barroisite).

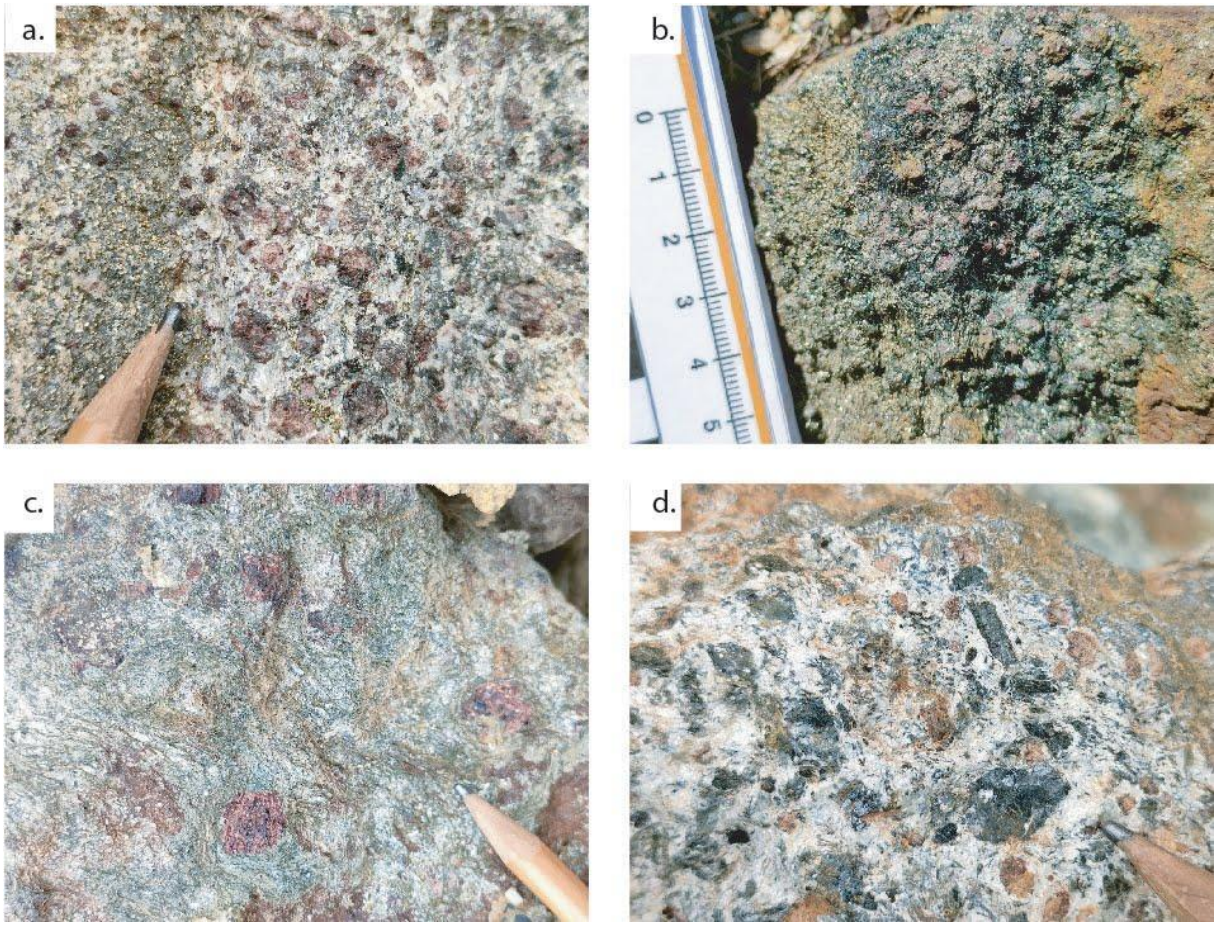

Fig. 23: *a) sulphide- garnet- bearing quartzite; b) mineralisation in chlorite schist; c) chlorite schist; d) chloritoid bearing talc schist.*

(d) In talc schists (**Fig. 23d**), cm-sized zoned garnet crystals, characterized by pink core and red rim, and large, dark, chloritoid porphyroclasts up to 5 cm long are immersed in a fine-grained talc matrix. Only rutile and quartz occur as inclusions in garnet cores, whereas chloritoid and talc also occur in rims. Garnet, glaucophane, chloritoid, rutile and sulphides are irregularly disseminated in the matrix. Chloritoid shows chlorite + paragonite rims that are due to a retrograde reaction such as chloritoid + glaucophane = chlorite + paragonite. Glaucophane is rare and not retrograded.

Fig. 24: *Pseudomorphs after lawsonite in glaucophanite.*

(e) Glaucophanite (**Fig.24**) is composed of glaucophane, garnet, chloritoid, epidote, paragonite and accessory phengite, rutile, magnetite and ilmenite. Glaucophane is strongly aligned in the main foliation and is microboudinaged parallel to the N-S trending lineation. Talc + magnetite ± albite and paragonite aggregates fill the stretching related fractures and glaucophane is rimmed by blue-green secondary hornblende. Garnet crystals show different sizes. The biggest, up to 5 mm in diameter, are zoned with core enclosing quartz and titanite. The inner rims include rutile, quartz, chloritoid, pseudomorphs after lawsonite, ilmenite and glaucophane elongated according to the outside main foliation.

In the outermost rims, which grew after the external foliation, inclusions are rare, as in the smaller unzoned garnet crystals of the matrix. Prisms with a lozenge- shaped basal section are frequent in this rock. They consist of zoisite, and/or clinozoisite, paragonite, ±calcite, albite and chlorite, and are interpreted as pseudomorphs after lawsonite.

Glaucophanite in contact with talc schists is generally characterized by absence of lawsonite, abundance of glaucophane and small garnet crystals, whereas the associated talc schists have abundant talc and large garnets. In these transitional rocks, chloritoid may reach 3-4 cm in length, and is generally inclusion-free (**Fig. 25**).

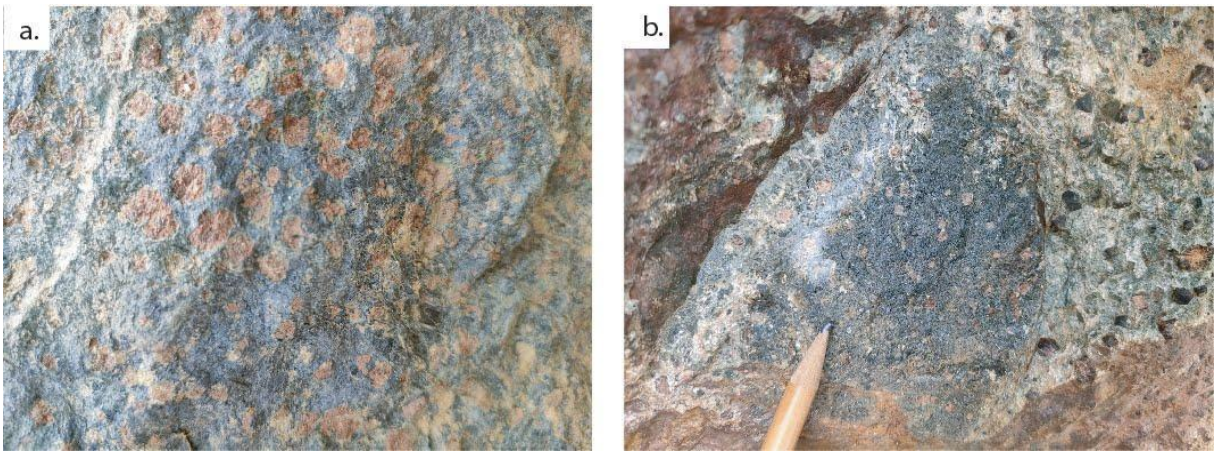

Fig. 25: *a) omphacite, glaucophane garnet rock; b) interlayering of chlorite schist (left) glaucophanite (center) and talc schist (right).*

(f) At times, Cr- and Mg-rich light-coloured flaser eclogite-facies metagabbro with cm-sized garnet porphyroclasts and large green Cr-rich omphacite are found in the debris, as well as omphacite bearing bands within glaucophanite.

(g) Micaschists and calcschists are interlayered rocks. The former may contain garnet and chloritoid, whereas the latter contain glaucophane and pseudomorphs after lawsonite.

The interlayering of glaucophanite, chlorite schists and talc schists (**Fig. 25b**) has been interpreted as resulting from hydrothermal oceanic alteration and deformation under highpressure metamorphic conditions of quartz-rich sediments, mafic and ultramafic materials (Martin & Tartarotti, 1989; Martin et al., 2008; Rebay & Powell, 2012). Thermodynamic modelling has been performed showing that all lithologies can be the result of HP metamorphism in compositions corresponding to those found in present day hydrothermally altered oceanic crust (Rebay &Powell, 2012; **Fig. 26**).

The metamorphic evolution of the Servette rocks can be summarized as follows (Martin et al., 2008). In quartzite, the presence of deerite and that of cummingtonite and crossite included in garnet evidence the early prograde evolution. In glaucophanite, this evolution is revealed by pseudomorphs after lawsonite and some relics of an early mineral assemblage preserved in garnet cores as inclusions of chlorite, lawsonite pseudomorphs, glaucophane, paragonite and chloritoid.

The main paragenesis in glaucophanite is characterized by the equilibrium assemblage garnet + chlorite + glaucophane + paragonite + talc. Martin et al. (2008) have estimated the peak metamorphic P-T conditions

for the main 3 different rocks (glaucophanite, chlorite schists and talc schists), as 550 ± 60°C and 2.0 ± 0.3 GPa.

Finally, greenschist-facies partial retrogression is testified by several observations: garnet is partially substituted by chlorite and quartz; chlorite and paragonite replace chloritoid and glaucophane.

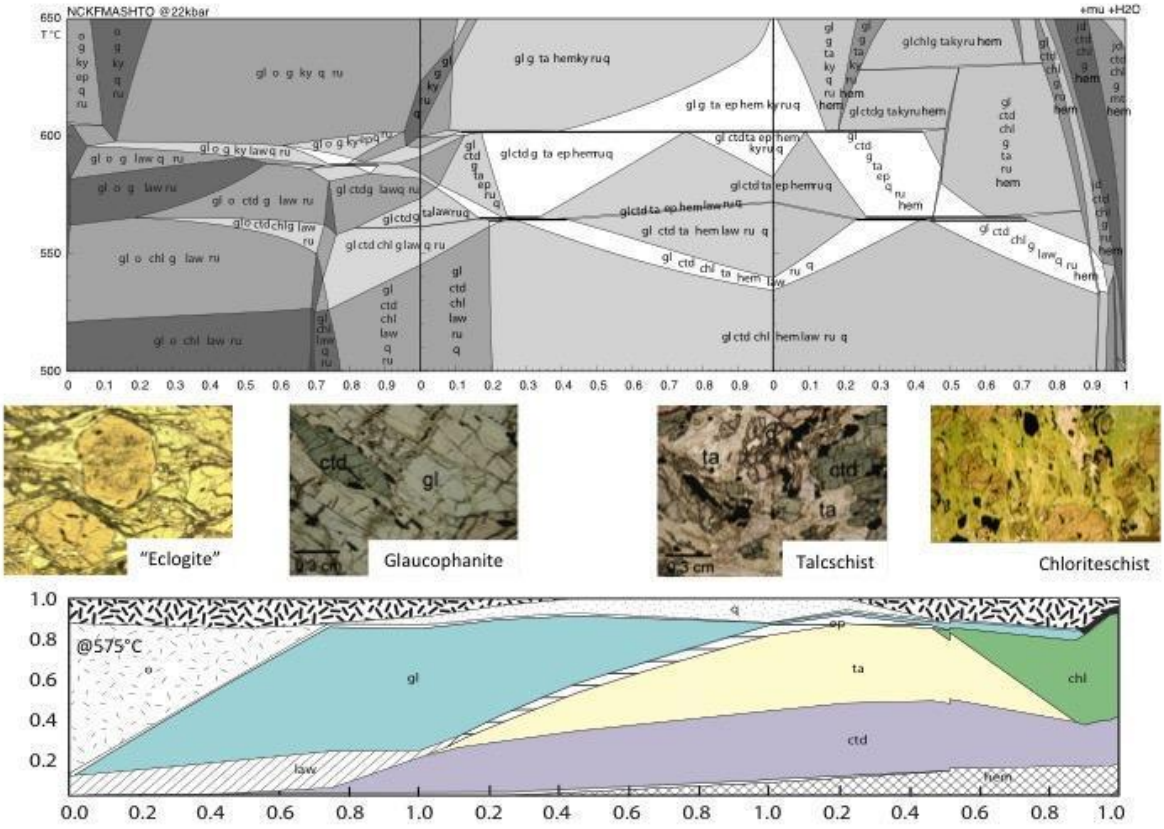

Fig. 26: *TX pseudosection (top) showing the parageneses predicted at P=2.2 GPa for compositions varying from that of unaltered MORB (to the left) to that of Chlorite schist (right), passing through glaucophanite and talc schist. The bottom diagram shows calculated modal compositions for the same rocks at 575°C (after Rebay & Powell, 2012).*

While descending please note the mine from antiquity (*45.7011°N ; 7.45467°E*, alt. 1792 m) a 7-8 m long cleft opened in the wall but partly hidden by debris. This cavity results from the excavation of a sulphide-rich layer. Because of the old-fashioned technique used, which has preserved part of the ore as pillars, Nicolis de Robilant (1786-87) and several authors after him attributed this excavation to the Roman and even pre-Roman (i.e., Celtic) times, without much proof.

Once you are back to the main path, head to Praborna (**stop 2.4**).

3. Praborna

The manganese mine of Praborna is known since at least 1415. This braunite (Mn_7SiO_{12}) ore was utilized for the glassmaking in Venice and in southern France. The mine was closed at the beginning of the 20th century. The most thriving time for the exploitation of the Praborna mine was probably the period between the mid 15th-century and the end of the 17th century. We know from the work of Antonio Neri *L'Arte Vetraria* (1612) that the manganese of Praborna was employed massively for the realization of the Venetian *Cristallo*

glass, whose innovation dated back to the middle of the 15th century. The *Cristallo* glass was an especially clear and colourless glass developed for luxury glassmaking in Murano, up to the development of the England lead-crystal in the late 17th-century. The addition of manganese to glass melt was practiced for centuries prior to Renaissance. Ancient glassmakers, on the basis of their practice, knew that the addition of Mn to melt decolourises glasses, minimising the colouring effect of accidentally introduced iron. On the other side, manganese was deliberately used to obtain colours ranging from purple-to-brown glasses, by controlling the oxygen fugacity in the furnace.

The Praborna ore, hosted in the Zermatt-Saas metaophiolites, has been interpreted as a hydrothermal Mn-oxide deposit embedded in cherts covering the Jurassic oceanic lithosphere of the Alpine Tethys, subducted to eclogite-facies conditions during the Alpine orogeny (e.g., Tumiati et al. 2010; **Fig. 27**). Hydrothermalism is likely constrained to Late Jurassic during an advanced stage of the opening of the Alpine Tethys, as demonstrated in the adjoining Aouliletta unit in the adjacent Cogne area (Toffolo et al. 2018). High-pressure metamorphic peak conditions of P = 2.1–2.3 GPa and T = 540–550, recorded in the nearby meta-ophiolite of the Saint-Marcel valley (Martin et al. 2008; Angiboust et al. 2009), are assumed to also represent the eclogite-facies peak conditions of the Praborna metacherts (Tumiati et al. 2015).

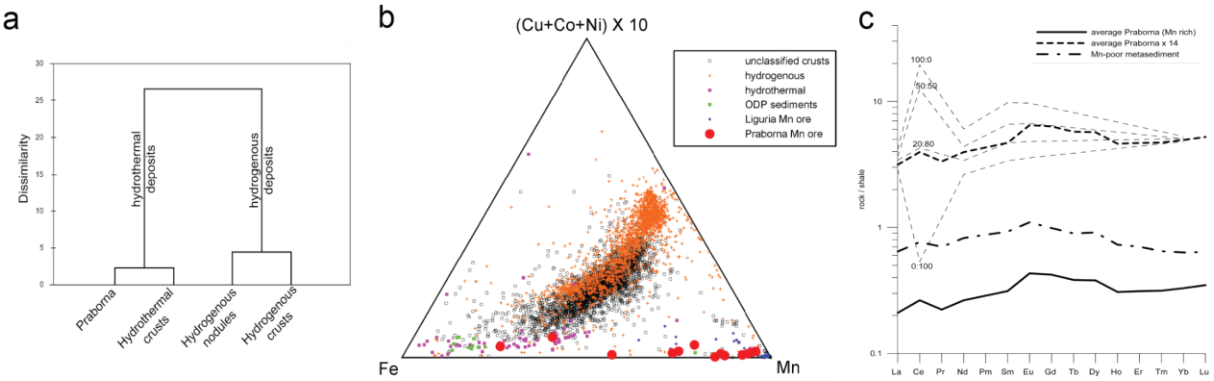

Fig. 27: *Hydrothermal origin of the Praborna ore (after Tumiati et al., 2010). a) Agglomerative hierarchical clustering comparing typical manganese deposits and Praborna Mn-rich rocks on the basis of their bulk composition; b) Mn–Fe–(Co + Ni + Cu)×10 ternary diagram of hydrogenous and hydrothermal Mn-rich deposits. Data of Praborna, Liguria ores and ODP sediments are displayed for comparison; c) Shale-normalized REE of the Praborna Mn-rich rocks. Thin dashed lines represent hypothetical mixtures of average hydrothermal and hydrogenous ferromanganese deposits; the first and second values in ratios represent the percentages of hydrogenous vs. hydrothermal, respectively. According to this model, Praborna REE composition is consistent with about 80% hydrothermal input.*

The Praborna Mn-deposit displays a continuous change in mineralogy from the basal levels in contact with lawsonite-bearing glaucophanite, partly retrogressed to greenschist facies, towards the upper levels in contact with Mn-poor metasediments (**Fig. 28, 29**). This layering is mostly due to an oxygen fugacity gradient between the strongly oxidized basal levels rich in braunite (mostly Mn^{3+}) and the less oxidized upper levels rich in Mn^{2+}-bearing minerals. The basal levels (ΔFMQ > +12.5; Tumiati et al. 2015) contain braunite ($Mn^{2+}Mn^{3+}{}_6(SiO_4)O_8$, the ore mineral), the epidote piemontite and a purple, Mn^{3+}-bearing semiprecious variety of omphacite called "violane" (**Fig. 30**), characterized by up to 64 mol% jadeite content (Tumiati et al. 2015). The upper levels are characterized by the assemblage garnet (spessartine–grossular ± calderite) + aegirine-rich clinopyroxene ± pyroxmangite, the high-pressure polymorph of $MnSiO_3$. Because of the strongly oxidized conditions, sulfides are not stable in any Mn-rich level. Therefore, chalcophile elements enter the structures of silicates and oxides, in particular ardennite-(As) (hydrous silico-arsenate of aluminum and manganese), hydroxycalcioroméite (calcium antimonate, Sb-rich pyrophanite ($MnTiO_3$) and rutile, and As-bearing apatite (Tumiati et al. 2015; **Fig. 32**). They also enter braunite, which contains

2500 ppm Co, 2000 ppm Cu and 1100 ppm Zn, and piemontite, with 450 ppm As, 450 ppm Ni and 360 ppm Zn (Tumiati et al. 2010).

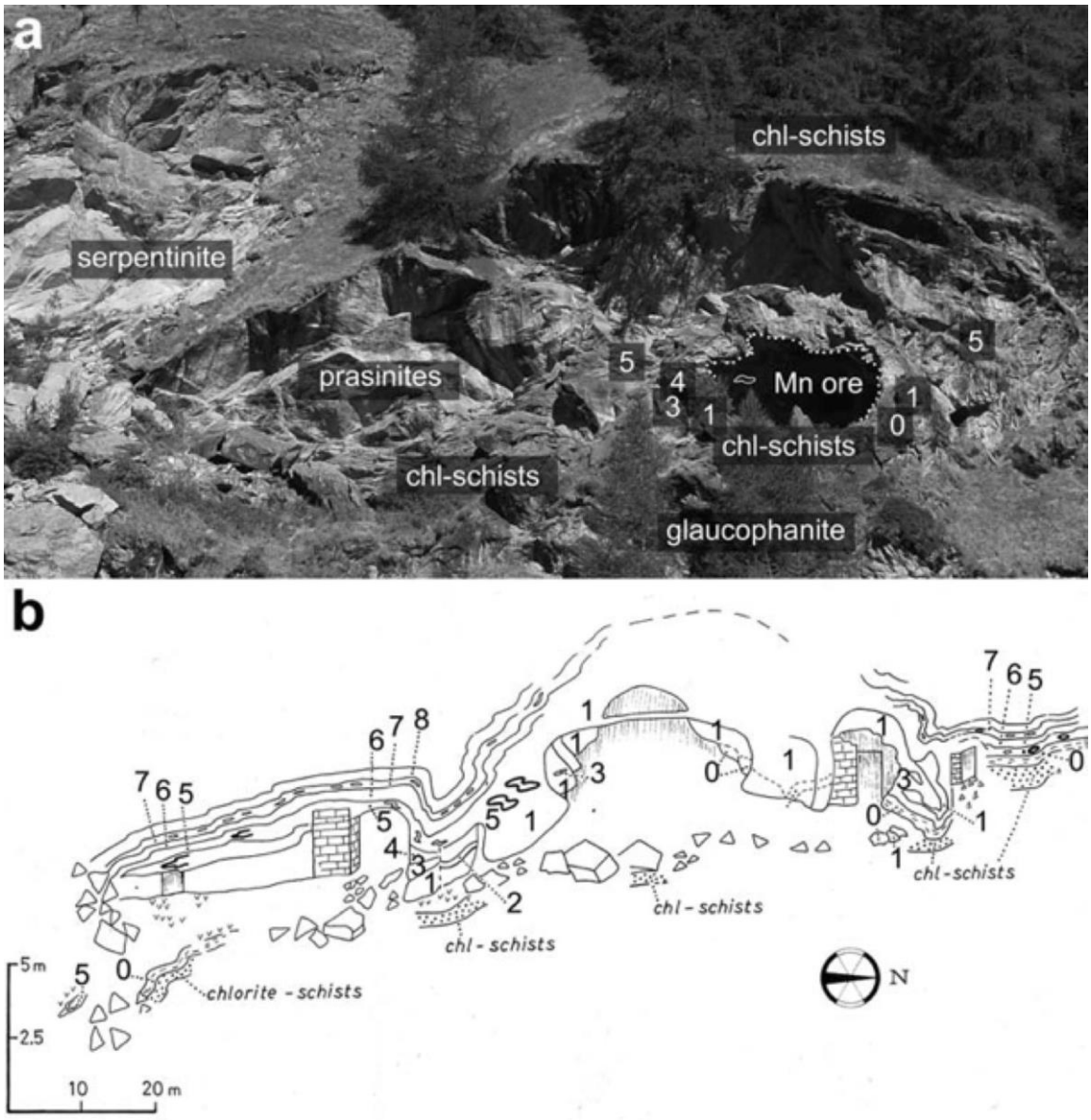

Fig. 28: *(a) Overview of the mine entrance; (b) schematic drawing of the typical sequence of levels constituting the ore. Level 0: this is the footwall of the Mn-rich ore in contact with the underlying garnet-bearing glaucophanite, partially retrogressed to prasinite. Micaschists and chlorite schists also occur; Level 1: the basal Mn-rich level is a massive braunite- and clinopyroxene-rich layer. The pyroxene is a violet Mn-bearing omphacite–aegirine-augite solid solution (i.e., ''violan''). Other minerals are: quartz, piemontite, clinopyroxene and phengite. This level is highly fractured and piemontite-sodic amphibole- jadeite-phengite-albite- phlogopite-quartz veins fill the fractures (Fig. 3); Level 2: this ore-body level is dominated by piemontite, braunite and quartz. Yellow layers of spessartine-rich garnet are common (Fig. 4 c). In late fractures, albite, microcline, piemontite, Na–Ca amphibole and barite occur. As and Sb minerals, such as ardennite and romeite, can be found as accessory minerals (Fig. 6); Level 3: This is a discontinuous emerald-green layer (10–20 cm), composed of quartz and Cr-bearing, aegirine-rich omphacite (Figs. 3, 4 b). This layer contains, e.g., native gold, Cr-rich epidote Cr-rich muscovite (fuchsite) and (Ca, REE) vanadates (Fig. 7); Levels 4, 5: These levels of Praborna contain calderite-rich garnet and minor hematite in a quartz-rich matrix (level 4). In some cm-thick layers, garnet grows together with a brownish aegirine-rich clinopyroxene (level 5) and dark-green Na–Ca amphibole; Level 6: This outer level (Fig. 4c) is composed of cm thick pinkish-orange*

boudins of quartz, pyroxmangite, strongly zoned garnet, and dark-coloured Mn-rich cummingtonite. Manganiandrosite-(Ce) and hematite occur as accessory minerals. Sb-rich pyrophanite developed after hematite; Level 7: The hanging wall of the ore, in contact with the country-rock, is composed of quartz, spessartine-rich garnet and Mn–Ca carbonates (rhodochrosite, kutnahorite). Some Na–Ca amphibole and secondary Mn oxides and chlorite are also present; Level 8: the contact country-rock is an eclogite/blueschist facies quartzite and quartz-rich micaschist.

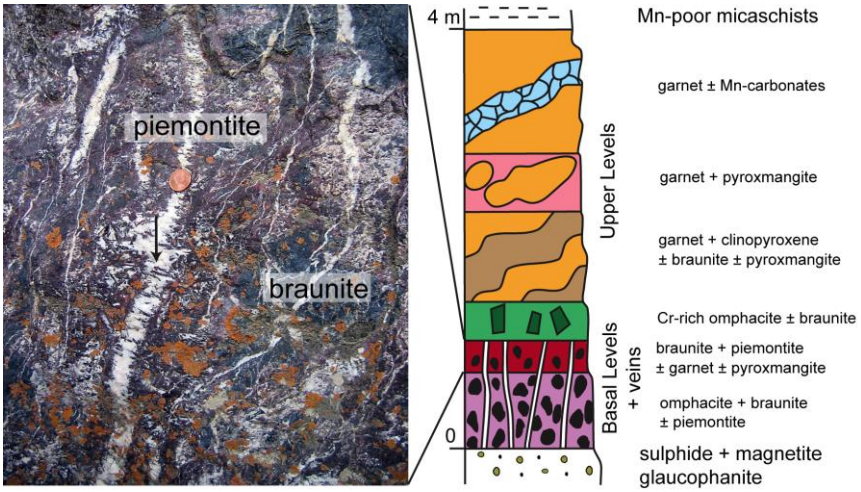

Fig. 29: *Schematic section of the Mn ore of Praborna (Tumiati et al. 2015). Basal levels are highly fractured and show pervasive veining. The enlargement shows a stockwork of quartz- and feldspar-filled veins cutting the massive ore mainly consisting of braunite (black) and piemontite (purple) (orange crusts are lichens). Note that the growth of "pegmatoid" piemontite crystals is perpendicular to the fracture walls (black arrow). Basal levels and veins contain omphacite in equilibrium with quartz and are in contact with glaucophanites. The upper part of the ore grades into garnet + quartz ± pyroxmangite assemblages, and is overlaid by Mn-poor micaschists.*

Fig. 30*: Details of the outcrops occurring at the mine entrance. (a) Mn-bearing omphacite "violane"; (b) emerald-green layer; (c) transition from basal braunite+piemontite to the upper garnet+pyroxmangite levels, folded and showing interference patterns.*

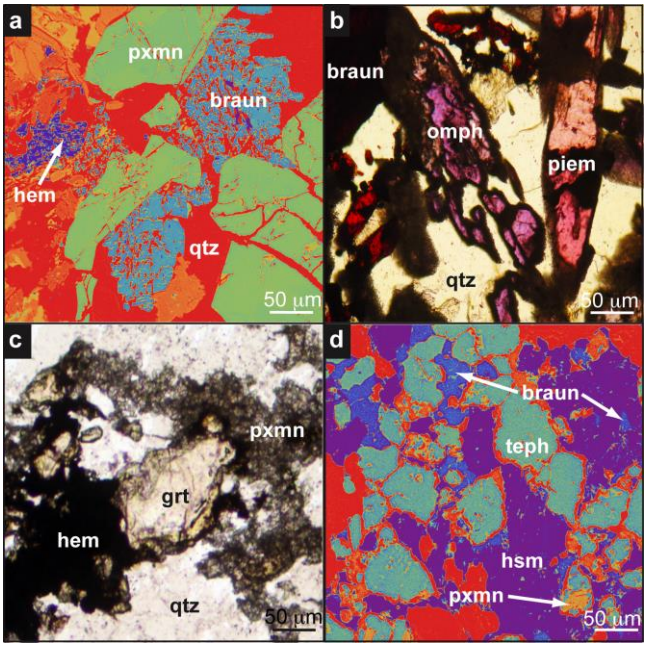

***Fig. 31**: Representative mineral assemblages characterizing the Mn ore of Praborna (Tumiati et al. 2015). (a) Colorized Back Scattered Electron (CBSE) image of braunite (blue), pyroxmangite (green) and hematite (violet) coexisting with quartz in the basal level. (b) Transmitted Light Photomicrograph (TLP) of the vein containing Mn-rich purple omphacite (violan) in equilibrium with quartz, braunite and piemontite. (c) TLP of hematite in equilibrium with garnet, pyroxmangite and quartz in the silica-rich assemblages of the upper level. (d) CBSE image of a quartz-free sample from the upper level, showing the replacement of pyroxmangite (yellow) + braunite (blue) by tephroite (blue-green) and hausmannite (violet). Rhodochrosite (red) forms as a late mineral.*

At Praborna, several minerals rich in rare earths have been described. Veins crosscutting the basal levels contain *REE*-rich piemontite, with maximum *REE* = 0.24 atoms per formula unit (a.p.f.u.) on the basis of 12.5 equivalent oxygens and Ce/La = 2.36 (Tumiati et al. 2015). In the upper levels, manganiandrosite-(Ce) occurs instead of piemontite as an accessory phase (Cenki-Tok et al. 2006). It is characterized by Ce/La = 8.53 and contains 1800 ppm Ni, 1680 ppm Zn, 1400 ppm Cu and 1400 ppm Co (Tumiati et al. 2010).
Between the basal braunite-piemontite-rich level and the upper garnet-rich levels, a dm-sized Mn-poor emerald-green layer (green in **Fig. 30**) contains vanadium-bearing, aegirine-rich omphacite (Jd_{70}) together with quartz. Accessory phases are Cr-rich phengite, Mn-rich epidotes bearing *REE* and Cr, Cr-bearing hematite and braunite, As-bearing apatite, native gold and the (*REE*, Ca)-vanadate wakefieldite (Tumiati et al., 2020; **Fig. 31**).

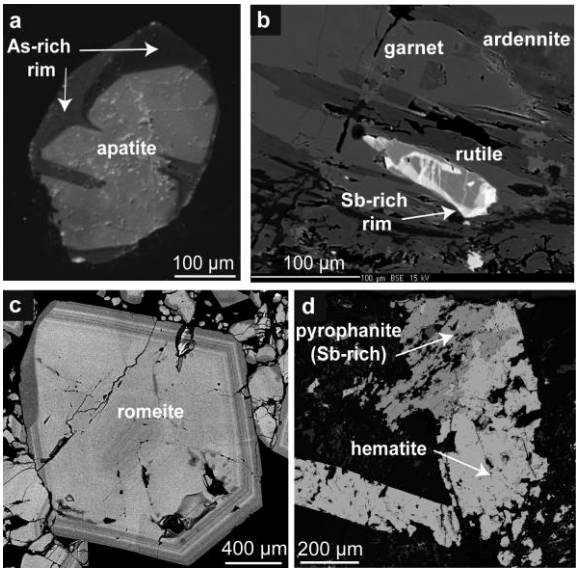

***Fig. 32:** As- and Sb-bearing minerals characterizing the parageneses of Praborna (Tumiati et al. 2015). (a) basal levels; zoned apatite crystal richer in As at the rim (cathodoluminescence image); (b) basal levels; ardennite-(As) $(Mn,Ca,Mg)_4(Al,Mg,Fe)_6(SiO_4)_2(Si_3O_{10})(AsO_4,VO_4)(OH)_6$ in equilibrium with garnet and rutile showing a Sb-rich rim (BSE image); (c) basal levels; romeite $(Ca,Fe,Mn,Na)_2(Sb,Ti)_2O_6(O,OH,F)$ showing oscillatory zoning (BSE image); (d) upper levels; hematite associated to Sb-rich pyrophanite ($MnTiO_3$) (BSE image).*

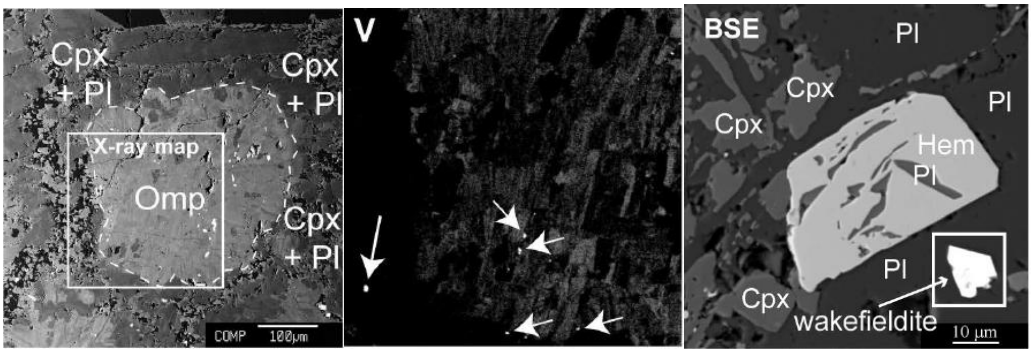

Fig. 33: Back-scattered electron and X-ray vanadium map of omphacite in the emerald-green basal level, delimited by dashed line, surrounded by retrograde symplectites consisting of Jd-poor clinopyroxene and albitic plagioclase. The tiny (REE, Ca)-vanadate wakefieldite occurs in symplectites as shown by arrows. Symplectites also contain minor hematite, phlogopite and K-feldspar. Rutile and apatite are present as accessory minerals. Epidote and braunite are peak eclogite-facies minerals involved in the wakefieldite minerogenesis (Tumiati et al. 2020).

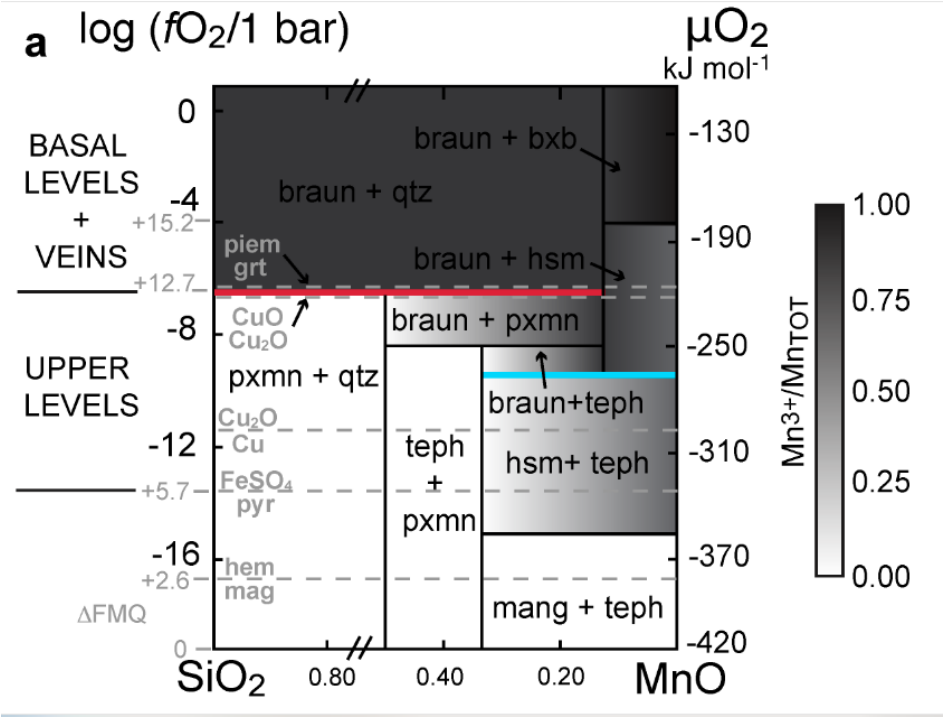

Fig. 34: Thermodynamic model of the phase stability of Mn minerals as a function of $SiO_2/(MnO+SiO_2$ and oxygen chemical potential, calculated for P = 2.1 GPa and T = 550 °C (Tumiati et al., 2015). Considered phases are: quartz (qtz); manganosite (mang); pyroxmangite (pxmn); tephroite (teph); hausmannite (hsm); braunite (braun); bixbyite (bxb); pyrolusite (not stable at these conditions). In addition to μO_2 (right vertical axis), the corresponding log (fO_2/1 bar) and ΔFMQ values (black and grey numbers, respectively, on the left vertical axis) are also reported for comparison. Dashed grey lines are the reference univariant equilibria piemontite = garnet + H_2O + O_2, $CuO = Cu_2O + O_2$, $Cu_2O = Cu+O_2$, $FeSO_4$ = pyrite + hematite + O_2, hematite = magnetite + O_2, and magnetite + quartz = fayalite + O_2. The red and blue horizontal lines indicate the associations quartz–braunite–pyroxmangite (basal levels) and braunite–haussmanite–tephroite (upper levels), respectively. Shaded fields represent in gray scale the ratio Mn^{3+}/Mn_{tot}.

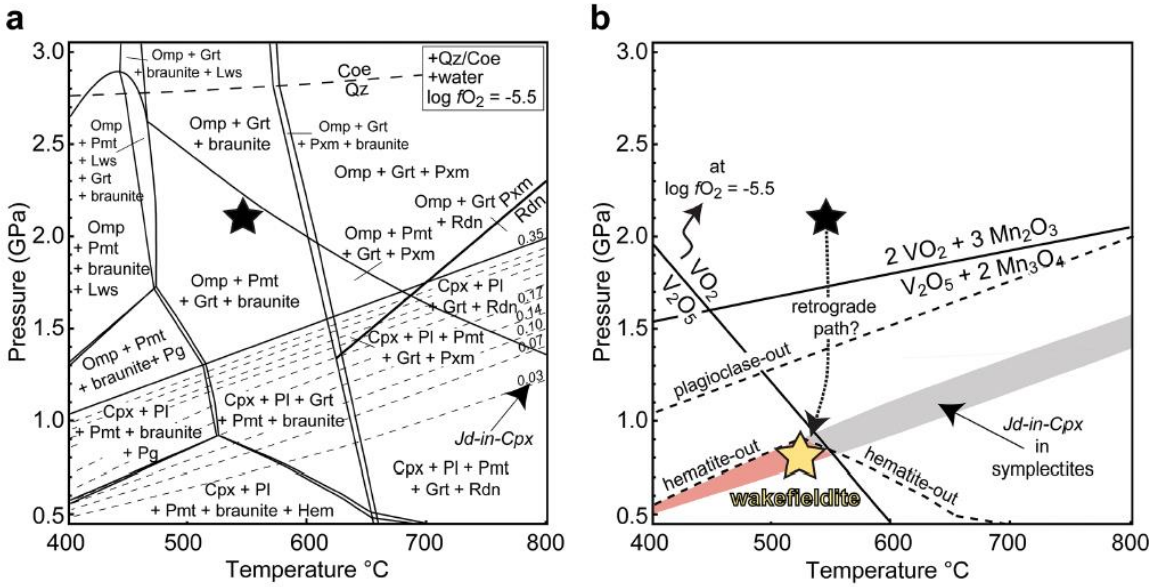

Fig. 35 *Pseudosection (isochemical diagram) calculated by thermodynamic modeling for the fixed bulk composition Na_2O = 0.709; MgO = 0.423; Al_2O_3 = 0.655; CaO = 0.832; FeO = 0.698; MnO = 1.60 (molar amounts), representing the model composition of the wakefieldite-bearing symplectite (emerald-green level) as derived from mass-balance calculations (Tumiati et al. 2020). Excess quartz + water and log (fO_2/1 bar) = –5.5 corresponding to ΔFMQ = +13 at P = 2.1 GPa and T = 550°C have been assumed for the calculations, in agreement with the occurrence of quartz and epidote at metamorphic peak conditions (black star; see Tumiati et al. 2015). b) univariant curves in the systems V–O and Mn–V–O showing the stability field of $V^{5+}{}_2O_5$, indicative of the stability of wakefieldite. Grey field: symplectitic clinopyroxene characterized by Jd-in-Cpx = 0.06–0.13 (Table 1). The upper boundary of the stability of symplectites is represented by the "plagioclase-out" curve. Red field: subset of the grey field where V_2O_5 and hematite are both stable at log (fO_2/1 bar) = –5.5. Yellow star: preferred retrograde P–T estimate of wakefieldite conditions of formation at Praborna.*

FIELD TRIP 3:

Panorama on the deep structure of the Western Alps orogenic wedge – On the foots of Matterhorn/Cervino –

(*upper Valtournanche valley – Zermatt-Saas zone*)

The aim of this short excursion is (i) to provide a panorama on the inner structure of alpine antiformal nappe stack (ii) observe some of the typical eclogite-facies lithologies forming the Liguro-Piemontese seafloor (now visible in the Zermatt-Saas unit) including the mafic crust, the serpentinized mantle and the sedimentary cover.

NB: this excursion may be canceled and replaced by a visit to Dent Blanche rocks in the Valpelline valley (North of Aosta city) in case of cloudy/rainy weather.

1. *Localization of the excursion, tectonic framework and itinerary*

We drive to Breuil (Cervinia) and take the cableways to Plan Maison (*45.94154° N, 7.65576° E,* **Fig. 36**) from where we have a spectacular view of the collisional zone of the Western Alps, particularly on the tectonic units we have crossed in the previous days. If the weather is clear, we can see the inner structure of the Matterhorn/Cervino that has been first studied by the famous Swiss geologist Emile Argand in the early 1900's.

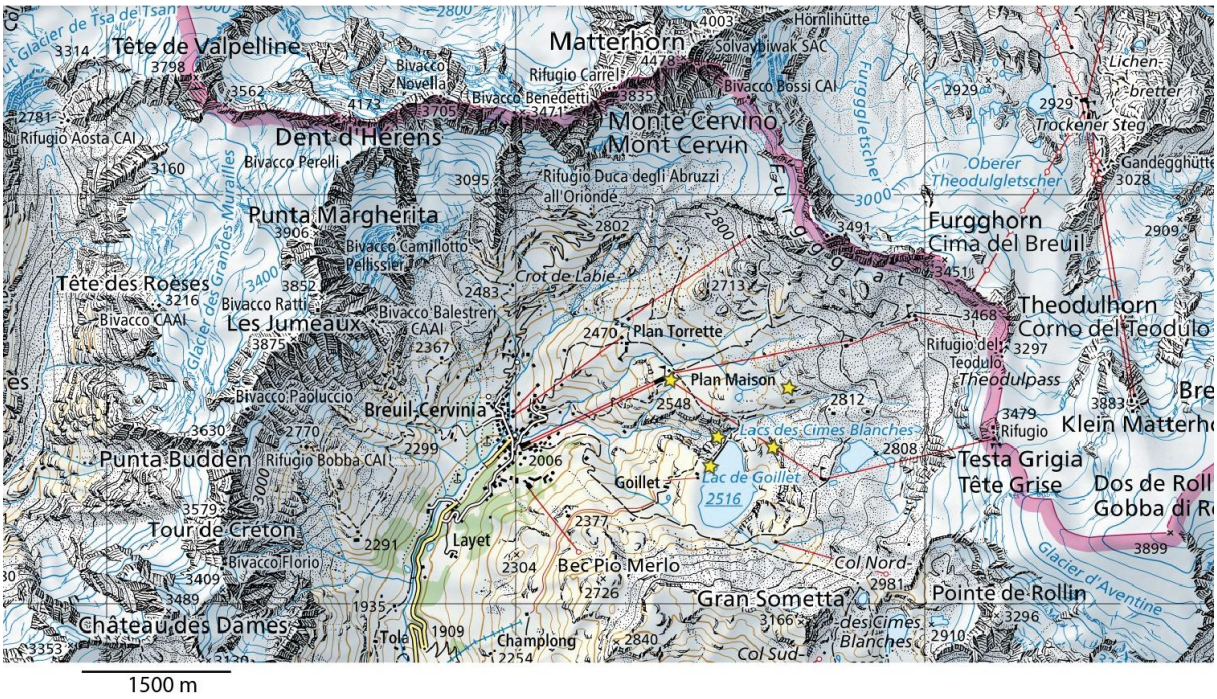

Fig. 36: *Topographic map of the excursion area (© Swisstopo) showing the location of the Plan Maison locality together with the yellow stars that localize the place that will be visited during this excursion (depending on conditions and available time).*

We first stop on a promontory next to the Plan Maison cable car arrival. From the top to the base of the Cervino (**Fig.37,39**), we observe the Dent Blanche (i) kinzigitic gneiss (with some mafic intercalations, all having experienced Permian granulite-facies metamorphism), (ii) the gneissic metagranitoids of the Arolla series, (iii) a thick mylonitic horizon of metagranitoids and metagabbros, (iv) the huge Early Permian metagabbro body, underlain by (v) thin basement mylonites, and (vi) the underlying ophiolitic Combin unit.

The Dent Blanche – Combin (i.e., Adria microplate – Tethys ocean) tectonic contact (Dent Blanche Thrust) is visible along the whole ridge, between Cervino and Monte Rous, through the Grandes et Petites Murailles. The whole nappe stack, from the Zermatt-Saas ophiolite to Dent Blanche-Mont Mary system through the Combin unit and the Etirol-Levaz slice, can be seen along the western flank of the upper and middle Valtournanche.

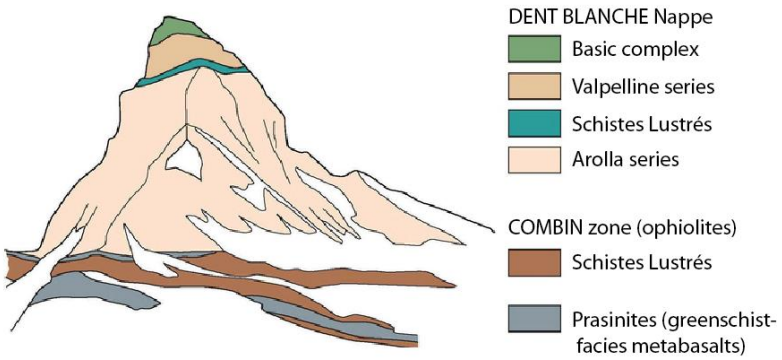

Fig. 37: Sketch of the Swiss side of the Matterhorn from Emile ARGAND, reproduced by Escher & Masson (1984). Note the intercalation of ocean-derived sediments within the continental slice-stack (i.e. between Valpelline granulites and Arolla orthogneisses). The Dent Blanche Thrust passes at the base of the peak, forming the contact with the Combin zone.

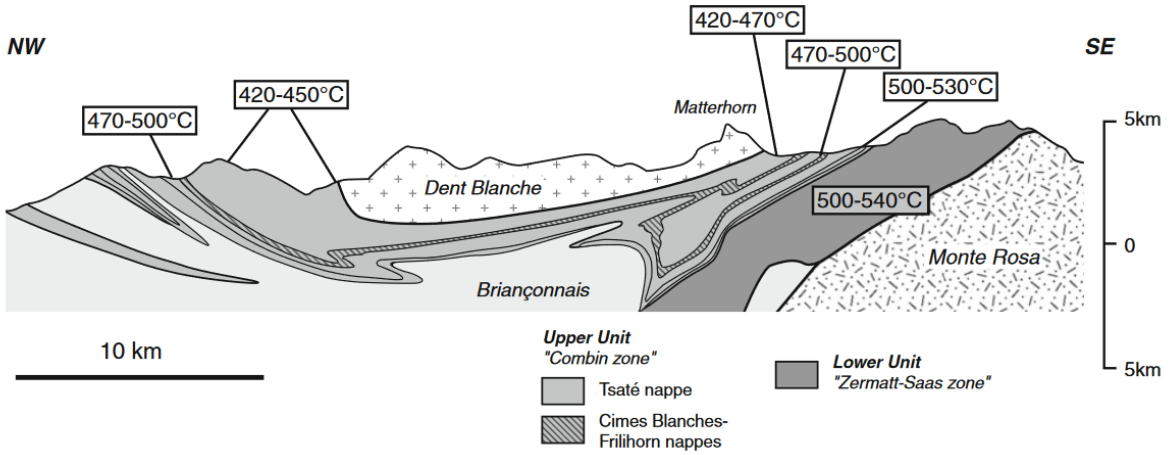

Fig. 38: Simplified cross-section across the Penninic units of the NW Alps (modified after Escher et al., 1993) showing the range of estimated RSCM (Raman Spectroscopy of Carbonaceous Matter) peak metamorphic temperatures in the Combin/Tsaté and underlying Zermatt-Saas units (Negro et al., 2013).

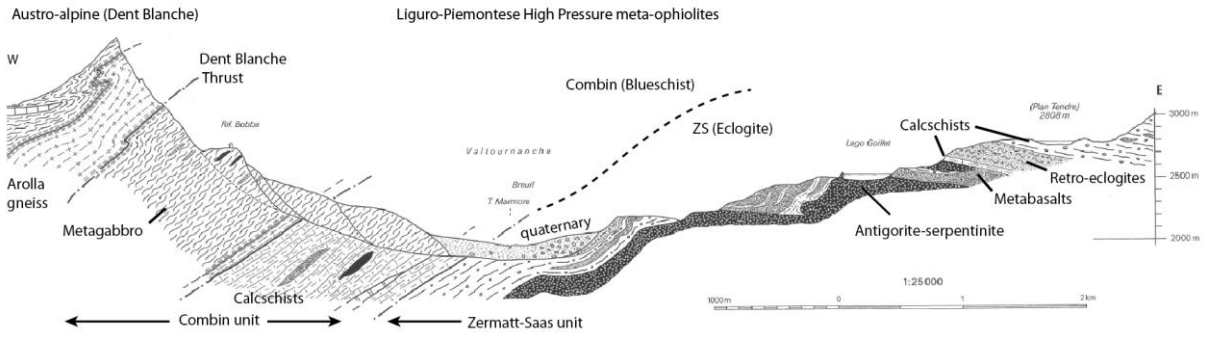

Fig. 39: Detailed geological cross section of the southwestern part of the Breuil-Cervinia circus (modified after Bucher et al., 2003: Geological Atlas of Switzerland, 1:25000). We stop by the lakeside in Lago Goillet (45.93384° N, 7.66503° E).

We then stop near the dam of Lago Goillet (**Fig. 40**) when we can see typical Jurassic and Early Cretaceous metasediments (metapelites and calcschists) that were covering the top of the Tethyan seafloor. In some

places, meter-thick levels of Mn-quartzites can be identified in the field further north (Dal Piaz et al., 1979). The metasediments exhibit extensive evidence of plastic deformation, mylonitization and boudinage of mafic levels (**Fig. 42**). Some of the mafic blocks found embedded within the calcschists were originally emplaced as boulders in conglomeratic levels formed during basin filling in the late Jurassic (called Rifelberg-Garten mélange in the literature; Dal Piaz, 1992). The NNE surroundings of the lake also contain deep green albite-rich amphibolites derived from a MORB protolith with relicts of garnet and locally eclogitic remnants. We walk along a stream coming from Cime Bianche lake (**Fig. 36**), and interlayered, typical mafic and pelitic eclogite-facies rocks can be observed on both sides of the creek.

On the eastern ridge (Plateau Rosa and further east) can be found the first occurrence of the Monte Rosa basement (internal crystalline massif; **Fig. 38**) which is abundantly documented by the orthogneiss blocks found in the moraine covering the Breuil circus.

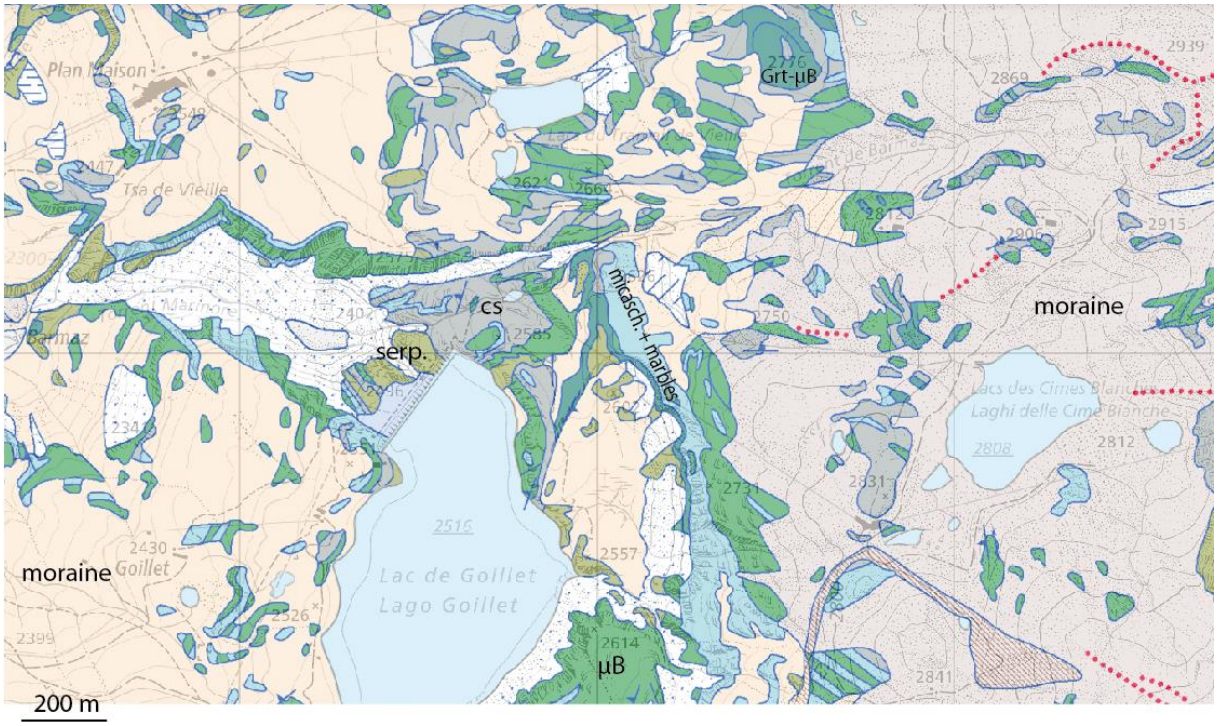

Fig. 40: *Detailed of the regional geological map showing the lithologies in the region of Lago Goillet. Serp: serpentinites; cs: calcschists; µB: metabasites. (downloaded from the Swisstopo © website).*

2. Petrographic observations and PT paths

- *Metasedimentary lithologies*

Around the Lago Goillet are only visible lithologies forming the seafloor of the Zermatt-Saas unit. The calcschists are characterized by the formation of a deep red garnet with chloritoid found both within garnet and also in the matrix (commonly chloritized because of retrogression; **Fig. 41**). The white mica is a highly substituted phengite (3.5-3.6 apfu). Lawsonite is occasionally observed pseudomorphed by clinozosoite and paragonite (**Fig. 43**). Other major phases are quartz and carbonates (calcite and ankerite). Organic matter, apatite and titanite also occur as accessory phases in the matrix. Available PT estimates point to 2.0 to 2.5 GPa and 500-550°C as recorded by metasediments (see Negro et al., 2013 and references therein; **Fig. 41**). This estimate contrasts with the underlying Combin/Tsaté unit for which lower pressures and lower temperatures (<500°C) are reported (Angiboust et al. 2014; **Fig.41**). In these lower grade rocks (not seen in the excursion), we have similar protoliths but garnet is generally absent and chloritoid extremely rare (Negro et al., 2013). Fresh aragonite and lawsonite have been recently reported by Manzotti et al. (2021) in similar rocks on the western side of the Dent Blanche.

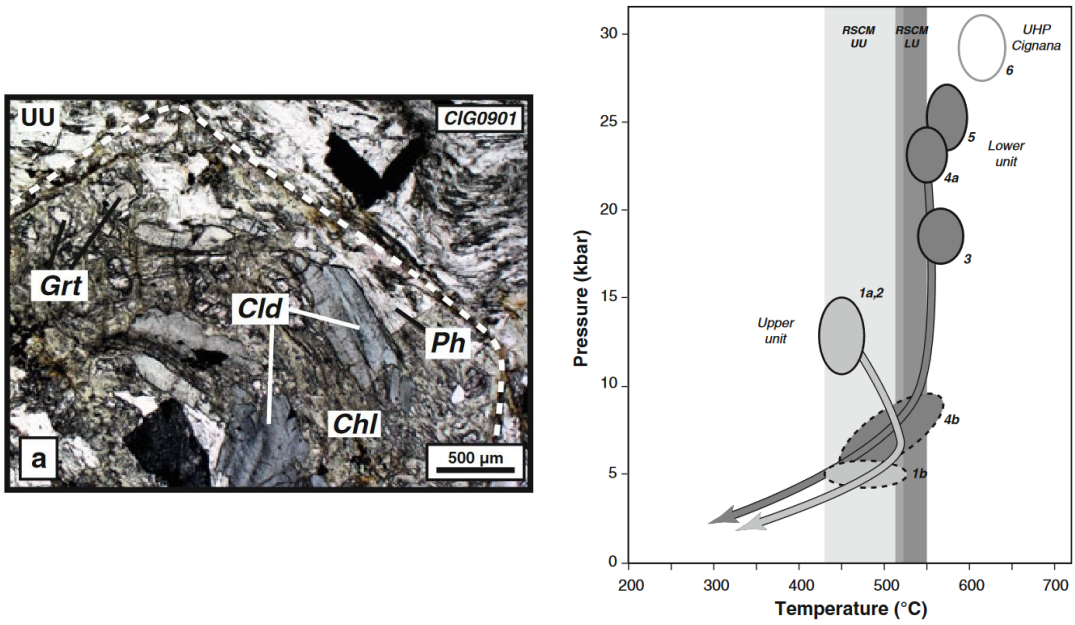

Fig. 41: *(left) Optical microscopy picture showing the typical peak burial assemblage in Zermatt-Saas metasediments where garnet (Grt), chloritoid (Cld) and phengite (Ph) grow together in the metapelitic matrix. Negro et al., 2013. (right) Summary of PT paths for the Combin/Tsaté unit (light gray; upper unit) and for the Zermatt-Saas unit (dark gray; lower unit). From Negro et al., 2013.*

Fig. 42: *(left) Field picture of a mafic pod wrapped within an alternation of impure marbles and calcschists (Lago Goillet dam). (right) View of an eclogitized conglomerate (Rifelberg garten mélange) with mafic pebbles floating in a calcschist matrix (Cime Bianche Laghi).*

- *Metabasaltic lithologies*

The Lago Goillet metabasalts all derive from MORBs emplaced on the Tethyan seafloor. They have been variably retrogressed during exhumation when crossing the epidote-blueschist facies and subsequently the

greenschist facies (**Fig.41** and **Fig.44**). When preserved, the metabasalts exhibit pillow-shaped morphologies (well-known and described by Bearth, 1968 in the Zermatt area further north). The cores contain garnet, omphacite, phengite, rutile together with pseudomorphs after lawsonite (**Fig.43**). PT estimates calculated for these lithologies point to c. 550°C and 2.4 GPa (**Fig. 44**; Angiboust et al., 2009).

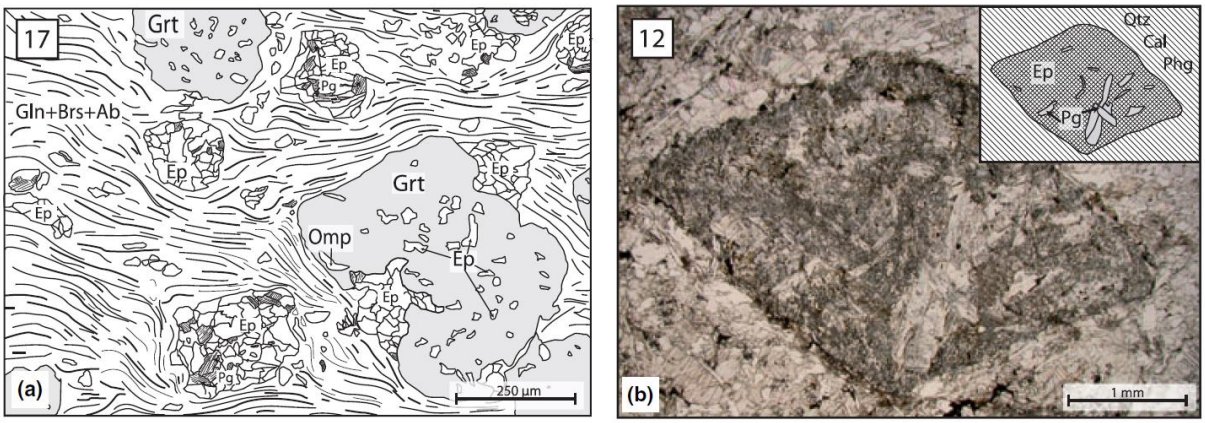

Fig. 43: *(left) Sketch depicting a typical mildly retrogressed Zermatt-Saas metabasite where the eclogite facies paragenesis is preserved in the garnet and where the sheared matrix has recrystallized into a blue-amphibole rich domain. (right) Optical microscope picture showing a pseudomorph after lawsonite in a calcschist from the ZS unit (both figures from Angiboust et al., 2009).*

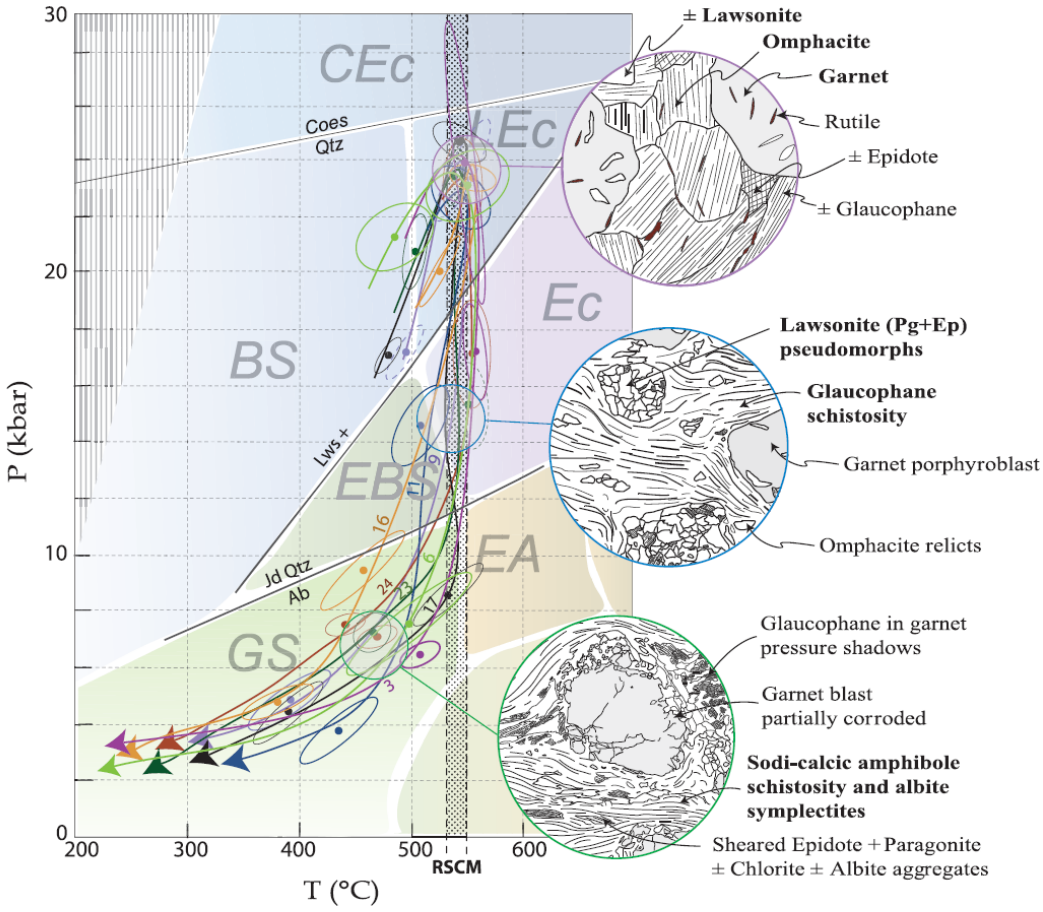

Fig. 44: *Summary of PT paths for various Zermatt-Saas metabasalts samples showing the three main metamorphic stages recorded in the rocks (Angiboust et al., 2009). RSCM: Raman Spectroscopy of Carbonaceous Matter.*

Upon exhumation, the omphacite from the matrix broke down into a glaucophane-rich assemblage (see the picture on the front page) which has been subsequently transformed into a sodic-calcic + albite assemblage below 0.8 GPa and in the T range 400-500°C. Garnet is gradually transformed into chlorite and a pervasive greenschist foliation is commonly observed (**Fig. 44**). These green rocks are called "prasinites" in the alpine literature. Locally rodingitization of mafic lithologies is observed with a marked Ca-enrichment and the growth of grossular-bearing lithologies. Some are visible on the W shore of the Goillet lake.

- *Ultramafic lithologies*

In the Zermatt-Saas unit the oceanic mantle has been extremely serpentinized on the seafloor and more than 95% of the ultramafic matrix has been transformed into antigorite schist during oceanic subduction (e.g. Li et al., 2004; Fontana et al., 2008). The lowermost part of the Zermatt Saas unit systematically comprises a several hundred-meters thick serpentinite sole as visible both on the Swiss side (Li et al., 2004), in the Valtournanche-Ayas area (Dal Piaz, 1992; Rebay et al., 2012) but also in the southern Aosta valley region (Mt Avic massif; Fontana et al., 2015). The thickness, the location and the structural position of this sole recalls the basal serpentinite sole also evidenced in the Monviso massif further south (Angiboust & Agard, 2010; Lombardo et al., 1978; Schwartz et al., 2001).

In the excursion area, the bottom of Lago Goillet is made of these tightly folded ZS serpentinites with a regional gentle dip to the W (**Fig. 39**). The typical assemblage comprises a groundmass of fine-grained antigorite with widespread magnetite and locally chromian spinel. The ultramafic assemblage has recorded a long hydrothermal/metamorphic history from the seafloor stage until subduction and exhumtion (e.g. Li et al., 2004; Kempf et al., 2020; Luoni et al., 2021; **Fig. 45**). Primary magmatic olivine is rare. Accessory phases are diopside, clinochlore, carbonates (dolomite/magnesite) and locally some talc approaching metasediments. Along veins are commonly found secondary (metamorphic) olivine, Ti-clinohumite, Ti-chondrodite, tremolite, diopside and further magnetite. Peak burial conditions have been estimated at near 550°C and 2.5 GPa (Kempf et al., 2020; **Fig.46**).

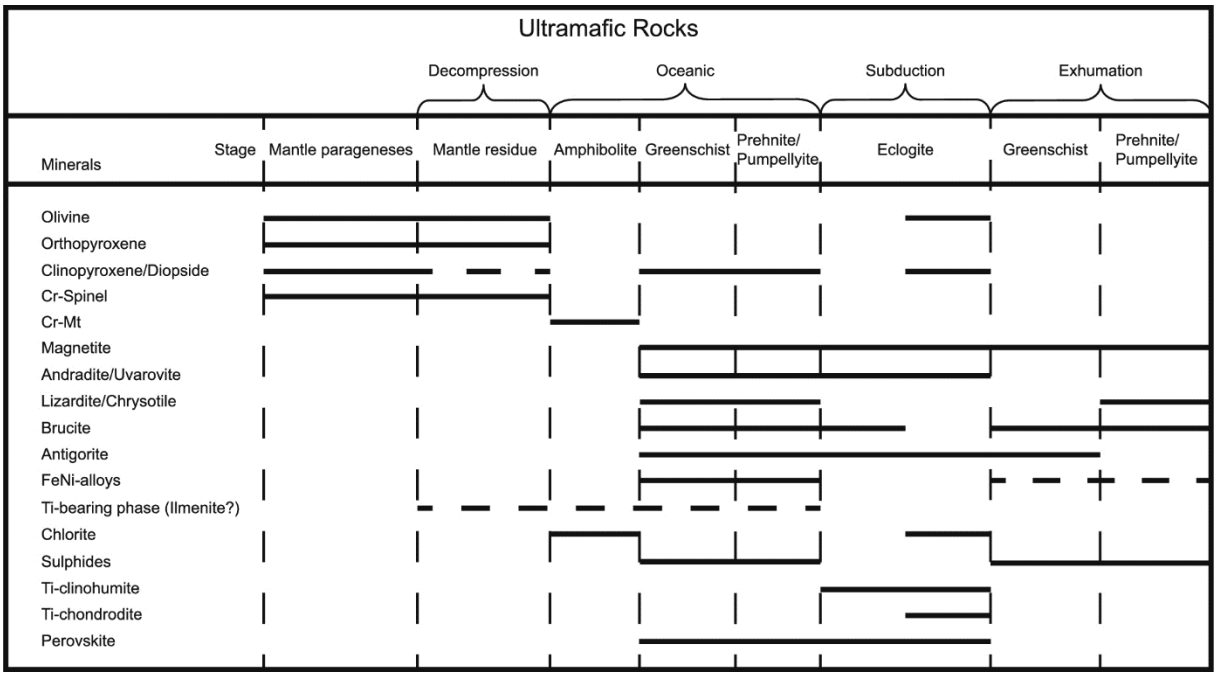

Fig. 45: *Summary of the protracted sequence of metamorphic events recorded in the ultramafics from the Zermatt-Saas unit (Kempf et al., 2020).*

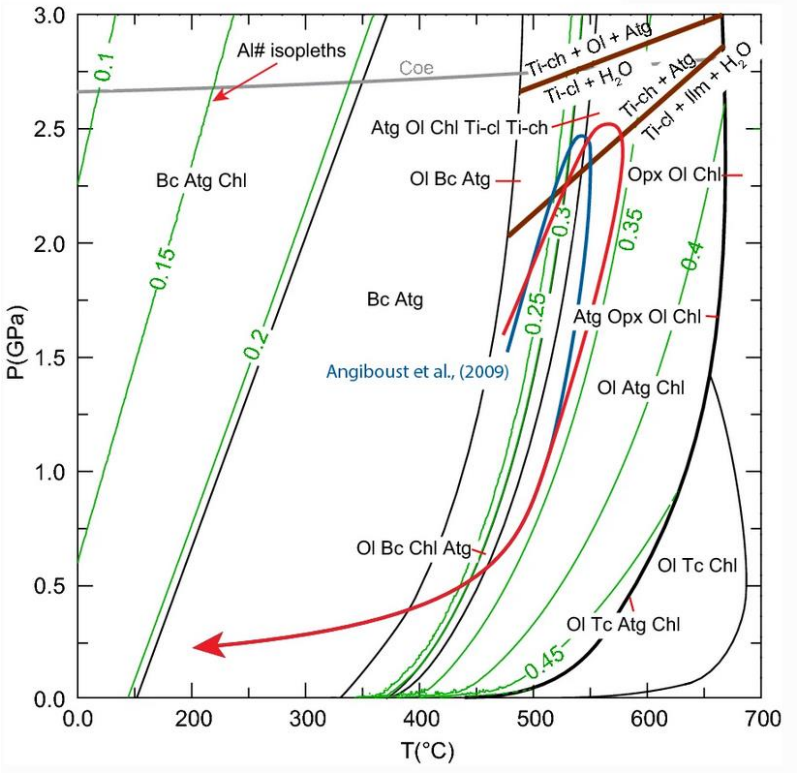

***Fig. 46**: Pseudosection modelling of ultramafics of the Zermatt-Saas unit (Swiss side) (red path: preferred PT path derived from petrological observations). after Kempf et al. (2020).*

REFERENCES

Agard P., Jolivet L., Goffé B. (2001) - Tectonometamorphic evolution of the Schistes Lustres Complex; implications for the exhumation of HP and UHP rocks in the Western Alps. Bull. Soc. Géol. France 172 (5), 617-636.

Agard P., Monié P., Jolivet L., Goffé B. (2002) - Exhumation of the Schistes Lustrés complex: *in situ* laser probe $^{40}Ar/^{39}Ar$ constraints and implications for the Western Alps. J. Metamorph. Geol. 20 (6), 599-618.

Agard, P., Lemoine, M. (2005) - Faces of the Alps: structure & geodynamic evolution. Commission for the geological map of the World.

Agard P., Yamato P., Jolivet L., Burov E. (2009) - Exhumation of oceanic blueschists and eclogites in subduction zones: Timing and mechanisms. Earth-Science Reviews 92 (1-2), 53-79.

Agard P., Handy M.R. (2021) - Ocean subduction dynamics in the Alps. Elements: An International Magazine of Mineralogy, Geochemistry, and Petrology 17 (1), 9-16.

Agard P., Soret M., Bonnet G., Ninkabou D., Plunder A., Prigent C., Yamato P. (2022) - Subduction and obduction processes: the fate of oceanic lithosphere revealed by blueschists, eclogites and ophiolites. Catlos; Cehmen; Dalziel (Eds.). Compressional Tectonics: Plate Convergence to Mountain Building – Volume 2, American Geophysical Union (AGU), In press.

Ahrendt H., (1969) - Tertiärer Vulkanismus in der Canavese-Zone? Neues J. Geol. Pal. Mon. (Stuttgart), 9, 513–516.

Angiboust S., Agard P., Jolivet L., Beyssac O. (2009)- The Zermatt-Saas ophiolite: the largest (60-km wide) and deepest (c. 70-80 km) continuous slice of oceanic lithosphere detached from a subduction zone? Terra Nova 21, 171–180.

Angiboust S., Agard P. (2010) – Initial water budget: The key to detaching large volumes of eclogitized oceanic crust along the subduction channel? Lithos 120 (3-4), 453-474.

Angiboust S., Langdon R., Agard P., Waters D., Chopin C. (2012) – Eclogitization of the Monviso ophiolite (W. Alps) and implications on subduction dynamics. J. Metamorph. Geol. 30 (1), 37-61.

Angiboust S., Glodny J., Oncken O., Chopin C. (2014) - In search of transient subduction interfaces in the Dent Blanche-Sesia Tectonic System (W. Alps). Lithos 205, 298-321.

Angiboust S., Yamato P., Hertgen S., Hyppolito T., Bebout G. E., Morales L. (2017) - Fluid pathways and high-P metasomatism in a subducted continental slice (Mt. Emilius klippe, W. Alps). Journal of Metamorphic Geology *35* (5), 471-492.

Angiboust S., Glodny J. (2020) - Exhumation of eclogitic ophiolitic nappes in the W. Alps: New age data and implications for crustal wedge dynamics. Lithos *356*, 105374

Argand E. (1916) - Sur l'arc des Alpes occidentales. Bridel G.

Ayrton S., Bugnon C., Haarpainter T., Weidmann M., Frank E. (1982) – Géologie du front de la nappe de la Dent Blanche dans la region des Monts-Dolins, Valais. Eclogae Geologicae Helvetiae 75, 269-286.

Babist J., Handy M.R., Konrad-Schmolke M., Hammerschmidt K. (2006) - Precollisional, multistage exhumation of subducted continental crust: the Sesia Zone, western Alps. Tectonics, 25/6, 1-25.

Ballèvre M., Kienast J.R., Vuichard J.P. (1986) - La "nappe de la Dent-Blanche" (Alpes occidentales): deux unites austroalpines indépendantes. Eclogae Geologicae Helvetiae 79 (1), 57-74.

Barnicoat A.C, Cliff R.A, Inger S., Rex D.C. (1993) – Assessing the age of high-pressure metamorphism in the western Alps using Sm-Nd and $^{40}Ar/^{39}Ar$. Terra Nova 5, 380.

Barnicoat A.C, Bowtell S.A. (1995) – Seafloor hydrothermal alteration in metabasites from high-pressure ophiolites of the Zermatt-Aosta area of the western Alps. Boll. Mus. Sci. Nat. Torino 13, 191-220.

Bearth P. (1967) - Die Ophiolithe der Zone von Zermatt-Saas Fee (p.130). Bern: Kümmerly & Frey.

Beltrando M., Compagnoni R., Lombardo B. (2010) - (Ultra-) High-pressure metamorphism and orogenesis: An Alpine perspective. Gondwana Research 18 (1), 147-166.

Beltrando M., Rubatto D., Manatschal G. (2010) - From passive margins to orogens: The link between ocean-continent transition zones and (ultra) high-pressure metamorphism. Geology *38* (6), 559-562.

Beltrando M., Manatschal G., Mohn G., Dal Piaz G.V., Brovarone A.V., Masini E. (2014) - Recognizing remnants of magma-poor rifted margins in high-pressure orogenic belts: The Alpine case study. Earth-Science Reviews 131, 88-115.

Beccaluva L., Macciotta G., Piccardo G.B., Zeda O. (1984) – Petrology of lherzolitic rocks from the Northern Apennine ophiolites. Lithos 17, 299-316

Bigi G., Cosentino D., Parotto M., Scandone P. (1990) - Structural model of Italy. Progetto Finalizzato Geodinamica CNR. Quad Ricerca Scientifica 114.

Bistacchi A., Massironi M. (2000) – Post-nappe brittle tectonics and kinematic evolution of the north-western Alps: an integrated approach. Tectonophysics 327 (3-4), 267-292.

Bonnet G., Chopin C., Locatelli M., Kylander-Clark A.R., Hacker B.R. (2022) - Protracted Subduction of the European Hyperextended Margin Revealed by Rutile U-Pb Geochronology Across the Dora-Maira Massif (Western Alps). Tectonics 41 (4), e2021TC007170.

Botwell S.A., Cliff R.A., Barnicoat A.C. (1994) – Sm-Nd isotopic evidence on the age of eclogitization in the Zermatt-Saas ophiolite. J. Metam. Geol. 12, 187-196.

Bucher K., Fazis Y., de Capitani C., Grapes R. (2005) - Blueschists, eclogites and decompression assemblages of the Zermatt-Saas ophiolite: High-pressure metamorphism of subducted Tethys lithosphere. American Mineralogist 90 (5-6), 821-835.

Bucher K., Weisenberger T. B., Weber S., Klemm O., Corfu F. (2020) - The Theodul Glacier Unit, a slab of pre-Alpine rocks in the Alpine meta-ophiolite of Zermatt-Saas, Western Alps. Swiss Journal of Geosciences *113* (1), 1-22.

Bussy F., Venturini G., Hunziker J., Martinotti G. (1998) - U–Pb ages of magmatic rocks of the western Austroalpine Dent–Blanche–Sesia Unit. Schweiz. mineral. petrogr. Mitt., 78, 163–168.

Callegari E., Cigolini C., Medeot O., D'Antonio M. (2004) – Petrogenesis of calc-alkaline and shoshonitic post-collosional Oligocene volcanics of the Cover Series of the Sesia Zone, Western Italian Alps. Geodinamica Acta 17 (1), 1-29.

Canepa A., Castelletto M., Cesare B., Martin S., Zaggia L. (1990) - The Austroalpine Mont Mary nappe (Italian Western Alps). Memorie di Scienze Geologiche *42*, 1–17.

Cartwright I., Barnicoat A.C. (1999) - Stable isotope geochemistry of Alpine ophiolites: a window to ocean-floor hydrothermal alteration and constraints on fluid-rock interaction during high-pressure metamorphism. International Journal of Earth Sciences (Geologische Rundschau). 88, 219-235.

Castello, P. (1979). Studio geologico-giacimentologico nelle valli di St. Marcel e Fenis. Tesi Univ. Torino, 328 p.

Castello, P., Dal Piaz, G.V., Gosso, G., Kienast, J.-R., Martin, S., Natale, P., Nervo, R., Polino, R., Venturelli, G. (1980). The Piedmont ophiolite nappe in the Aosta valley and related ore deposits. In: Gruppo di Lavoro sulle Ofioliti Mediterranee, VI ophiolite field conference, Field excursion book, Firenze, 1980, 171-192.

Castello P. (1981) -Inventario delle mineralizzazioni a magnetite, ferro-rame e manganese del complesso piemontese dei calcescisti con pietre verdi in valle d'Aosta. Ofioliti. 6, 5-46.

Castello P. Cesti G. (2017). Il sito fusorio di epoca romana di Eteley (Saint-Marcel - Ao). Bull. d'Etudes prehistoriques et archeologiques alpines. Aoste. v. 28, pp. 121-132.

Cenki-Tok, B., Chopin, C. (2006). Coexisting calderite and spessartine garnets in eclogite-facies metacherts of the Western Alps. Mineral. Petrol. 88, 47–68.

Cesare B., Martin S., Zaggia L. (1989) - Mantle peridotites from the Austroalpine Mt. Mary nappe (Western Alps). Schweitzerische mineralogische und petrographische Mitteilungen 69, 91-97.

Chopin C. (1984) - Coesite and pure pyrope in high-grade blueschists of the Western Alps: a first record and some consequences. Contr. Mineral and Petrol. 86, 107-118.

Compagnoni R. (1977) - The Sesia-Lanzo Zone: high pressure-low temperature metamorphism in the Austroalpine continental margin. Rend. Soc. Ital. Mineral. Petrol., 33, 335-375.

Compagnoni R., Dal Piaz G.V., Hunziker J.C., Gosso G., Lombardo B., Williams P.F. (1977) - The Sesia-Lanzo zone, a slice of continental crust with alpine high pressure–low temperature assemblages in the Western Italian Alps. Rend. Soc. It. Min. Petr. 33, 281–334.

Compagnoni R.,Maffeo B. (1973) - Jadeite-bearing metagranites l.s. and related rocks in the Mount Mucrone area (Sesia-Lanzo zone, Western Italian Alps). Schweiz. mineral. petrogr. Mitt., 53, 355-378.

Compagnoni, R., Rolfo, F., Groppo, C., Hirajima, T., & Turello, R. (2012). Geological map of the ultra-high pressure Brossasco-Isasca unit (Western Alps, Italy). Journal of Maps, 8(4), 465-472.

Compagnoni R., Engi M., Regis D. (2014). Valle d'Aosta section of the Sesia Zone: multi-stage HP metamorphism and assembly of a rifted continental margin. Geological Field Trips, 6(1.2), 1-44.

Cortiana G., Dal Piaz G. V., Del Moro A., Hunziker J. C., Martin, S. (1998) - ^{40}Ar–^{39}Ar and Rb–Sr dating of the Pillonet klippe and Sesia-Lanzo basal slice in the Ayas valley and evolution of the Austroalpine-Piedmont nappe stack. Memorie di Scienze Geologiche *50*, 177–194.

Coward M., Dietrich D., (1989) - Alpine tectonics – an overview. Geological Society, London, Special Publications, 45, 1-29, 1.

De Graciansky P.C., Roberts D.G., Tricart P. (2011) - The Alps: Present Day Structure. In *Developments in Earth Surface Processes* Elsevier 14, 29-53

Dal Piaz G.V. (1965) – La formazione mesozoica dei calcesti con pietre verdi fra la Valsesia e la Valtournanche ed I suoi rapport strutturali con il ricoprimento Monte Rosa e con la Zona Sesia-Lanzo. Boll Soc Geol Ital 84 (1), 67-104.

Dal Piaz G.V., Hunziker J.C., Martinotti G. (1972) - La zona Sesia-Lanzo e l'evoluzione tettonico-metamorfica delle Alpi nord-occidentali interne. Mem. Soc. Geol. It., 11, 433-460.Dal Piaz G.V. (1974) – Le metamorphisme de haute pression et basse temperature dans l'evolution structurale du bassin ophiolitique alpino-apenninique; 1ere partie; Considerations paleogeographiques. Boll. Soc. Geol. Ital. 93 (2), 437-467.

Dal Piaz G.V. (1976) - Il lembo di ricoprimento del Pillonet (falda della Dent Blanche nelle Alpi Occidentali). Memorie di Scienze Geologiche (Padova) *31*, 1–60.

Dal Piaz G.V. (1978) – Areal geology and petrology of eclogites and associated metabasites of the Piemonte ophiolite nappe, breuil-st Jacques area, Italian Western Alps. Tectonophysics 51 (1-2), 99-126.

Dal Piaz, G. V., De Vecchi, G., & Hunziker, J. C. (1977). The Austroalpine layered gabbros of the Matterhorn and Mt. Collon–Dents de Bertol. Schweizerische Mineralogische und Petrographische Mitteilungen*, 57*, 59–88.

Dal Piaz G.V., Omenetto P. (1978) - Brevi note su alcune mineralizzazioni della falda piemontese in Valle d'Aosta. Ofioliti 3 (2-3), 161-176.

Dal Piaz G.V., Venturelli G., Scolari A. (1979) – Calk-alkaline to ultrapotassic post-collisional volcanic activity in the Internal Northwestern Alps. Mem. Sci. Geol. Padova 32, 4-16.

Dal Piaz, G.V., Di Battistini, G., Kienast, J.-R., and Venturelli, G. (1979). Manganiferous quartzitic schists of the Piedmont ophiolite nappe in the Valsesia-Valtournanche area. Memorie di Scienze geologiche [di Padova]. 32, 24 p.

Dal Piaz G.V. (1981) – Geochemical features of metabasalts and metagabbros from the Piemonte ophiolite nappe; Italian Western Alps. Schweizerbart.

Dal Piaz G.V., Martin S. (1988) – Dati microchimici sul metamorfismo alpino nei lembi Austroalpini del Pillonet e di Chatillon (Valle d'Aosta). Rendiconti della Società geologica italiana 9, 15-16.

Dal Piaz, G.V. [ed.] 1992. Le Alpi dal M. Bianco al lago Maggiore. Guide geologiche regionali, Società geologica italiana, 1/3, 311 p.; 2/3, 211 p.

Dal Piaz G.V. (1999) - The Austroalpine-Piedmont nappe stack and puzzle of Alpine Tethys. Memorie di Scienze Geologiche 51 (1), 155-176.

Dal Piaz G.V., Cortiana G., Del Moro A., Martin S., Pennacchioni C., Tartarotti P. (2001) - Tertiary age and paleostructural inferences of the eclogitic imprint in the austroalpine outliers and Zermatt-Saas ophiolite, Western Alps. Intern. J. Earth Sci. 90, 668-684.

Dal Piaz, G.V., Bistacchi, A., Massironi,M., 2003. Geological outline of the Alps. Episodes 26 (3), 175-180.

Delleani F., Rebay G., Zucali M., Tiepolo M., Spalla M.I. (2018) - Insights on Variscan geodynamics from the structural and geochemical characterization of a Devonian-Carboniferous gabbro from the Austroalpine Domain (Western Alps). Ofioliti, 43(1), 23-39.

Deville E., Fudral S., Lagabrielle Y., Marthaler M., Sartori M. (1992) – From oceanic closure to continental collision: A synthesis of the "Schistes lustrés" metamorphic complex of the Western Alps. Geological Society of America Bulletin 104 (2), 127-139.

Diehl E.A., Masso R., Stutz A.H. (1952) – Contributo alla conoscenza del ricoprimento della Dent Blanche. Memorie degli Istituti di Geologia e Mineralogia dell'Università di Padova 17, 1-52.

Dragovic, B., Angiboust, S., Tappa, M.J. (2020) -Petrochronological close-up on the thermal structure of a paleo-subduction zone (W. Alps). Earth and Planetary Science Letters 547, 116446.

Duchêne S., Blichert-Toft J., Luais B., Télouk P., Lardeaux J.M., Albarède F. (1997) - The Lu-Hf dating of garnets and the ages of the Alpine high-pressure metamorphism. Nature 387 (6633), 586-589.

Elter G. (1960) – La Zona Pennidica dell'alta e media Val d'Aosta e le unita limitrofe. Mem. Ist. Geol. Univ. Padova 22, 1-113.

Elter G. (1971) - Schistes lustrés et ophiolites de la zone piémontaise entre Orco et Doire Baltée (Alpes Graies). Hypothèses sur l'origine des ophiolites. Géologie Alpine 47, 147-169.

Ernst W.G., Dal Piaz G.V. (1978) - Mineral parageneses of eclogitic rocks and related mafic schists of the Piemonte ophiolite nappe, Breuil-St. Jacques area, Italian Western Alps. American Mineralogist, 63(7-8) 621-640.

Escher A., Beaumont C. (1997) - Formation, burial and exhumation of basement nappes at crustal scale: a geometric model based on the Western Swiss-Italian Alps. Journal of structural Geology 19 (7), 955-974.

Escher, A., Masson, H., & Steck, A. (1993). Nappe geometry in the western Swiss Alps. Journal of structural Geology, 15(3-5), 501-509.

Escher, A., & Masson, H. (1984). Le Cervin: un dessin géologique inédit d'Emile Argand (1929) et son interprétation actuelle. Travaux du Comité français d'Histoire de la Géologie, 2(tome 2), 95-127.

Fassmer K., Obermüller G., Nagel T. J., Kirst F., Froitzheim N., Sandmann S., ... Muenker C. (2016). High-pressure metamorphic age and significance of eclogite-facies continental fragments associated with oceanic lithosphere in the Western Alps (Etirol-Levaz Slice, Valtournenche, Italy). Lithos *252*, 145-159.

Fontana E., Tartarotti P., Panseri M., Buscemi S. (2015) – Geological map of the Mount Avic massif (western Alps Ophiolites). Journal of Maps 11 (1), 126-135.

Fontana, E., Panseri, M., & Tartarotti, P. (2008). Oceanic relict textures in the Mount Avic serpentinites, Western Alps. Ofioliti, 33(2), 105-118.

Ford M., Duchêne S., Gasquet D., Vanderhaeghe O. (2006) – Two-phase orogenic convergence in the external and internal SW Alps. Journal of the Geological Society 163 (5), 815-826.

Forster M., Lister G., Compagnoni R., Giles D., Hills Q., Betts P., Tamagno E. (2004) – Mapping of oceanic crust with "HP" to "UHP" metamorphism: The lago di Cignana Unit (Western Alps). In *Mapping geology in Italy*. Geological Society of London.

Franchi S. (1900) – Sopra alcuni giacimenti di rocce giadeitiche nelle Alpi Occidentali e nell'Appennino Ligure. Boll. R. Comitato Geologico d'Italia 31, 119-146.

Franchi S. (1902) – Uber Feldspath-Uralitisierung der Natron-Thonerde-pyroxene aus den eklogitischen Glimmerschiefern der Gebirge von Biella (Graiische Alpen). Neues Jahrbuch für Mineralogie, Geologie und Palaeontologie 2, 112 - 158

Frezzotti M.L., Selverstone J. Sharp Z.D., Compagnoni R. (2001) – Carbonate dissolution during subduction revealed by diamond-bearing rocks from the Alps. Nature Geoscience 4 (10), 703-706.

Gasco I., Gattiglio M., Borghi A. (2013) - Review of metamorphic and kinematic data from Internal Crystalline Massifs (Western Alps): PTt paths and exhumation history. Journal of Geodynamics *63*, 1-19.

Gastaldi B. (1871) – Studi geologici sulle Alpi Occidentali. Parte I, Memorie del Regio Comitato Geologico d'Italia 1, 1-47.

Giuntoli F., Engi M. (2016) - Internal geometry of the central Sesia Zone (Aosta Valley, Italy): HP tectonic assembly of continental slices. Swiss Journal of Geosciences 109(3), 445–471.

Giuntoli F., Lanari P., Burn M., Kunz B.E., Engi M. (2018) - Deeply subducted continental fragments-Part 2: Insight from petrochronology in the central Sesia Zone (western Italian Alps). Solid Earth, 9(1), 191–222.

Goffé B., Velde B. (1984) - Contrasted metamorphic evolutions in thrusted cover units of the Briançonnais zone (French Alps): A model for the conservation of HP-LT metamorphic mineral assemblages. Earth Planet. Sci. Lett. 68 (2), 351 – 360.

Gosso G. (1977) - Metamorphic evolution and fold history in the eclogite micaschists of the upper Gressoney valley (Sesia-Lanzo zone, Western Alps). Rendiconti della Società Italiana di Mineralogia e Petrologia *33*, 389–407.

Gosso G., Dal Piaz G. V., Piovano V., & Polino R. (1979) - High pressure emplacement of Early-Alpine nappes, postnappe deformations and structural levels (Internal Northwestern Alps). *Memorie degli Istituti di Geologia e Mineralogia dell'Università di Padova, 32*, 5–15.

Groppo C., Beltrando M., Conpagnoni R. (2009) – The P-T path of the ultra-high pressure Lago Di Cignana and adjoining high-pressure meta-ophiolitic units: insights into the evolution of the subductiong Tethyan slab. J. Metamorph. Geol. 27 (3), 207-231.

Gruppo di Lavoro sulle Ofioliti Mediterranee (1977). Escursione ad alcuni giacimenti a Cu-Fe e Mn della falda piemontese, Alpi occidentali: 10-13 ottobre 1977. Ofioliti, 2, pp. 241-263.

Halama R., Konrad-Schmölke M., Sudo M., Marschall H. R., Wiedenbeck M. (2014) - Effects of fluid-rock interaction on $^{40}Ar/^{39}Ar$ geochronology in high-pressure rocks (Sesia-Lanzo Zone, Western Alps). Geochimica et Cosmochimica Acta *126*, 475–494.

Inger S., Ramsbotham W., Cliff R. A., Rex D. C. (1996) - Metamorphic evolution of the Sesia-Lanzo Zone, Western Alps: time constraints from multi-system geochronology. Contributions to Mineralogy and Petrology 126 (1), 152-168

Jervis, G. (1873). I tesori sotterranei dell'Italia. Parte prima, regione delle Alpi. Torino, Gribaudi Ed., new edition 1974, 81-114.

Kapferer N., Mercolli I., Berger A., Ovtcharova M., Fuegenschuh (2012) - Dating emplacement and evolution of the orogenic magmatism in the internal Western Alps: 2. The Biella Volcanic Suite. Swiss Journal of Geoscience, 105, 67-84.

Kempf, E. D., Hermann, J., Reusser, E., Baumgartner, L. P., & Lanari, P. (2020). The role of the antigorite+ brucite to olivine reaction in subducted serpentinites (Zermatt, Switzerland). Swiss journal of geosciences, 113(1), 1-36.

Kiénast J. R. (1973) - Sur l'existence de deux séries différentes au sein de l'ensemble "schistes lustrés-ophiolites" du val d'Aoste: quelque arguments fondés sur l'étude des roches métamorphiques. Comptes Rendus de l'Académie des Sciences de Paris, *D-276*, 2621–2624.

Konrad-Schmolke M., Halama R. (2014) - Combined thermodynamic-geochemical modeling in metamorphic geology: Boron as tracer of fluid–rock interaction. Lithos 208, 393–414.

Krutow-Mozgawa A. (1988) - Métamorphisme dans les sédiments riches en fer ou magnesium de la couverture des ophiolites piémontaises (mine de Servette, Val d'Aoste). Thèse de 3ème cycle, Université P. et M. Curie, Paris VI.Lagabrielle Y., Cannat M. (1990) - Alpine Jurassic ophiolites resemble the modern central Atlantic basement. Geology 18 (4), 319-322

Lagabrielle Y., Lemoine M. (1997) - Alpine, Corsican and Apennine ophiolites: the slow-spreading ridge model. Comptes Rendus de l'Académie des Sciences-Series IIA-Earth and Planetary Science 325 (12), 909-920.

Lapen T. J., Johnson C. M., Baumgartner L. P., Dal Piaz G. V., Skora S., Beard B. L. (2007) - Coupling of oceanic and continental crust during Eocene eclogite-facies metamorphism: Evidence from the Monte Rosa nappe, western Alps. Contributions to Mineralogy and Petrology, *153*, 139–157.

Lardeaux J. M., Gosso G., Kienast J. R., Lombardo, B. (1983) - Chemical variations in phengitic micas of successive foliations within the Eclogitic Micaschists complex, Sesia-Lanzo zone (Italy, Western Alps). Bulletin de minéralogie, 106 (6), 673-689.

Lardeaux J.M., Spalla M.I. (1991) - From granulites to ecogites in the Sesia zone (Italian Western Alps): a record of the opening and closure of the Piedmont ocean. J. Metamorph. Geol. 9 (1), 35-59.

Lemoine M., Bas T., Arnaud-Vanneau A., Arnaud H., Dumont T., Gidon M., Bourbon M., de Graciansky P-C., Rudkiewicz J-L., Megard-Galli J., Tricart P. (1986) - The continental margin of the Mesozoic Tethys in the Western Alps. Marine and Petroleum Geology 3 (3), 179-199.

Le Pichon X., Bergerat F., Roulet M.J. (1988) - Plate kinematics and tectonics leading to the Alpine belt formation: a new analysis. Geol. Soc. Am. Spec. Pap. 218, 111-131.

Li, X. P., Rahn, M., & Bucher, K. (2004). Serpentinites of the Zermatt-Saas ophiolite complex and their texture evolution. Journal of metamorphic Geology, 22(3), 159-177.

Liermann H.-P., Isachsen C., Altenberger U., Oberhänsli R. (2002) - Behavior of zircon during high-pressure, low-temperature metamorphism: Case study from the Internal Unit of the Sesia Zone (Western Italian Alps). Eur. J. Mineral., 14, 61–71.

Lombardo, B., Nervo, R., Compagnoni, R., Messiga, B., Kienast, J., Mevel, C., Fiora, L., Piccardo, G. and Lanza, R. 1978. Osservazioni preliminari sulle ofioliti metamorfiche del Monviso (Alpi Occidentali. Rendiconti Società Italiana di Mineralogia e Petrologia, 34: 253–305.

Lorenzini C. (1995) - Saint-Marcel, miniera di Chuc e Servette. In: "Le antiche miniere della Valle d'Aosta", Lorenzini C. (a cura di), Musumeci Editore Quart; 165p.

Lorenzini, C. (1998). Le antiche miniere della Valle d'Aosta. Quart (Aosta), Musumeci, 165 p.

Luoni, P., Zanoni, D., Rebay, G., & Spalla, M. I. (2019). Deformation history of Ultra High-Pressure ophiolitic serpentinites in the Zermatt-Saas Zone, Créton, Upper Valtournanche (Aosta Valley, Western Alps). Ofioliti, 44(2), 111-123.

Manzotti, P., Ballèvre, M., Zucali, M., Robyr, M., & Engi, M. (2014). The tectonometamorphic evolution of the Sesia–Dent Blanche nappes (internal Western Alps): review and synthesis. Swiss Journal of Geosciences, 107(2), 309-336.

Manzotti, P., Zucali, M., Ballevre, M., Robyr, M., & Engi, M. (2014). Geometry and kinematics of the Roisan-Cignana Shear Zone, and the orogenic evolution of the Dent Blanche Tectonic System (Western Alps). Swiss Journal of Geosciences, 107(1), 23-47.

Manzotti, P., Ballèvre, M., Pitra, P., & Schiavi, F. (2021). Missing lawsonite and aragonite found: P–T and fluid composition in meta-marls from the Combin Zone (Western Alps). Contributions to Mineralogy and Petrology, 176(8), 1-27.

Martin S., Kienast J.R. (1987) – The HP-LT manganiferous quartzites of Praborna; Piemonte ophiolite nappe, Italian western Alps. Schweizerische Mineralogische und Petrographische Mitteilungen 67 (3), 339-360.

Martin, S., Tartarotti, P. (1989) -Polyphase HP metamorphism in the ophiolitic glaucophanites of the lower St. Marcel Valley (Aosta, Italy). Ofioliti. 14, 135-156.

Martin-Vernizzi S. (1982) – La mine de Praborna (Val d'Aoste, Italie): une série manganesifère métamorphisée dans le faciès eclogite. Unité d'enseignement et de recherche des sciences de la terre 494.

Martin S., Cortiana G. (2001) – Influence of the whole-rock composition on the crystallization of sodic amphiboles (Piemonte zone, Western Alps). Ofioliti 26 (2b), 445-456.

Martin S., Rebay G., Kienast J.R., Mevel C., (2008). An eclogitised oceanic palaeo-hydrothermal field from the St. Marcel Valley (Italian Western Alps). Ofioliti, 33, 49-63.

Masini E., Manatschal G., Mohn G. (2013) - The Alpine Tethys rifted margins: Reconciling old and new ideas to understand the stratigraphic architecture of magma-poor rifted margins. Sedimentology 60 (1), 176-196.

Mattauer M. (1986) – Intracontinental subduction, crust-mantle décollement and crustal-stacking wedge in the Himalayas and other collision belts. Geological Society, London, Special Publications 19 (1), 37-50.

Mayer A., Abouchami W., Dal Piaz G.V. (1999) – Eocene Sm-Nd age for the eclogitic metamorphism of the Zermatt-Saas ophiolite in Ayas valley, western Alps. Eur. Union GEosc. 10, Abstr 809.

Natale, P. (1969). Recrystallization and remobilisation in some pyrite deposits of the Western Alps. In: Convegno sulla rimobilizzazione dei minerali metallici e non metallici, Cagliari, 23 p.

Negro, F., Bousquet, R., Vils, F., Pellet, C. M., & Hänggi-Schaub, J. (2013). Thermal structure and metamorphic evolution of the Piemont-Ligurian metasediments in the northern Western Alps. Swiss Journal of Geosciences, 106(1), 63-78.

Nicot, E. (1977) - Les roches méso- et catazonales de la Valpelline (nappe de la Dent Blanche, Alpes Italiennes). *PhD dissertation*, Université de Paris VI, Paris, France, 211p.

Oberhänsli R., Martinotti G.M., Hunziker J.C., Stern W.F. (1982) - Monte Mucrone; eoalpin eklogitisierter permischer Granit. Schweitzerische mineralogische und petrographische Mitteilungen 62, 486-487.

Oberhänsli R., Hunziker J.C., Martinotti G., Stern W.B. (1985) - Geochemistry, geochronology and petrology of Monte Mucrone: an example of eo-Alpine eclogitisation of Permian granitoids in the Sesia Lanzo zone, western Alps, Italy. Chem. Geol., 52, 165-184.

Oberhänsli R., Bousquet R., Engi M., Goffé B., Gosso G., Handy M.R., Höck V., Koller F., Lardeaux J.M., Polino R., Rossi P.L., Schuster R., Schwartz S., Spalla I. (2004) - Metamorphic Structure of the Alps. CCGM Commission of the Geological Maps of the World.

Passchier C.W., Urai J.L., van Loon J., Williams P.F. (1981) - Structure and metamorphism in the central Sesia-Lanzo. Geol. Mijnbouw, 60, 497–507.
Perseil E.A. (1988) – La présence du strontium dans les oxydes manganésiféres du gisement de St-Marcel-Praborna-V.Aoste, Italie. Mineralium Deposita 23 (4), 306-308.
Perseil E.A., Smith D.C. (1995) – Sb-rich titanite in the manganese concentrations at St. Marcel-Praborna, Aosta Valley, Italy: petrography and crystal-chemistry. Mineralogical Magazine 59 (397), 717-734.
Pfeiffer H.R, Colombi A. Ganguin J. (1989) – Zermatt-Saas and Antrona Zone : A petrographic and geochemical comparison of polyphase metamorphic ophiolites of the West-Central Alps. Schweiz. Mineral. Petrogr. Mitt. 69, 217-236.
Philippot P., Kienast J-R. (1989) - Chemical-microstructural changes in eclogite-facies shear zones (Monviso, Western Alps, north Italy) as indicators of strain history and the mechanism and scale of mass transfer. Lithos 23 (3), 179-200.
Pognante U. (1979) - Studio geologico-petrografico del complesso dei micascisti eclogitici lungo la Valle d'Aosta tra Quincinetto, Ivozio e la Colma di Mombarone. Ist. Petrografia Univ. Torino, Unpubl. Thesis.
Pognante U. (1989) - Tectonic implications of lawsonite formation in the Sesia zone (Western Alps). Tectonophysics, 162, 219-227.
Pognante U., Compagnoni R., Gosso G. (1980) - Micro-mesostructural relationships in the continental eclogitic rocks of the Sesia-Lanzo zone: a record of a subduction cycle (Italian Western Alps). Rend. Soc. It. Min. Petr., 36, 169-186.
Pognante U. (1991) - Petrological constraints on the eclogite- and blueschistfacies metamorphism and P-T-t paths in the Western Alps. J. Metamorph. Geol. 9 (1) 5-17.
Polino R., Dal Piaz G.V., Gosso G. (1990) - Tectonic erosion at the Adria margin and accretionary processes for the Cretaceous orogeny of the Alps. Mém. Soc. Géol. Fr. 156, 345-367.
Rebay G. & Messiga B. (2007) - Prograde metamorphic evolution and development of chloritoid-bearing eclogitic assemblages in subcontinental metagabbro (Sesia–Lanzo zone, Italy). Lithos, 98, 275–291.
Rebay, G. & Powell, R. (2012). Eclogite-facies sea-floor hydrothermally-altered rocks: calculated phase equilibria for an example from the western Alps at Servette. Ofioliti, 37 (1), 55-63.
Rebay G. & Spalla M.I. (2001) - Emplacement at granulite facies conditions of the Sesia-Lanzo metagabbros: an early record of Permian rifting? Lithos, 58, 85-104.
Regis D. (2012) - High-pressure evolution in the Sesia terrane (Italian Western Alps), PhD thesis, Department of Geological Sciences, University of Bern, 161 p.
Regis D., Rubatto D., Darling J., Cenki-Tok B., Zucali M., Engi M. (2014) - Multiple metamorphic stages within an eclogite-facies terrane (Sesia Zone, Western Alps) revealed by Th–U–Pb petrochronology. Journal of Petrology, 55(7), 1429-1456.
Reinecke T. (1991) – Very-high-pressure metamorphism and uplift of coesite-bearing metasediments from the Zermatt-Saas zone, Western Alps. European Journal of Mineralogy, 7-18.
Reinecke T. (1998) - Prograde high- to ultrahigh-pressure metamorphism and exhumation of oceanic sediments at Lago di Cignana, Zermatt-Saas Zone, western Alps. Lithos 42 (3-4), 147-189.
Roda M., Zucali M., Regorda A., Spalla M.I. (2019) Formation and evolution of a subduction-related mélange: The example of the Rocca Canavese Thrust Sheets (Western Alps). GSA Bulletin; 132 (3-4): 884–896. doi: https://doi.org/10.1130/B35213.1.
Rosenbaum G., Lister G. S. (2005) - The Western Alps from the Jurassic to Oligocene: spatio-temporal constraints and evolutionary reconstructions. Earth-Science Reviews 69 (3-4), 281-306.
Rubatto D. (1998) - Dating of pre-Alpine magmatism, Jurassic ophiolites and Alpine subductions in the Western Alps. Unpubl. PhD thesis, ETH Zuerich, 173 p.
Rubatto D., Gebauer D., Fanning M. (1998) - Jurassic formation and Eocene subduction of the Zermatt-Saas-Fee ophiolites: implications for the geodynamic evolution of the Central and Western Alps. Contrib. Mineral. Petrol. 132 (3), 269-287.
Rubatto D., Gebauer D. & Compagnoni R. (1999) - Dating of eclogite-facies zircons: the age of Alpine metamorphism in the Sesia-Lanzo Zone (Western Alps). Earth Planet. Sci. Lett., 167, 141-158.
Rubatto D., Hermann J., (2001) - Exhumation as fast as subduction? Geology 29 (1), 3-6.
Rubatto D., Hermann J. (2003) - Zircon formation during fluid circulation in eclogites (Monviso, Western Alps): implications for Zr and Hf budget in subduction zones. Geochimica et Cosmochimica Acta 67 (12), 2173-2187.
Rubatto D., Regis D., Hermann J., Boston K., Engi M., Beltrando M., McAlpine S. (2011) - Yo-Yo subduction recorded by accessory minerals (Sesia Zone, Western Alps). Nature Geosc., 4, 338-342.
Rubbo M., Borghi A., Compagnoni R. (1999) - Thermodynamic analysis of garnet growth zoning in eclogite facies granodiorite from M. Mucrone, Sesia zone, Western Italian Alps. Contributions to Mineralogy and Petrology 137, 289-303.
Ruffini R., Polino R., Callegari E., Hunziker J.C., Pfeifer H.R. (1997) – Volcanic clast-rich turbidites of the Taveyanne sandstones from the Thônes syncline (Savoie, France): Records for a Tertiary postcollisional volcanism. Schweizerische mineralogische und petrographishe Mitteilungen 77, 161-174.
Schwartz, S., Allemand, P., & Guillot, S. (2001). Numerical model of the effect of serpentinites on the exhumation of eclogitic rocks: insights from the Monviso ophiolitic massif (Western Alps). Tectonophysics, 342(1-2), 193-206.
Sinclair H.D., Allen P.A. (1992) - Vertical versus horizontal motions in the Alpine orogenic wedge: stratigraphic response in the foreland basin. Basin Research 4 (3-4), 215-232.
Spalla M.I., Lardeaux J-M., Dal Piaz G.V., Gosso G., Messiga B. (1996) - Tectonic significance of Alpine eclogites. Journal of Geodynamics 21 (3), 257-285.
Spalla M.I., Zulbati F. (2003) - Structural and petrographic map of the southern Sesia-Lanzo zone (Monte Soglio - Rocca Canavese, western Alps, Italy). Memorie di Scienze Geologiche 55, 119-127
Stampfli G.M., Mosar J., Marquer D., Marchant R., Baudin T., Borel G. (1998) - Subduction and obduction processes in the Swiss Alps. Tectonophysics 296 (1-2), 159-204.
Stella A. (1894) – Relazione sul rilevamento eseguito nell'anno 1893 nelle Alpi Occidentali (Valli dell'Orco e della Soana). Bollettino del Regio Comitato geologico d'Italia 25, 343-371.
Sturani C. (1973) - Considerazioni sui rapporti tra Appennino settentrionale ed Alpi occidentali. Rend. Acc. Lincei 183, 119-142.

Stutz A.H., Masson R. (1938) - Zur Tektonik der Dent Blanche-Decke. Schweiz Mineral. Petrogr. Mitt. 18, 40-53.
Sue C., Thouvenot F., Fréchet J., Tricart P. (1999) - Widespread extension in the core of the western Alps revealed by earthquake analysis. Journal of Geophysical Research: Solid Earth, *104* (B11), 25611-25622.
Tartarotti P., Caucia F. (1993) - Coexisting cummingtonitesodic amphibole pair in metaquartzites from the ophiolite's sedimentary cover (St. Marcel Valley, Italian Western Alps): A X-ray structure refinement and petrology study. Neues Jahrbuch fuïr Mineralogie, Abhandlungen 165, 223-243.
Tartarotti P., Martin S., Polino R. (1986) - Geological data about the ophiolitic sequences in the St. Marcel valley (Aosta Valley). Ofioliti 11, 343-346.
Todd C.S., Engi M. (1997) - Metamorphic field gradients in the Central Alps. Journal of Metamorphic Geology 15 (4), 513-530.
Toffolo L., Addis A., Martin S., Nimis P., Rottoli M., Godard G. (2018) - The Misérègne slag deposit (Valle d'Aosta, Western Alps, Italy): Insights into (pre-)Roman copper metallurgy. J. Archaeol. Sci. Reports 19, 248–260.
Tropper P., Essene E.J. (2002) - Thermobarometry in eclogites with multiple stages of mineral growth: an example from the Sesia-Lanzo Zone (Western Alps, Italy). Schweiz. mineral. petrogr. Mitt., 82, 487-514.
Tropper P., Essene E.J., Sharp Z.D., Hunziker J.C. (1999) - Application of K-feldspar - jadeite- quartz barometry to eclogite facies metagranites and metapelites in the Sesia Lanzo Zone (Western Alps, Italy). J. metam. Geol. 17, 195-209.
Tumiati S., Casartelli P., Mambretti A., Martin S., Frizzo P., and Rottoli M. (2005). The ancient mine of Servette (Saint-Marcel, Aosta Valley, Western Italian Alps): a mineralogical, metallurgical and charcoal analysis of furnace slags. Archaeometry 47 (2), 317-340.
Tumiati S., Godard G., Martin S., Malaspina N., Poli S., (2015) - Ultra-oxidized rocks in subduction mélanges? Decoupling between oxygen fugacity and oxygen availability in a Mn-rich metasomatic environment. Lithos 226, 116–130.
Tumiati S., Martin S., Godard G. (2010) - Hydrothermal origin of manganese in the high-pressure ophiolite metasediments of Praborna ore deposit (Aosta Valley, Western Alps). Eur. J. Mineral 22, 577–594.
Tumiati S., Merlini M., Godard G., Hanfland M., Fumagalli P. (2020) - Orthovanadate wakefieldite-(Ce) in symplectites replacing vanadium-bearing omphacite in the ultra-oxidized manganese deposit of Praborna (Aosta Valley, Western Italian Alps). Am. Mineral. 105, 1242–1253. Venturini G., Martinotti G., Armando G., Barbero M., Hunziker J.C. (1994) - The Central Sesia Lanzo Zone (Western Italian Alps): new field observations and lithostratigraphic subdivisions. Schweiz. mineral. petrogr. Mitt. 74, 115–125.
van der Klauw S.N.G.C., Reinecke T., Stöckhert B. (1997) – Exhumation of ultrahigh-pressure metamorphic oceanic crust from Lago di Cignana, Piemontese zone, western Alps: the structural record in metabasites. Lithos 41 (1-3), 79-102.
Venturelli, G., Thorpe, R. S., Dal Piaz, G. V., Del Moro, A., & Potts, P. J. (1984). Petrogenesis of calc-alkaline, shoshonitic and associated ultrapotassic Oligocene volcanic rocks from the Northwestern Alps, Italy. Contributions to Mineralogy and Petrology, 86(3), 209-220.
Venturini, G., Martinotti, G., Armando, G., Barbero, M., & Hunziker, J. C. (1994). The central Sesia Lanzo Zone (Western Italian Alps): new field observations and lithostratigraphic subdivisions. Schweizerische Mineralogische und Petrographische Mitteilungen, 74(1), 115-125.
Venturini, G. (1995). Geology, geochemistry and geochronology of the inner central Sesia Zone (Western Alps, Italy). *Mémoires de Géologie (Lausanne), 25*, 1–143.
Vho A., Rubatto D., Lanari P., Regis D. (2020) - The evolution of the Sesia Zone (Western Alps) from Carboniferous to Cretaceous: insights from zircon and allanite geochronology. Swiss journal of geosciences 113 (1), 1-33.
Weber S., Bucher K. (2015) - An eclogite-bearing continental tectonic slice in the Zermatt–Saas high-pressure ophiolites at Trockener Steg (Zermatt, Swiss Western Alps). Lithos *232*, 336-359.
Wheeler J., Butler R.W. (1993) - Evidence for extension in the western Alpine orogen: the contact between the oceanic Piemonte and overlying continental Sesia units. Earth and Planetary Science Letters, *117* (3-4), 457-474.
Widmer T., Ganguin J., Thompson A.B. (2000) – Ocean floor hydrothermal veins in eclogite facies rocks of the Zermatt-Saas zone, Switzerland. Schweiz. Mineral. Petrogr. Mitt. 80, 67-73.
Zanoni D., Corti L., Roda M. (2022) - Cooling history of the Biella pluton and implication for Oligocene to Miocene tectonics of the Sesia-Lanzo Zone, Austroalpine, Western Alps. International Geology Review 64 (2), 203-232.
Zinetti G. (2002) - Analisi ambientale del dissesto idrogeologico causato dallo stato di abbandono e di degrado della miniera di Cu e Fe di Servette nel versante destro della bassa valle di Saint – Marcel (AO) e proposta di recupero ambientale. – Tesi di Laurea – Università degli Studi dell'Insubria – Como.
Zucali M. (2002) - Foliation map of the "Eclogitic Micaschist Complex" (Monte Mucrone – Monte Mars – Mombarone, Sesia-Lanzo Zone, Italy). Mem. Sci. Geol. (Padova), 54, 87-100.
Zucali, M. (2011). Coronitic microstructures in patchy eclogitised continental crust: the Lago della Vecchia Permian metagranite (Sesia-Lanzo Zone, Western Italian Alps). In: (Ed.) Marnie A. Forster, and John D. Fitz Gerald, The Science of Microstructure - Part II, Journal of the Virtual Explorer, Electronic Edition, ISSN 1441-8142, volume 38, paper 7.
Zucali M., Spalla M.I., Gosso G. (2002) - Strain partitioning and fabric evolution as a correlation tool: the example of the Eclogitic Micaschists Complex in the Sesia-Lanzo Zone (Monte Mucrone-Monte Mars, Western Alps, Italy). Schweiz. mineral. petrogr. Mitt.., 82, 429-454.
Zucali M., Spalla M.I., Gosso G., Racchetti S., Zulbati F. (2004) - Prograde Lws-Ky transition during subduction of the Alpine continental crust of the Sesia-Lanzo Zone: the Ivozio Complex. In: Beltrando M., Lister G., Ganne J. & Boullier A. (Eds.), Evolution of the Western Alps: Insights from Metamorphism, Structural Geology, Tectonics and Geochronology. Journal of Virtual Explorer, 16, 4.
Zucali M. & Spalla M.I. (2011) - Prograde lawsonite during the flow of continental crust in the Alpine subduction: Strain vs. metamorphism partitioning, a field-analysis approach to infer tectonometamorphic evolutions (Sesia-Lanzo Zone, Western Italian Alps). J. Struct. Geol., 33, 381-398.

Horace-Bénédict de Saussure (1740–1799), portray by Jens Juel, 1778 (Geneva, Bibliothèque Publique et Universitaire).

Authors' affiliation:

Samuel ANGIBOUST : Laboratoire de Géologie de Lyon –TPE, Ecole Normale Supérieure de Lyon, France
Daniele CASTELLI: Dipartimento di Scienze della Terra, Torino University, Italy
Silvana MARTIN: Department of Geoscience, Università degli Studi di Padova, Italy
Gisella REBAY: Earth and Environmental Sciences Department, University of Pavia, Italy
Simone TUMIATI: Department of Earth Sciences, Università degli Studi di Milano, Italy
Michele ZUCALI: Department of Earth Sciences, Università degli Studi di Milano, Italy

Acknowledgements:

Tessa Adrian-Roux and Farah Daoulet from the Cellule Congrès (ENS Lyon) are greatly acknowledged for the logistical help us to organize this excursion. ENS Lyon and Lyon metropole are also acknowledged for the financial support for organizing this congress and the excursions. Clothilde Minnaert is also acknowledged for technical and editorial assistance.

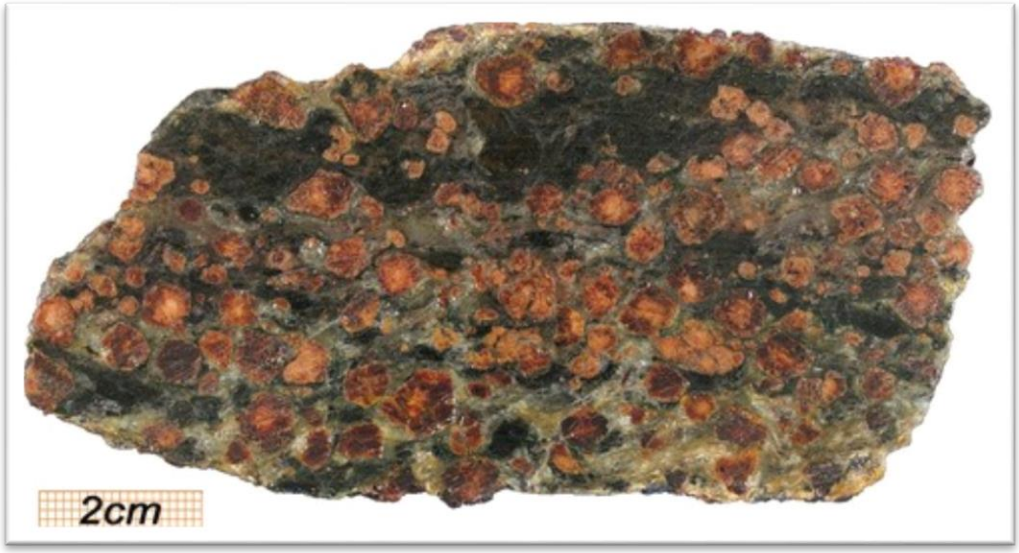

Garnet-talc-chloritoid metabasite, Servette mine, St Marcel valley